THE RESERVOIR BEHAVIOR OF ASSOCIATIVE POLYMERS

Diploma Thesis

FILIZ AKTAS

Submitted to the
Department of Petroleum Engineering
University of Leoben, Austria

December 2007

I declare in lieu of oath that I did this work by myself using only literature cited at the end this volume.

_____

AKTAS Filiz
Leoben, December 2007

Acknowledgements

First and foremost, I would like to thank Prof. Anthony Kovscek and Dr. Louis Castainer for their support, thoughtful advices, encouragement and friendship throughout my research. I have learned a tremendous amount while under their supervisions. Working with you has been a great experience for me. I also would like to thank my office mate, Bolivia Vega, for her help, guidance and friendship. I will never forget the steps Bolivia! Being a researcher at the Stanford University, getting to know very special people, gaining experiences by the help of great professors has been an enormous gift to me. Thanks to the students, faculty, and staff in the department for all their assistance. Also technical support during the course of this work of the Stanford University Petroleum Research Institute (SUPRI-A) Industrial Affiliates is gratefully acknowledgement.

I also would like to thank my advisor Prof. Leonhard Ganzer for his advices, support and help during my research time at Stanford University.

Financial support during the course of this work was provided by the OMV and the Department of Petroleum Engineering through the University of Leoben. I am very grateful to OMV and Dr. Torsten Clemens for giving me this big opportunity to pursue my master thesis at Stanford University.

Finally, I would like to dedicate this work to my family for their incredible support during my years in abroad. You made it a lot easier! Your endless love and understanding were the inspiration which made me pursue further achievement in this study. Dad, Mom, my dear sister, this thesis is dedicated to you. I love you.

Abstract

Waterflood accounts for roughly half of all oil recovered, but is generally limited to lighter oils with relatively low in-situ viscosity. Application of water injection for viscous oil recovery suffers from high mobility of water leading to unstable displacement. Addition of polymer to injected water reduces injected-phase mobility and provides a first order solution to the problem of unstable displacement. To decrease costs of polymer flooding, new types of polymers – so called "associative polymers" - have been developed.

This study investigates the displacement process of medium viscosity oil (10-100 cP) by aqueous solutions of associative polymers. Studies are conducted in two-dimensional etched-silicon micromodels under a reflected light microscope. The pore network pattern of the micromodel replicates Berea sandstone. Fluid advance is monitored at the pore level as well as over the entire micromodel. Visual observations are used to determine displacement fluid flow characteristics. Results include the sweep pattern, ultimate oil recovery, and the pore-level distribution of residual oil. Brine injection to displace crude oil is compared to the injection of associative polymer solutions as well as conventional polymers.

Associative polymers result in greater fluid viscosities at the same concentration as conventional polymers. Generally, we find that conventional polymers and brine result in severe fingering of the displacement fluid, however, associative polymers lead to more stable displacement characteristics at these concentrations. The displacement pattern while injecting brine displays fingers clearly. Injection of associative polymers after breakthrough mitigates fingering and improves viscous oil displacement accordingly.

Experimental results show that associative polymers are a promising method to improve the displacement efficiency of viscous oils.

Kurzfassung

Die Hälfte des weltweit geförderten Erdöls wird mit Hilfe des sogenannten Wasserflutens gewonnen. Diese Entölungsmethode beschränkt sich aber auf leichtere Öle mit relativ niedrigen in-situ Viskositäten. Durch die hohe Mobilität des injizierenden Wassers kommt es, vorallem bei der Entölung von viskosen Ölen, zu einer Instabilität der Verdrängung was den Erfolg des Wasserflutens beeinträchtigt. Durch die Zugabe von Polymeren zum injizierten Wasser wird die Mobilität der Wasserphase reduziert, was den erstrangigen Lösungsansatz für das Problem der instabilen Verdrängung darstellt. Um die Kosten des sogenannten Polymerflutens zu reduzieren, wurden neue Polymere, so genannte „Assoziative Polymere", entwickelt.

In der vorliegenden Arbeit wird die Verdrängung von moderat viskosem Öl (10-100 cP) durch eine wässrige Lösung mit assoziativen Polymeren untersucht. Die Experimente wurden mithilfe eines zwei-dimensionalem geätzten Silizium Mikromodells unter einem Lichtmikroskop durchgeführt. Die Porenstruktur des Silizium Modells repräsentiert Berea Sandstein. Der Durchfluss der Fluide durch das Modell wird sowohl auf Porenebene als auch durch das gesamte Mikromodell beobachtet. Das Verhalten der Fluide während der Verdrängung wurde mit Hilfe von visueller Überwachung der Experimente bestimmt. Die Ergebnisse dieser Untersuchungen beinhalten das Verdrängungsmuster (Sweep pattern), den ultimativen Entölungsgrad, sowie die Verteilung des Restöles auf Porenebene. Lagerstättenwasserinjektion zu verbesserten Entölung wird mit der Injektion von assoziativen Polymeren, sowie mit der Injektion von konventionellen Polymerlösungen verglichen.

Verglichen mit konventioneller Polymerinjektion resultiert die Injektion von assoziativen Polymeren, bei gleicher Polymerkonzentration, in höheren Viskositäten. Im allgemeinen, führt die Injektion von konventionellen Polymeren oder Lagerstättenwasser häufig zu sogenannten „viscous fingering" des Verdrängungsmediums, bei der Injektion von assoziativen Polymeren hingegen konnte eine stabilere Verdrängung bei gleicher Polymerkonzentration beobachtet werden. Dieses „viscous fingering" kann bei der Verdrängung des Öles mit Lagerstättenwasser bei der visuellen Untersuchung der „sweep pattern" sehr gut beobachtet werden. Die Injektion von assoziativen Polymeren nach dem Wasserdurchbruch verringert dieses „viscous fingering" und verbessert folglich die Verdrängung des viskosen Öles. Die Ergebnisse der Experimente zeigen deutlich, dass die Injektion assoziativer Polymere eine vielversprechende Methode zur verbesserten Entölung von viskosen Ölen ist.

TABLE OF CONTENTS

CHAPTER ONE

CHAPTER TWO

CHAPTER THREE

CHAPTER FOUR

CHAPTER FIVE

LIST OF FIGURES

LIST OF TABLES

CHAPTER ONE

1. INTRODUCTION

The purpose of this investigation is to observe and understand the differences between the displacement processes of medium viscous oil by conventional polymer and new kind of so called 'associative' polymers. Toward this goal, experiments were conducted in a micromodel whose homogenous pore space is geometrically and topologically similar to Berea sandstone. High-resolution, micro visual data, in the form of photographs and video footage, describes the front movement and the sweep efficiency at the pore and the ensemble pore network scale.

The use of crude oil plays an important role in the world economy today. There are three stages in hydrocarbon production which are primary, secondary and tertiary recoveries. Primary recovery is using the natural energy existing in the reservoir to produce the fluids. Secondary recovery is implemented after primary production declined. It includes water flooding and pressure maintenance. When a typical oil reservoir reaches its economic limit after primary and secondary recovery (water flooding), more than two-thirds of the original oil is left in place. Enhanced oil recovery (tertiary recovery) can begin after a secondary recovery process or any time during the productive life of an oil reservoir. Its purpose is not only to restore formation pressure, but also to improve oil displacement or fluid flow in reservoir. The four major types of enhanced oil recovery operations are Mobility-control, chemical flooding (alkaline flooding or micellar-polymer flooding), miscible displacement (carbon dioxide injection or hydrocarbon injection), and thermal recovery (steamflood or in-situ combustion). The optimal application of each type depends on reservoir temperature, pressure, depth, net pay, permeability, residual oil and water saturations, porosity and fluid properties such as oil API gravity and viscosity[(1)]. Polymer injection belongs to the mobility-control process in which water viscosity is increased through added polymers.

Oil recovery in petroleum reserves is extremely affected by fluid-rock and fluid-fluid interactions. These surface chemical interactions directly control rock wettability, capillary pressure curves and relative permeabilities [(2)]. The increasing use of high molecular weight polymers to improve water flood efficiency has resulted in increased interest on the part of potential users, polymer manufacturers and universities in the mechanisms by which these polymers exert their mobility control effects. This interest has resulted in a number of excellent publications on polymer behavior [(3)]. Polymer flooding is one of the more attractive recovery methods proposed in recent years. Compared to the conventional water flooding, it requires

more technology and equipment. It is also more complicated to observe and interpret the behavior of polymer solutions in porous media [4].

This report concerns new kinds of polymers which are manufactured by SNF Group and called associative polymers. SNF Group is the world's preeminent producer of water-soluble polymers. They are located in France and manufacture polymers. Polymer to control the mobility of injected water has been employed for many years in enhanced oil recovery applications. Polymer flooding to improve volumetric sweep efficiency and reduce channeling and breakthrough has been used by many operators to increase oil recovery. The same kind of polymers was also used with the surfactants and alkali agents to increase the sweep efficiency of the tertiary recovery floods. But in this study, only polymer solution is used and its flow mechanism is observed without surfactants or alkali agents.

The figure 1 below shows polymer flooding increases the areal sweep efficiency of the water so that the fingering is reduced.

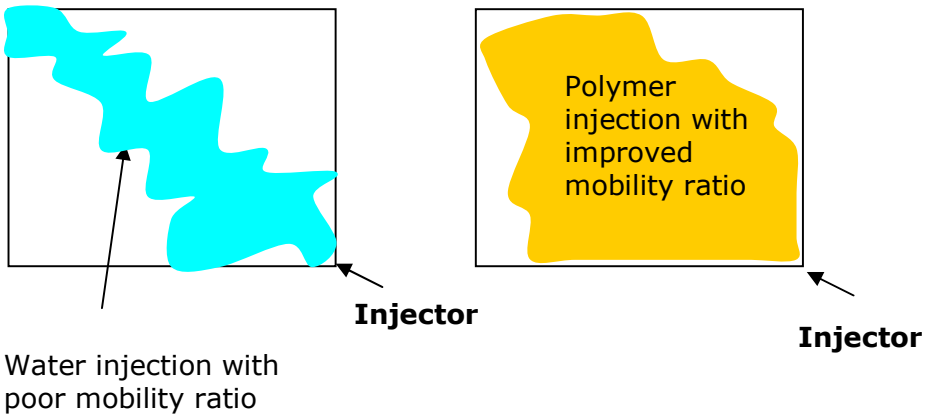

Figure 1: Differences between polymer and water floods [5]

The figure 2 shows the increase of the vertical sweep efficiency by the polymer flooding in a heterogeneous reservoir.

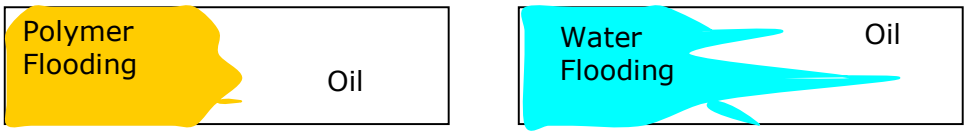

Figure 2: Schematic illustration of polymer and water flooding [5]

This project has attempted to study the pore level processes in polymer flooding in a silicon micro model. The micro model is an exact representation of a slice through Berea sandstone etched onto a silicon wafer. It honors the microscopic heterogeneity of the rock but being two-

dimensional loses some of the continuity of a three-dimensional sample [6]. Initial experimentation involved the saturation of the silicon micro model with a prepared brine solution. This liquid medium is then invaded by oil and observed. Next, varying concentrations of the polymer solution is injected into micro model. The displacement process of oil by polymer solution and its flow mechanism in the two phase run is observed.

As a prelude to these experiments, a literature survey of previous studies on polymer flow with oil, as well as the use of micro models themselves was conducted. This survey is given in the following section.

CHAPTER TWO

2. BACKGROUND AND LITERATURE REVIEW

This section will look into two-phase flow studies and also review the use of micromodels in pore level visualization work. There has been a great deal of work published concerning polymer research and a great deal of interest is being shown in the use of polymer solutions for secondary recovery and a number of polymer floods have been performed. A number of floods are still in progress and remain to be evaluated. With the advent of polymer flooding, the need developed to understand the mobility control mechanism in porous media. All the research and field applications done by the investigators and scientists so far used and evaluated the conventional polymer solutions. The polymers which are used in this research are so-called "Associative Polymers" which were manufactured by SNF Group and they have not been tested before neither in an experimental work nor in field application. This study is the first experimental work in which these new kind of polymers are being tested in a laboratory project by using silicon-micromodels. Associative polymers mean that their viscosity will depend on the shear history and the salinity of the solution. Their chemical description and the solution preparation are given in the further sections.

2.1. Mechanism of Polymer Flow in Porous Media

Depending on the wetting properties of the fluids, there are essentially two different types of displacement in two-phase flow in porous media. They are called drainage and imbibition. Drainage displacements are where a non-wetting invading fluid displaces a wetting fluid. The opposite case, imbibition, occurs when a wetting fluid displaces a non-wetting fluid. The mechanisms of the displacements in drainage and imbibition are quite different. Typically, slow drainage is characterized by piston-like motion inside the pores where the invading non-wetting fluid only enters a pore if the capillary pressure is equal to or greater than the threshold pressure of that pore. The threshold pressure corresponds to the capillary in the narrowest part of the pore. However, in imbibition at low injection rate the invading fluid will enter the narrowest pores before any other is considered. [7]

Rheologically, the polymer solutions behave as pseudo plastic fluids. Investigators have studied the rheology for this type of non-Newtonian fluid in porous medium. Results have also been reported on the ability of

the polymer solutions to decrease mobility. Some investigators indicated that polymer solutions show a different rheological behavior in cores than in the viscometer. A Newtonian fluid is a fluid that has a constant viscosity at all shear rates at a constant temperature and pressure, and can be described by a one-parameter rheological model. [1]

$$\mu = \tau / \gamma \quad \ldots\ldots(1)$$

In the equation 1 above, τ is the shear stress (Pa), γ is the shear rate (s) and μ (Pa.s) is the viscosity. Water, sugar solutions, glycerin, silicone oils, light-hydrocarbon oils, air and other gases are Newtonian fluids. Most drilling fluids are non-Newtonian. A non-Newtonian fluid is a fluid whose viscosity is not constant at all shear rates and does not behave like a Newtonian fluid. [1]

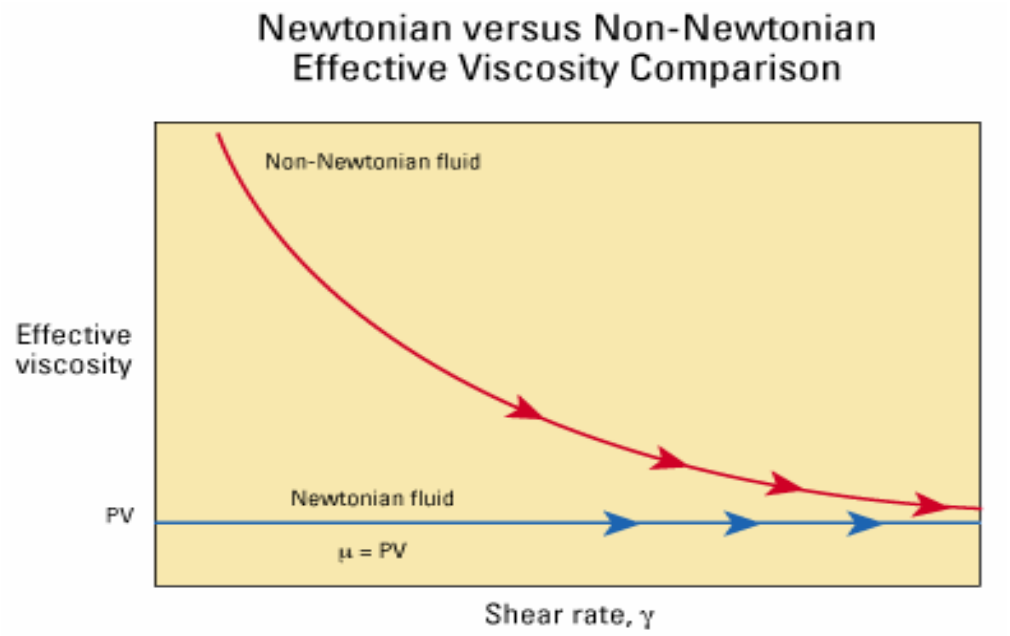

Figure 3: Comparison of Newtonian and Non-Newtonian fluids [1]

The figure above shows a comparison between a Newtonian and a non-Newtonian fluid. Most successful drilling fluids are non-Newtonian. Within that group are several general types and rheological mathematical models to describe them. The subject of 'Rheology' is devoted to the study of the behavior of such fluids. High molecular weight liquids which include polymer melts and solutions of polymers, as well as liquids in which fine particles are suspended are usually non-Newtonian. Pseudo plastic is a general type of shear-thinning. When the viscosity decreases with increasing shear rate, it is called shear-thinning fluid. A typical shear

stress versus shear rate plot for a shear-thinning fluid looks displayed in figure 4. [8]

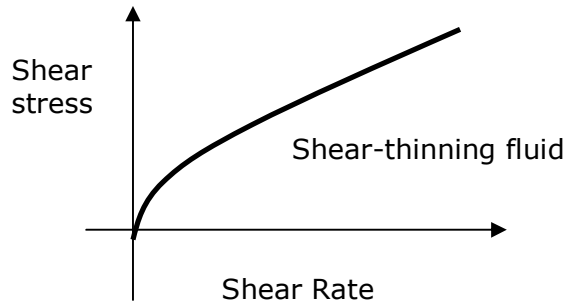

Figure 4: Shear – thinning fluid [8]

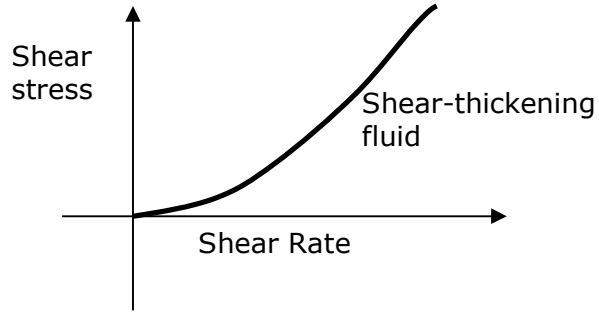

Figure 5: Shear – thickening fluid [8]

In the opposite case, where the viscosity increases as the fluid is subjected to a higher shear rate, the fluid is called shear-thickening. Shear-thinning behavior is more common than shear-thickening.

2.2. Sweep Pattern

Sweep efficiency is defined as a measure of the effectiveness of an enhanced oil recovery process that depends on the volume of the reservoir contacted by the injected fluid. The volumetric sweep efficiency is an overall result that depends on the injection pattern selected, off-pattern wells, fractures in the reservoir, position of gas-oil and oil/water contacts, reservoir thickness, permeability and areal and vertical heterogeneity, mobility ratio, density difference between the displacing and the displaced fluid, and flow rate [1]. The nature of the front movement in a displacement process differs very clearly depending on

whether the mobility ratio is greater or less than unity. For example, if a solvent displaces an oil phase with which it is miscible at M is less than or equal to 1.0 and there are no gravity effects, the displacement process is efficient [9]. The figure 6 below shows two kinds of displacement patterns. In this experimental work, the focus was on the displacement of oil by associative polymer and the aim was to observe whether it leads to a stable or an unstable displacement. In the figure 6 (a), an unstable displacement at different times is depicted. On the other hand, the figure 6 (b) depicts a stable displacement pattern at different times.

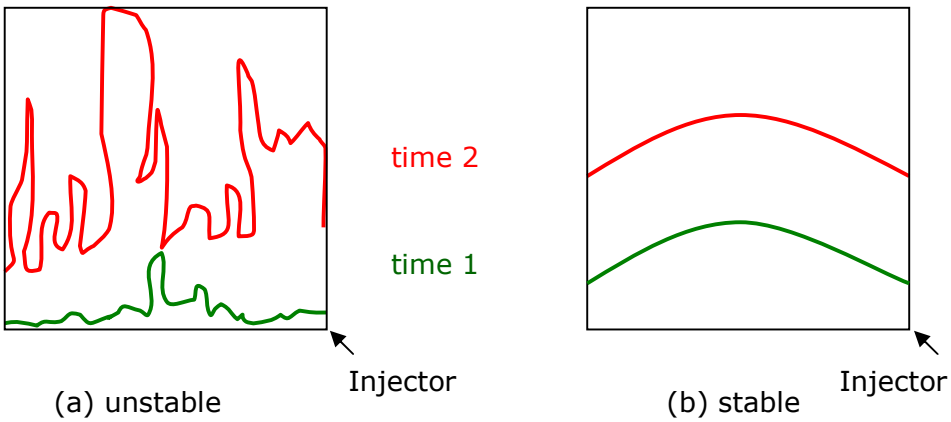

Figure 6: Stable and Unstable Displacement Patterns [10]

In stable displacement the principal force is due to viscous forces in the invading fluid. Opposite to viscous fingering the process is obtained by injecting a high viscosity fluid into a medium of low viscosity fluid with a high injection rate. Due the high injection rate the capillary forces vanish and the pressure drop across the sample corresponds to the pressure over the invading fluid. The structures are characterized by an almost flat front between the invading and the defending phases and some clusters of defending fluid are observed. The cluster sizes are bounded by the roughness of the front and as a consequence only small clusters can develop. In viscous fingering the principal force is due to viscous forces in the defending fluid. The process is obtained by injecting a low viscosity fluid into a medium of high viscosity fluid with a high injection rate. The capillary effects and the pressure drop in the invading fluid are negligible. The structures typically consist of fingers of invading fluid that propagate through the medium with only a few small trapped clusters of defending fluid left behind. [11]

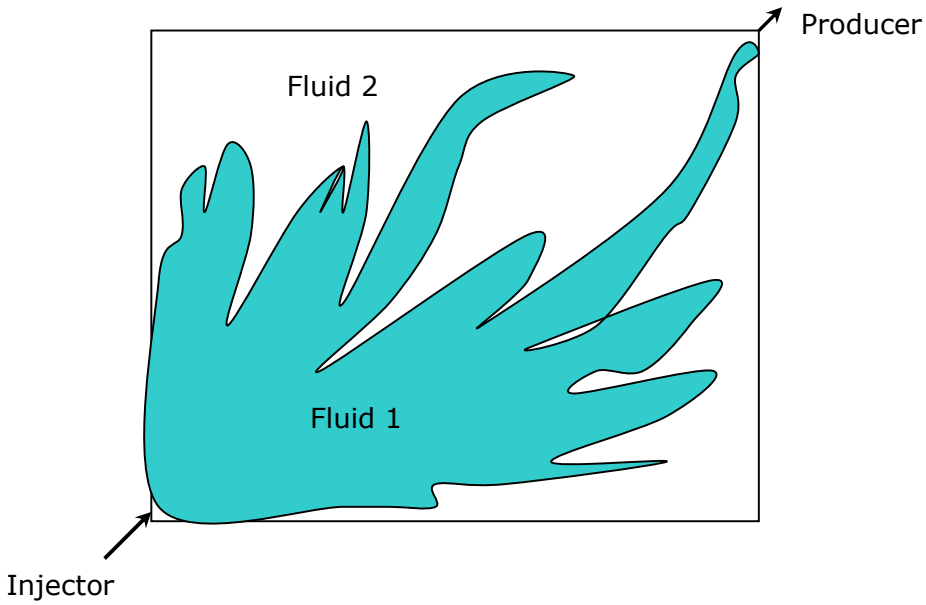

Figure 7: Viscous fingering in a quarter five-spot model [12]

2.3. Polymer Flood Field Applications

EOR projects have drawn great attention in the petroleum industry because of their high potential for recovering more oil from depleted reservoirs than conventional production methods.

Chemical enhanced oil recovery (EOR) methods have been used by the investigators by adding chemicals (surfactants, polymers) to the injected water to reduce residual oil saturation to very low values in the swept zone of an oil reservoir. Most chemical EOR projects have used polymer with surfactant for mobility control, and in recent years many of the projects have combined alkaline agents with the surfactant and polymer solutions.

There have been a great number of papers written by the investigators about polymer flood applications. Polymer flooding has been performed in oil reservoirs several decades around the world. The polymers basically increase the viscosity of the injected water and reduce the porous media permeability, allowing for an increase in the vertical and areal sweep efficiency of the water injection and consequently increasing the oil recovery. The interest in polymer flood is increasing by the successful trials on the fields. Between the years of 1978-1979, a Dow 500 Polymer injection program was carried out in the Cretaceous Newcastle Sandstone

reservoir by Michael A. Janeczko from the company Texaco Inc. Their description of the Newcastle reservoir is consolidated sandstone of lower cretaceous age containing three basic sand members separated by medium-hard, black shale deposits. They first started the water flooding operations in 1970. Then in 1972, they ran a polymer flood operation. It was concluded that the polymer floods were very successful, and an operation of a dry polymer injection system is very practical with the Petrofina flood reaching an average of 63 % increased recovery over conventional flooding. They also reported that the water-oil-ratio had been lower in the polymer area than in the non-polymer area. Based on these facts, together with the apparent polymer flooding success of the other operators, a 20% pore volume injection schedule was set up and the polymer project was initiated in 1974 with the addition of Dow 500 Polymer to the injection water. (13)

Canada's first polymer flood was initiated in 1967. The report was published by Ian Martin, Wally Lozanski. They reported that polymer flooding was economically successful and more profitable than a conventional water flood. Their use of polymer is estimated to increase the ultimate recovery over conventional flooding by at least 10 percent, or 4 million bbl. They also made a comparison between the plain water flood and the water flood with the addition of polymer. The conclusion of their comparison was reached that the mobility ratios were three times more favorable compared to the plain water flood. (14)

A pilot project for polymer mobility control was done by Ivonete P.Gonzalez de Silva, Jose Marcelo Luvizotto, Maria Aparecida de Melo from PETROBRAS and Elizabete F. Lucas from Federal University of Rio de Janeiro in the Carmopolis field, 1977. They also reached some positive results at the end. Their first experience with the polymers was in 1969, Carmopolis field, in the so called "Pusher" project, with the polymer injection which lasted until 1972. They did not get good results at the end of this project but instead of the results, they decided to invest in new polymer pilot, again in the same field, Carmopolis in September 1977. They first evaluated the fit of the polymer technology to that field, considering the particular characteristics of the field regarding rock heterogeneities, oil type, water salinity, temperature, pressure etc. Their second goal was to obtain know-how in all the project phases like lab tests, design and operation in field scale. The paper that they published shows a more economical evaluation of their experiences in this project and an evaluation of the world and Brazilian scenario of the polymer technology. (15)

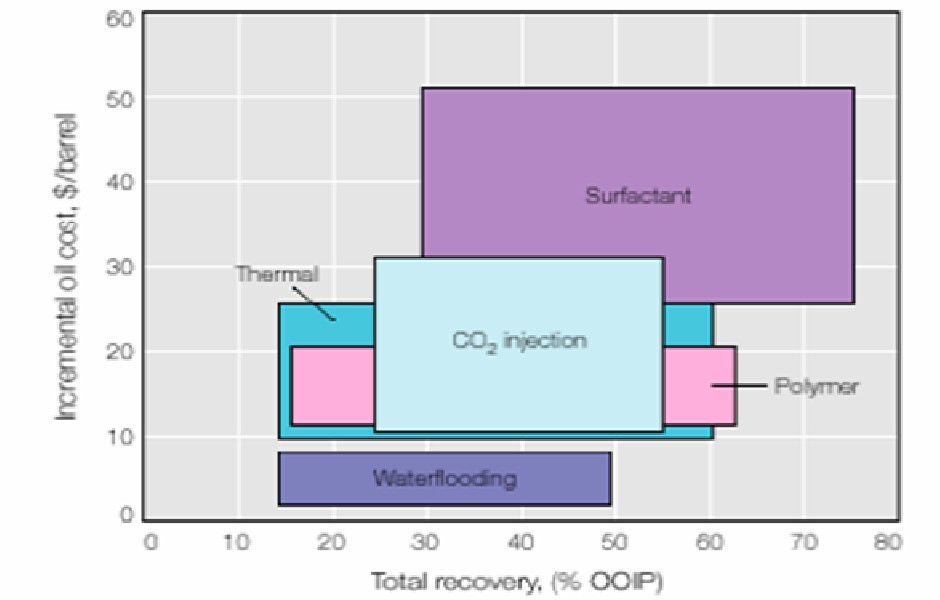

Figure 8: Cost and Recovery factor evaluation done by PETROBAS [15]

In the table above, it was shown that the methods of recuperation, the onshore polymer injection is one of the most common methods of easy application and with one of the lowest cost of additional oil. Their evaluation demonstrated that the injection process of polymer for mobility control is efficient even for heterogeneous reservoirs as Carmopolis field with the increase of the oil production. They also reported that the great Brazilian offshore reserves and the amount of the mature fields justify the investment in this advanced recovery technique to this type of production, in spite of challenges, in the logistics and in the polymer for hostile conditions of salinity and temperature, the polymer injection process seems to be one of the more feasible in these conditions. In this project, polymer injection reduced the use of water which consequentially reduced the water production and the costs related to this water. [15]

Deutsche Texaco AG carried out 2 polymer flood operations in the years of 1975 and 1977. The applications are conducted by Balram K. Maitin and Hartwig Volz. Their main object was to plug off a zone of high permeability in the reservoir and hereby improve the areal sweep efficiency of flood operations. The oil fields that they conducted the applications are called Oerrel and Hankensbuettel which are located in one of the main oil producing sediment basins of Germany. The sandstone of this basin belongs to different geological ages. They use the water soluble high molecular weight polymers offered by the chemical industry. They accomplished a decrease in water cut after a cumulative production of 30% of OOIP. After Polymer broke through early in the northern part of

the reservoir, and no injectivity problems occurred, they increased the liquid polymer concentration in 1978. After technical and economical evaluations, it was concluded that the incremental recovery was 23.5 and 12.9 % of OOIP in those two projects. They reported that positive results encouraged to extent polymer floods to larger parts of the reservoirs and considered that both floods are successful and then they extended the polymer application to larger parts of both fields. (16)

2.4. Previous Polymer Flood Experimental Studies

The goal of the polymer injection projects for mobility control is to increase the oil recovery factor, by reducing the mobility between the injected water and the oil. The reduction of the mobility ratio is achieved by increasing the viscosity of the aqueous phase, which increases the sweep efficiency and as a consequence, the oil recovery. There have been a number of laboratory experiments done by the use of polymers. Some of them used the polymer solution with foam, and some used it with water. It was also evaluated how to control mobility by using polymer solutions in some studies.

In 1967, a study was carried out by W.B. Gogarty in order to evaluate mobility control with polymer solutions. Mobility control was investigated by considering both permeability and rheological effects. A high molecular weight polymer was used in Berea cores having zero oil saturation. This experiment reached the results which are the decrease in permeabilities and stabilization with polymer flow. They reported that the flow of polymer solutions in cores reduces the permeability, the decrease continuing with the volume of fluid injected until stabilization takes place. The polymer solutions that they used in this experimental work are considered effective in reducing mobility below that obtained with water and the reduction takes place by both increased viscosity and decreased permeability. It was concluded that the measured effective viscosities showed that rheological properties play an important role in mobility control with polymer solutions. (17)

Frank W. Smith evaluated the behavior of partially Hydrolyzed Polycrylamide solutions in 1969. He used 3 kinds of polymers. One of them is called Polymer H, has the highest molecular weight, the others, polymer M and L, have the medium and lowest molecular weights, respectively. His results of laboratory tests showed that the extent of polymer adsorption from solution may be quite high if the solution is very saline or is in contact with carbonate rock. The experiments also suggest that solution salinity, rock pore size, flow rate and polymer molecular weight greatly influence the reduction of mobility and permeability by polymer solution. It was concluded that polymer adsorption increases with salt concentration. And Polymer effectiveness in reducing mobility is greatest at the low salinity and with the polymers having the highest

molecular weight. He used Berea sandstone for the experiments and concluded that in Berea sandstone there is an approximate correlation between permeability and polymer effectiveness in reducing permeability and mobility at low rates. He reported that the correlation seemed to be independent of wettability and the residual oil. [4]

A similar experiment was also done by R.R.Jennings, J.H.Rogers from The Dow Chemical Co in 1971. They evaluated the factors influencing the mobility control by polymer solutions. They used various polymer solutions of high molecular weight which are non-Newtonian and pseudo plastic in viscosity behavior. It was reported that different polymers produced decrease mobility in porous media by different mechanisms, which involve polymer-matrix interactions and solution rheology. It was also concluded that the mobility decrease did not correlate with adsorption of the polymers. [3]

Another economical analysis is conducted by R.L.Jewett, G.F.Schurz from The Dow Chemical Co. Their analysis includes some successful and unsuccessful polymer flood applications where they report the reasons of the unsuccessful floods. Some of the reasons reported are high oil viscosity, small polymer slug, injectivity problems. They also presented basic conditions and test results for a large number of polymer flood projects. As a conclusion of the test results, it was reported that polymer flood has been found to be successful over broad ranges of reservoir conditions and fluid characteristics. However they had difficulties in designing a polymer flood program as well as in calculations of many required variables which they handled with a computer. [18]

Another Polymer laboratory experiment was also reported by Sinclair oil& gas Co in 1966 by N. Mungan, F. W. Smith, J.L. Thompson. They carried out some laboratory experiments with polyacrylamides and polyethelyene oxides. They studied the flow behavior of the polymer solutions by three flow tests in cores. First water was injected and filtered polymer was flowed through the core. Eventually they saturated the core with water to evaluate the recover of mobility. It was concluded that the reduction of water mobility by polymers is due in part to increase in solution viscosity and in part to core permeability reduction. The factors which affect the mobility of polymer were evaluated such as polymer concentration, type and molecular weight as well as water salinity, pH, capillary properties of the porous rock and type of crude oil. They also carried out displacement tests where they used refined and crude oils. As the conclusion, they compared the crude oil recoveries and concluded that a considerable benefit of the polymer flooding is noted. [19]

2.5. Water flood – Previous Experimental Studies

Waterflood is one of the oldest oil recovery methods and is defined as a method of secondary recovery in which water is injected into the reservoir formation to displace residual oil. The water from injection wells physically sweeps the displaced oil to adjacent production wells. Potential problems associated with waterflood techniques include inefficient recovery due to variable permeability, or similar conditions affecting fluid transport within the reservoir, and early water breakthrough that may cause production and surface processing problems [(1)]. The typical case in a waterflood is viscous fingering which consequently leads to an unstable displacement. There has been a great deal of experimental studies and field applications conducted for waterflood.

An experimental study is carried out by Sarah Inwood and Anthony Kovscek at Stanford University in 2007. It was a waterflood process of so called Lost Hills medium crude oil without connate water. A 2-dimensional micromodel - which was used in this project for the displacement processes - is utilized for the experiment. The objective of the project was to observe the flow regime at pore network scale as well as at the pore scale. They also evaluated the parameters which influence the instabilities that were caused by waterflood. The micromodel was first oil saturated completely. The pore spaces are observed through the microscope to make sure that the oil saturation is 1. Following step was to inject water to observe the flow regime. The figure 9 shows six images of pore network scale of waterflood. The fingers can be clearly seen which results in unstable displacement.

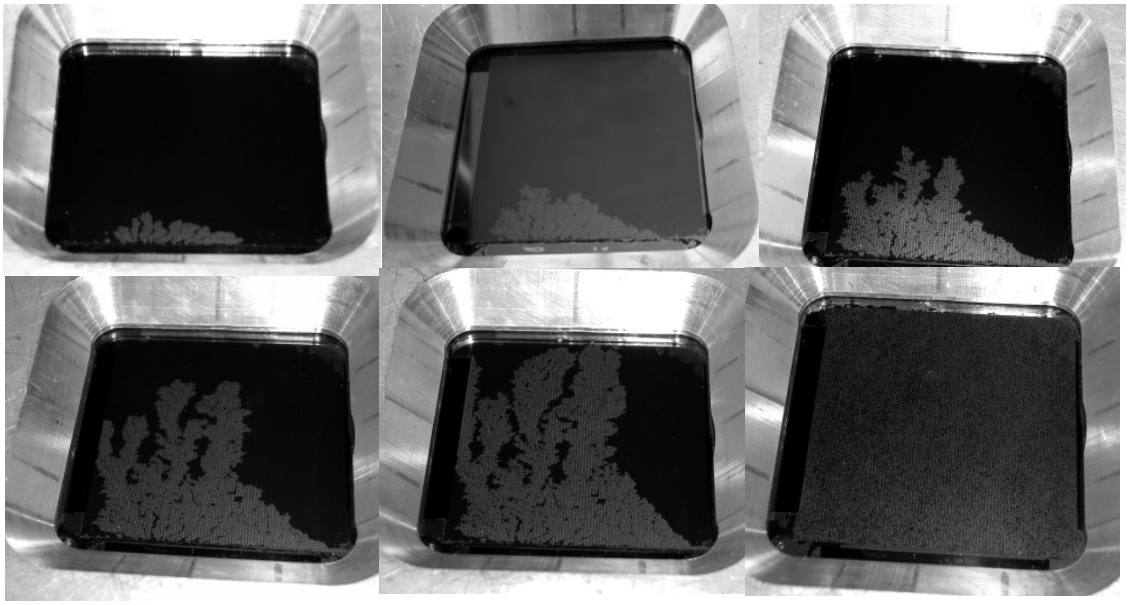

Figure 9: Waterflood of medium crude oil [10]

The conclusion of this laboratory work was that the displacement was unstable at meso scale (pore network scale), and viscous fingering on multiple scales are observed. [10]

2.6. Micromodels - Early Work

Micromodels have been used for many years to understand flow mechanisms taking place in rock cores, at the pore scale. More than 50 papers describe micromodel studies, and particular attention has been given to the investigation of enhanced oil recovery (EOR) process; e.g. flow of foam, water-alternating-gas (WAG) displacement, heavy oil displacement mechanisms, etc. Polymers were added to evaluate its effects on conventional flow and polymer-enhanced-foams.

The use of micromodels as a tool for understanding pore level processes has existed for quite some time. Throughout this literature review, different micromodels provided substance to theories exposed by their authors. Such micromodels include simple capillary tubes (Marsden and Khan, 1996 and Sanchez and Schechter, 1986), glass beadpack which can be homogenous or heterogeneous (Sharma, 1995 and Radke and Ransohoff, 1986), etched glass (Mattax and Kyte, 1961, Davis and Jones, 1968 and Mast, 1972), etched plastic (Bonnet, 1978), and etched silicon (Owete and Brigham, 1986 and Hornbrook et al. 1992). All of these models provided valued insights, the merits of which can and have been debated. [6]

The variety of micromodels employed for studies however, suggests an underlying problem with their usage. The objective of micromodels, and any other type of model for that matter, is to replicate the features of the medium it represents. Reservoirs are three dimensional and heterogeneous by rule. As Sarathi (1986) points out, micromodels in general suffer from several distinct limitations. They are a difficulty in obtaining a specific etch depth necessary for the sake of heterogeneity: the unintentional introduction of microscopic heterogeneities into the model through the etching processes themselves: the fact that two dimensional micromodels required for visualization cannot ever demonstrate the continuity with multiple phases that three dimensional models permit: that Peclet numbers defined as the ratio of convective to dispersive transport, are altered due to pores in micromodels generally being larger than true reservoir pores: and finally, differing pore structures from reservoirs due to an inability to capture rock characteristics such as heterogeneity, pore geometry and wettability. Their usage, Sarathi reasoned, should always be done with these limitations in mind. [6]

Owete and Brigham (1986) and Hornbrook et al. (1992) employed the use of silicon micromodels to study foam propagation. Due to a novel fabrication technique, these models were able to rule out all of the concerns of Sarathi (1986) except for the loss of three-dimensional continuity. [6] Micromodel construction will be described in Chapter 3.

CHAPTER 3

3. EXPERIMENTAL APPARATUS

3.1. THE SILICON MICROMODEL

A micromodel consists of a 2D etched network of the model porous medium on one plate of glass, resin or silicon covered with another transparent (usually glass) plate. Visualization through a microscope or using a video camera provides the micro-scale resolution required to see pore-scale processes. When multiphase systems are being studied the various fluids are frequently dyed in different colors in order to distinguish them. The micromodel etch patterns were initially simple geometries such as connected capillary channels, manufactured by moulding techniques using transparent polyester resin or glass and a photographically etched mould. These models allowed a reasonably good resolution with capillary diameters of the order of 100s of μm. Several disadvantages are inherent in these early procedures such as the pore size being too large, variation of the etch depth, surface roughness, enlargement of the pores, narrowness of the pore size distribution. Many of these problems were solved by the Stanford university group (Owete and Brigham, 1986: Hornbook et al., 1991, 1992) using a very novel technique adapted from the computer chip industry involving etching a silicon wafer. It should be noted that, however, that even this objection was considered in Hornbook's design, as three dimensional connectivity characteristics were "sculpted" into the micromodel by computer. This model is composed of silicon, and its pattern replicates that of Berea Sandstone. A detailed description of the fabrication of the model can be found in Hornbook et al. (1992). This section contains the summary of micromodel construction, description of its pore structure, and fluid flow analysis. [6]

3.1.1. Micromodel Construction

The micromodel employed is made of silicon. A detailed heterogeneous network is etched onto the silicon wafer. In order to get to the point of etching, and to complete micromodel construction, the following steps are required;

Micromodel fabrication follows seven steps. They are respectively:

1- Coat
2- Expose
3- Develop
4- Deep Etch

5- Drill four holes
6- Clean
7- Anadonic bond to pyrex wafer

The manufacturing process is shown schematically in Figure below. First, the digitized Berea sandstone image is engraved on a glass-chrome mask; this step is not depicted. Next, silicon wafers are uniformly coated with photoresist, a photosensitive chemical that is then exposed to the pattern from the mask by a photolithographic process. The silicon wafers are developed in a chemical solution to remove the unexposed photoresist. Then, using a deep reactive ion etching method, the exposed silicon wafers are etched to the desired depth of 25 μm. Holes are drilled through each corner of the etched pattern and the wafers are cleaned in sulfuric acid/ hydrogen peroxide piranha solution (9:1 H_2SO_4:H_2O_2).

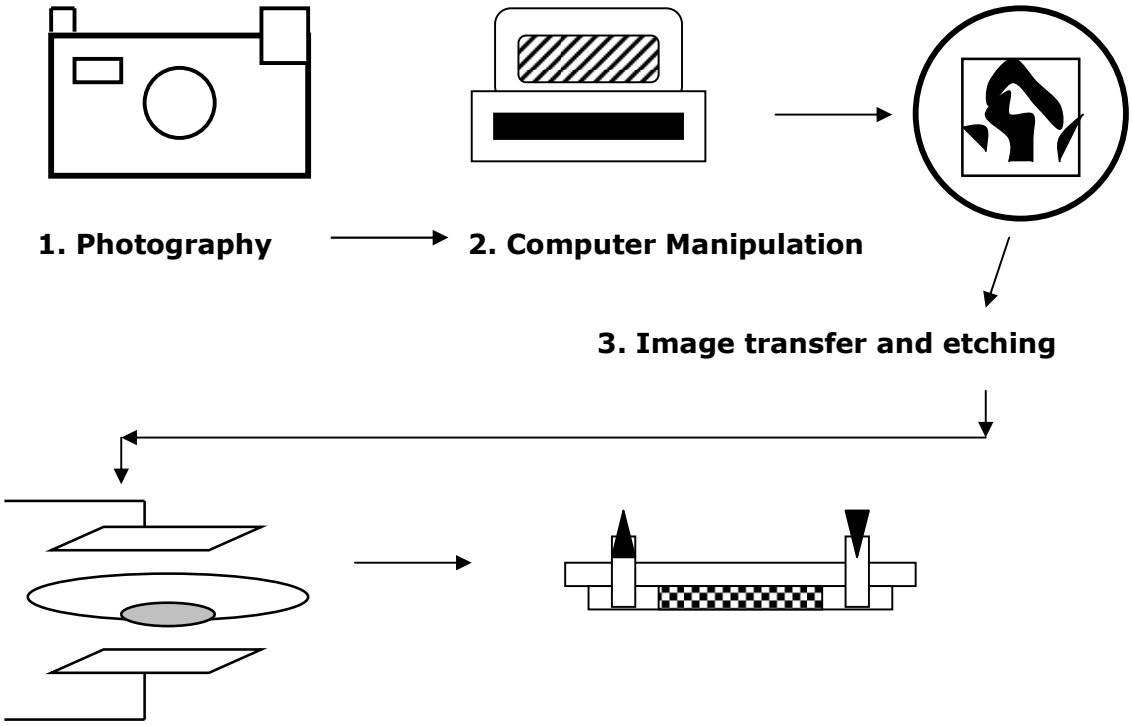

Figure 10: Step-by-Step model construction [6]

To seal the etched pore pattern, each silicon wafer is anodically bonded to a 500 μm thick glass Pyrex wafer. The micromodel is then mounted in an aluminum holder to enable connection to an injection pump. [19]

❖ The imaging process

Imaging of the model onto the silicon wafer involves the digitization of a rock section into a computer from a high quality photograph. The section, which is approximately 500 µm across, is replicated many times to fill an area 5 cm squared. Assurance of two- dimensional connectivity is made, and this image is reproduced as chrome on a glass. The grains are now opaque and the pores are transparent. A coating of photoresist is placed on a silicon wafer. As ultraviolet light kills photoresist, it is shined through the mask onto the wafer. After exposure, the flow path image exists as clean silicon for the pores and photoresist coated silicon for the grains. [20]

The pore network pattern etched onto the silicon wafer possesses geometrical and topological proportions similar to Berea sandstone at a 1:1 size scaling, see Figure below.

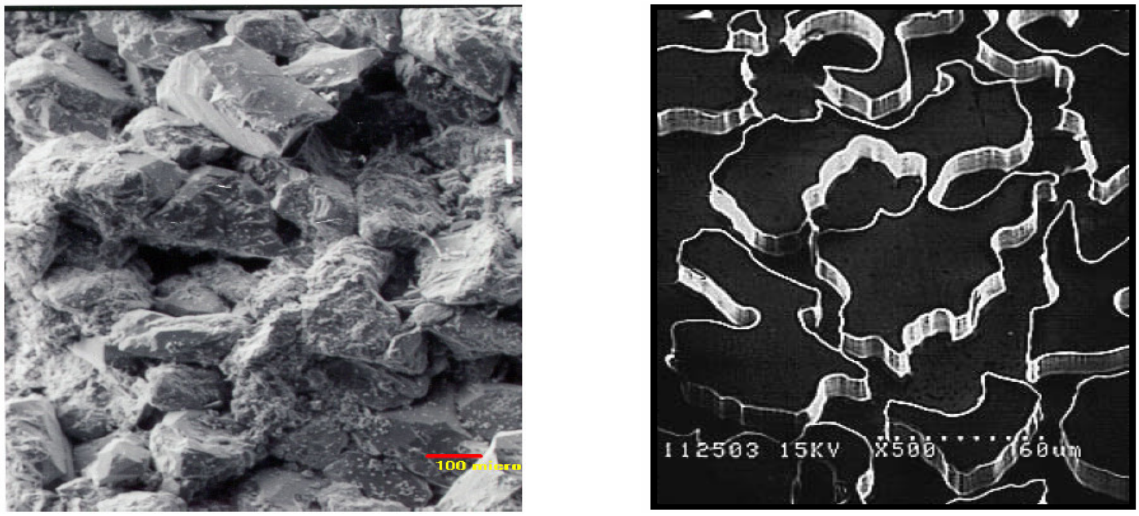

(a) (b)

Figure 11: (a) The first step: A high quality photograph of Berea sandstone [10] (b) The second step: Digital modification of the photograph [10]

❖ The etching process

The micromodels were fabricated at the Stanford Nanofabrication Facility, using a procedure depicted in the figure below.

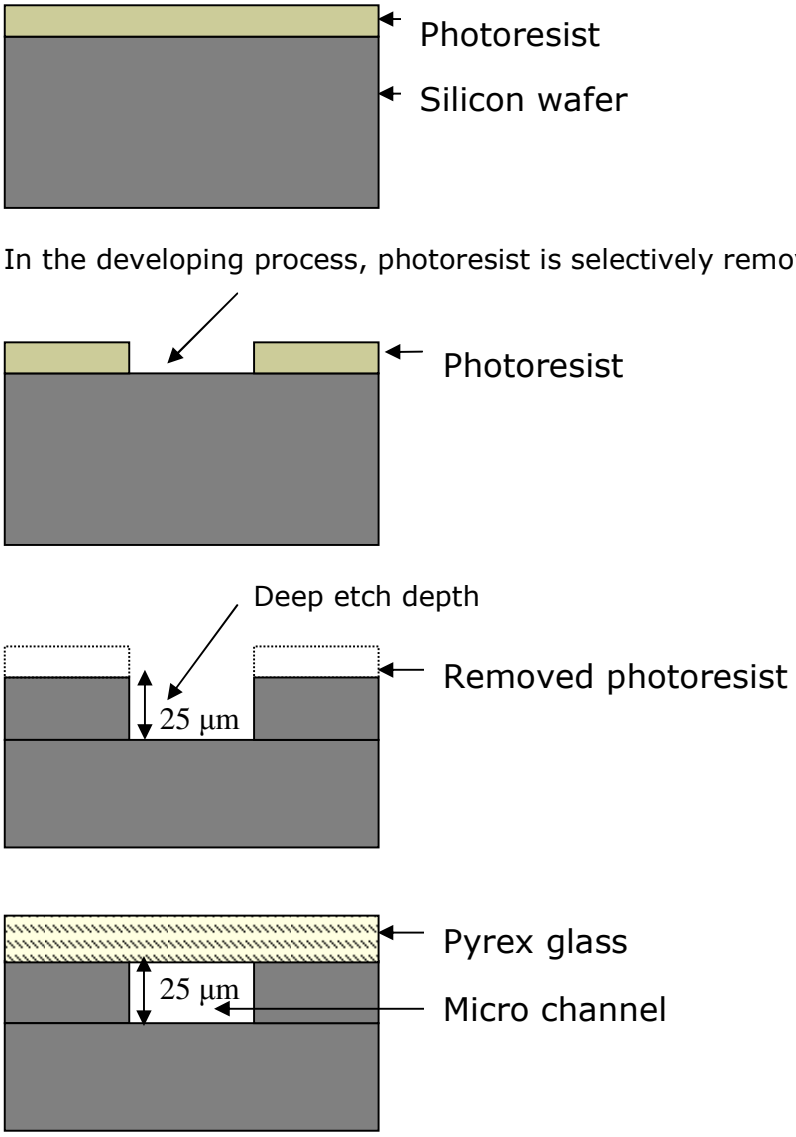

Figure 12: Manufacturing the micromodel. Note: diagrams are not drawn to scale. [20]

Using the pattern provided by the photoresist, a dry etch technique is used to create the network of pores and grains in the wafer. As the micromodel is an exact replica of Berea sandstone in two dimensions, this is not true in its third dimension – etch depth. Since exact duplication of three-dimensional flow is impossible for direct visualization purposes, a uniform etch depth is made throughout the micromodel. Owete and Brigham (1986), and Hornbook et al. (1991, 1992) both used an etch depth of 5 μm. It is, however, possible to etch to a depth of 30 μm

without the loss of detail. The micromodels used in this project were etched to 25 μm.

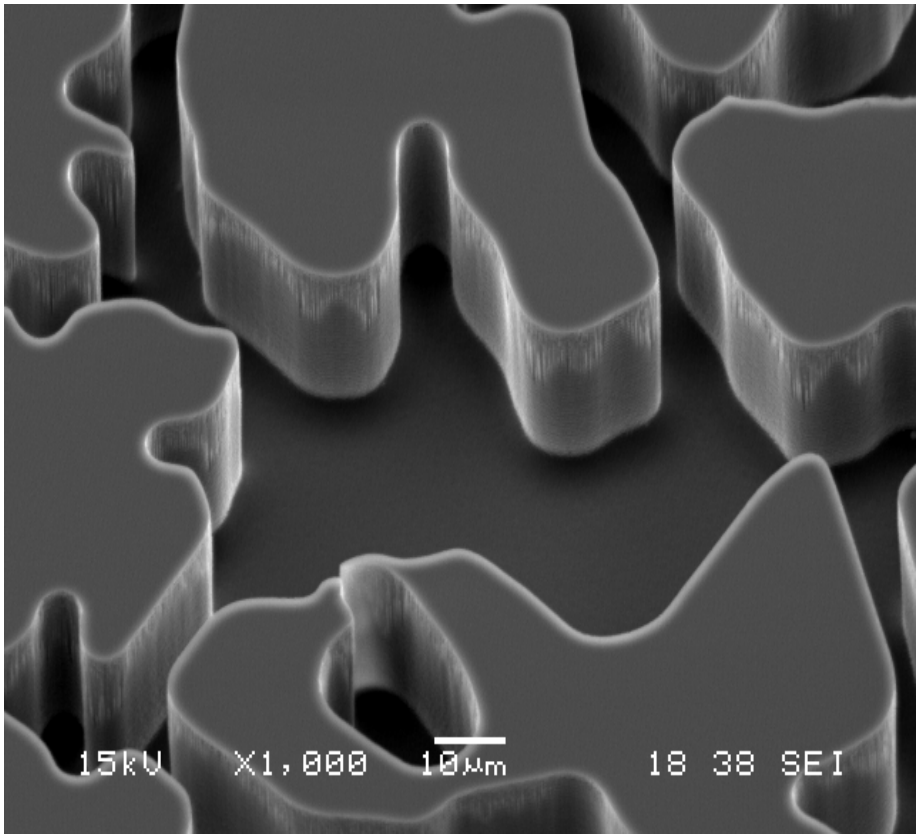

Figure 13: The depth of etch: 25 μm [10]

❖ Anodic Bonding Process

After construction of the flow model, as described above, it was necessary to isolate the individual etched flow channels. The most efficient means to isolate the flow channels was determined to be the bonding of the etched wafer to a flat piece of glass. The bonding procedure was required to form an irreversible bond between the surface of the glass and the unetched portions of the wafer. Anodic bonding was found to provide the simplest means to fulfill the stated requirements.

- A cleaned wafer is placed on a hotplate to 600 °F, with its etched side facing up. The wafer is left on the hotplate for around 45 minutes, by which a very thin SiO2 film is formed on the wafer surface and the wafer, initially non-wetting, becomes water wetting.

- Then the temperature is reduced down to 500 °F and wait for the temperature to be stabilized. Wafer surface should be cleaned from any dust that might deposit during preheating period.
- The next step is to place a clean glass wafer right on the top of the wafer, and align as desired. The wafers are heated for at least 1 minute.
- The voltage of the power supply should be preset between 900 and 1200 volts. But first the power supply stays at the standby mode to warm up for 2 minutes. The anode of the power supply was connected to the hotplate and the other electrode (cathode) was connected to an aluminum plate wrapped by a copper mesh. The aluminum plate was placed on the top of the glass wafer gently, and then power supply was turned on to apply a high voltage.
- After 50 minutes, bonding is achieved.

The electricity should be turned off, and the new micromodel should be removed from the hotplate using tweeze to allow it to cool to room temperature.

3.1.2. Micromodel Pattern

The figure below shows the micromodel pattern. The pattern has a unit cell that repeats and it incorporates futures of a porous medium which are small and large pores, also channels with large and narrow throats. Pore grains range is from 30 – 200 μm. And the resolution is 2 μm. [10]

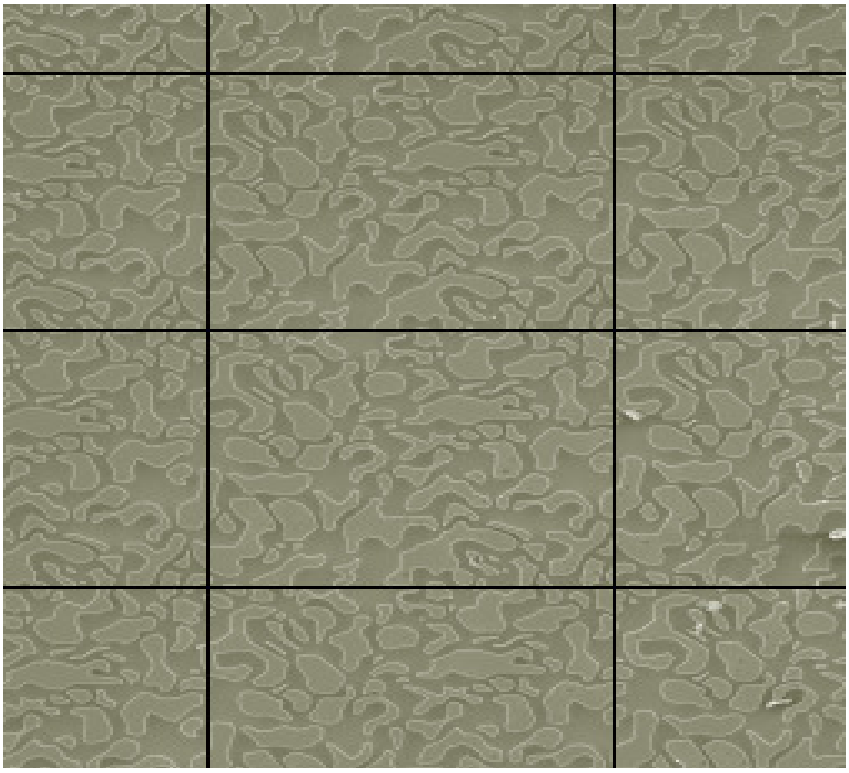

Figure 14: Micromodel pattern [10]

3.1.3. Micromodel Pore Structure

A silicon micromodel is used for this experiment. The dimensions of the micromodel are 5 cm by 5 cm with a channel depth of 25 μm. This depth was selected to minimize the three-dimensional effects of the flow through the micromodel, in effect creating a two-dimensional flow regime. The 25 cm^2 corresponds to 600 by 600 pores, which is a sufficient number of pores to meet the scaling requirements for a representative elementary volume in two dimensions. [R. Lenormand, et al (1988)]. The apparatus is shown schematically in the figure below. [20]

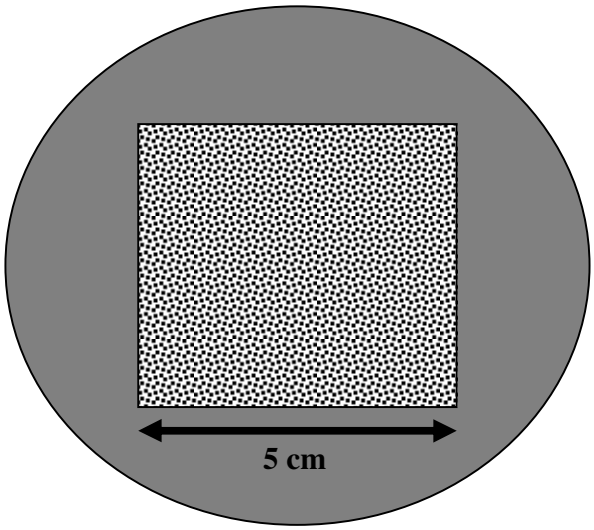

Figure 15: Depiction of top – view of a completed silicon wafer. [20]

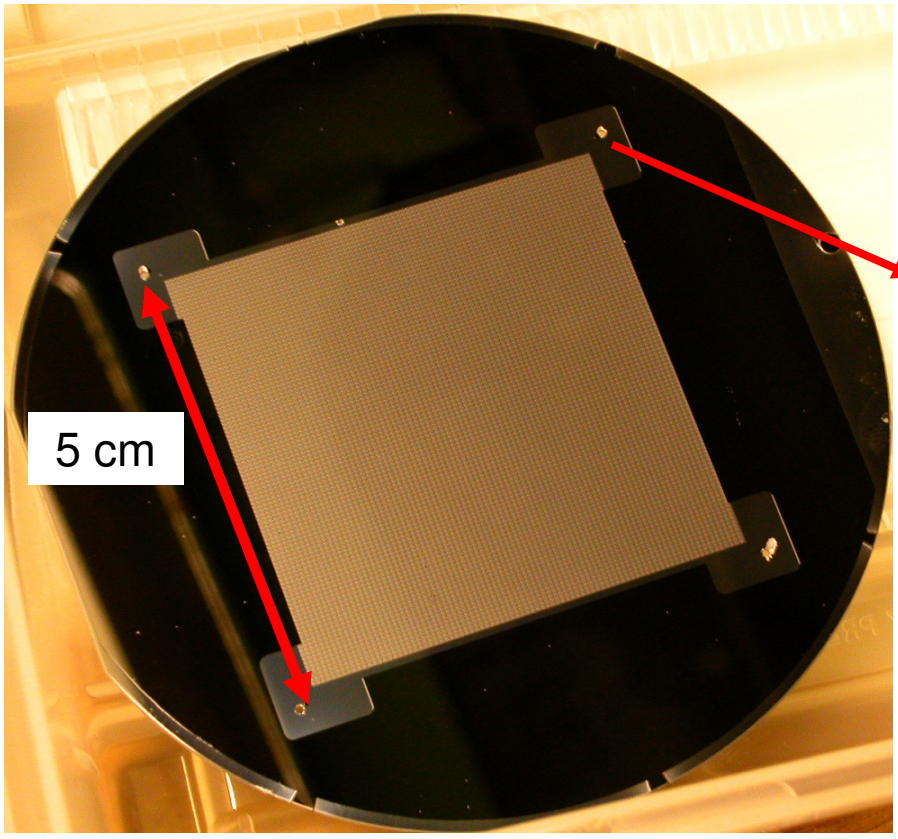

Figure 16: A finished silicon wafer [10]

3.1.4. Micro Plate

Each port of entry in the aluminum holder represents a data volume of approximately 0.9 mL; this volume must be filled before the injected phase can enter the micromodel pore space. The data volume is almost 15 times larger than the micromodel's total volume of 0.0625 mL, and about 65 times larger than the micromodel's pore volume of 0.01375 mL. This disparity in scale renders calculations that pertain to time and injected volume profoundly inaccurate and practically meaningless. As a result, it is not always possible to compare the findings in the micromodel experiments to findings from core experiments, data from field production or predictions from numerical simulations. [16]

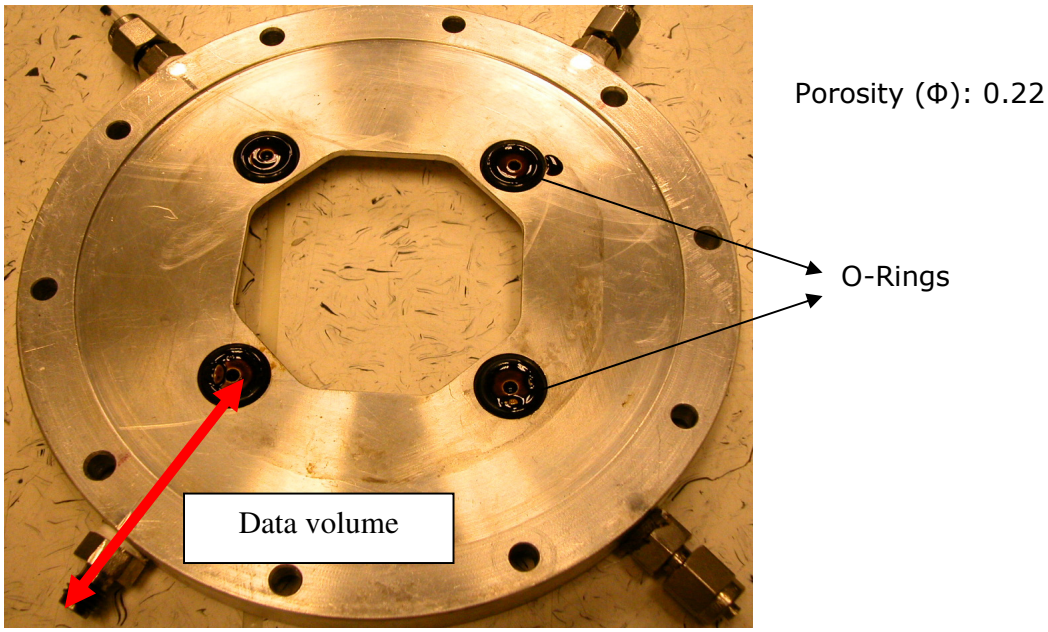

Figure 17: Aluminum holder. Note the crude oil that is pooled at each port of entry [10]

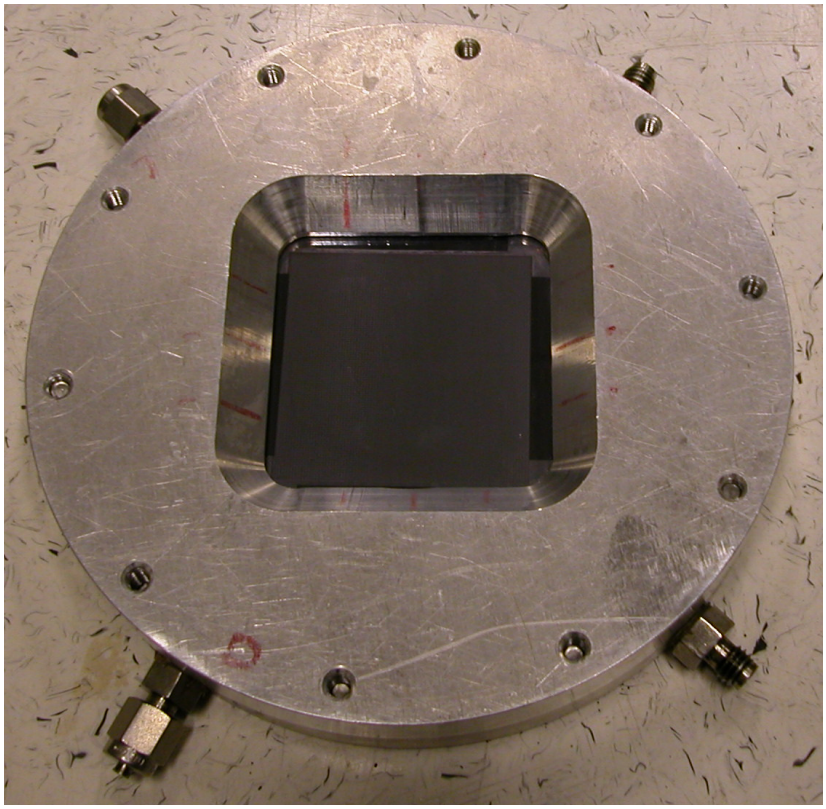

Figure 18: Mounted micromodel in an aluminum holder with four ports of entry. [10]

3.2. THE PREPARATION PROCEDURE OF THE SOLUTIONS

3.2.1. Brine Solution Preparation

The reagents and the apparatus used to prepare the brine solution are the following;

- 1000 mL Beaker
- A mechanical Stirrer
- A digital Scale

Figure 19: Mechanical stirrers and a digital Scale

The following chemical substances that are used in the solution:

Sodium Chloride	**(NaCl)**	**19.75 grams**
Potassium Chloride	**(KCl)**	**0.19 grams**
Calcium Chloride 2-Hydrate	**($CaCl_2.2H_2O$)**	**0.66 grams**
Magnesium Chloride 6-Hydrate	**($MgCl_2.6H_2O$)**	**0.59 grams**
Sodium Sulfate 10-Hydrate	**($Na_2SO_4.10H_2O$)**	**0.05 grams**
Sodium Bicarbonate	**($NaHCO_3$)**	**0.92 grams**

Table 1: The chemical content of brine solution

First, a water flask which was filled with 1000 mL water is put on the mechanical stirrer and stirring was started. While stirring, the chemical substances are scaled for the given amount and put into the beaker one by one. After stirring the solution for half an hour, the beaker is removed from the stirrer and the injection cylinder is filled up with the brine solution in order to get the silicon wafer brine saturated.

3.2.2. Polymer Solution Preparation

The reagents and the apparatus for the polymer solution preparation are the following;

- Mechanical stirrer with a variable speed electric motor fitted with a stainless steel shaft equipped at the end with approximately 3 cm. radius long blades, propeller type
- 400 mL Beaker
- Balance with an accuracy of 0.001 g
- Deionised water or field test brine

All polymer solutions were prepared carefully to avoid the mechanical degradation of the polymer molecules. For all the flow experiments, the same instruction is followed. The instruction is described below.

- The active content of the polymer sample is called "x".
- Place (200-1/x) g of freshly prepared brine or deionised water into a 400 mL beaker.
- Weight out accurately 1.0/x g of polymer.
- Set the stirrer at a rate high enough to create a strong vortex and add slowly the polymer by sprinkling into the wall of the vortex.
- After 1 minute stirring, reduce the rate allowing sufficient stirring condition.
- Stir 2 hours (until the polymer is completely dissolved)

The active content of the polymer sample was 83.879 g. According to the instructions, (200-1 / 83.879) g of freshly prepared field brine is placed into the beaker or as another option; the same amount of deionised water can be also put. But in this work, only brine is used for the polymer solutions. 1.0 / 89.879 g of polymer is weighted out accurately. The stirring took about 2,5 hours.

Figure 20: The powder Polymer before preparing its solution

3.3. FLUID INJECTION SYSTEM

In order to evaluate the pore level interactions occurring in the micro model, it was necessary to use both visual and indirect means to gather supporting data. In order to get fluids into the micro model, two distinct injection systems were utilized. In this study, two syringe pumps are used in order to carry out two experiments at the same time.

1. A syringe pump for liquids (water, brine, oil, polymer)
2. High pressure tanks for gas (CO_2)

3.3.1. Syringe Pump:

The syringe pump was a Teledyne Isco Model 100 DM. The capacity of the pump is 103 mL.

The limits of the pump were set as;

- The minimum flow rate: 0.00010 mL/min
- The maximum flow rate: 25.00000 mL/min
- The minimum pressure: 10 psi
- The maximum pressure: 52 psi

Before starting the experiment and mounting the micromodel to the pump, the flow is started to make sure the flow of fliud into the micromodel. The water flow is continued until the fluid which is going to be injected to the micromodel, came out a bit from the plastic tubings. This way, it was avoided that any gas bubbles or other fluid to enter into the micromodel. It is also avoided to apply more than 55 psi pressure to protect the pyrex glass which was bounded to the silicon wafer in the construction step.

Figure 21: Syringe pump

3.3.2. Cylinders:

In order to provide a fluid connection between the injection pump and the micromodel, metal tubes are used with plastic tubings connected to them. Plastic tubings are chosen transparent to observe the fluid flow between the cylinders. The volume of the cylinders is 180 cc. There was a gauge connected to every cylinder to control the fluid flow.

Figure 22: Injection cylinders

3.3.3. Microscope

A Nikon Eclipse ME 600L model microscope is used for this study. It has a phototube which allows for video imaging. There are three objective lenses attached which allows the different magnification of surveillance of the pore spaces.

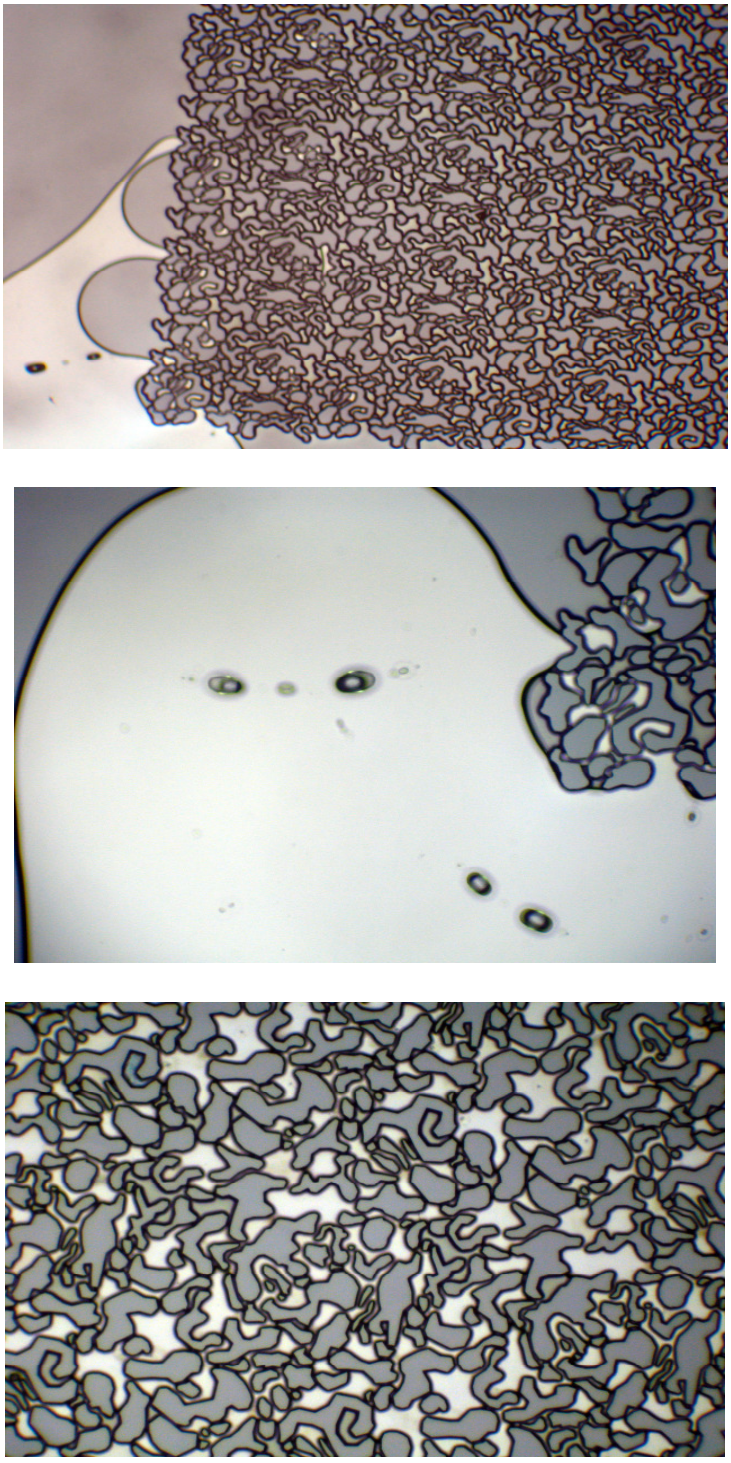

Figure 23: The images of the pore spaces photographed though the microscope.

The figures above show the pore spaces at different magnifications. Different magnifications allow a good observation of the pore spaces. Sometimes, during the anodic bonding of the pyrex glass to the silicon wafer, pore spaces could get dirty if it is not done carefully. In order to avoid this problem, the micromodel should be controlled through the microscope very carefully before every experiment to make sure that the pore spaces are clean.

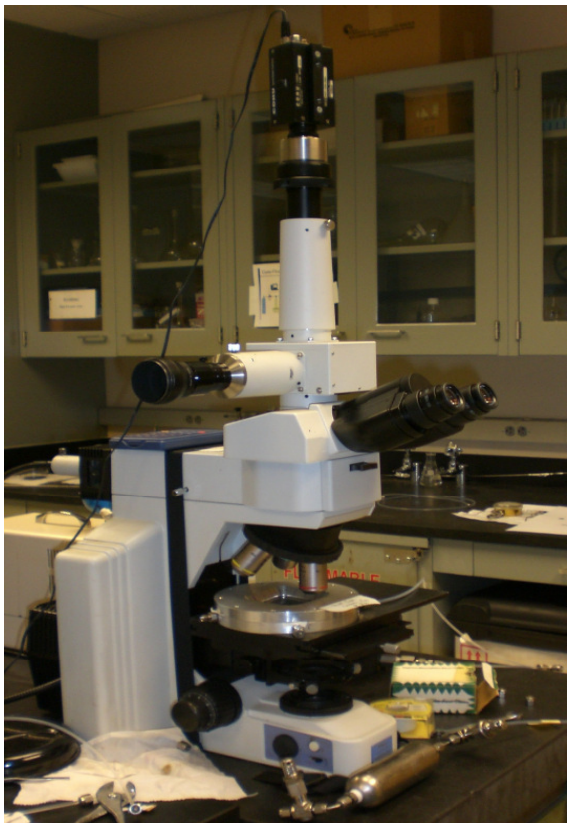

Figure 24: Microscope

3.3.4. Viscometer:

A Brookfield Dial reading Viscometer is used for the viscometer measurements of the fluids. The viscometer was calibrated by using oil samples whose viscosity was already determined before. This step is repeated before every measurement. The viscosity of the oil samples were already determined before. The minimum amount of fluid is 0.1 mL which should be put in the viscometer.

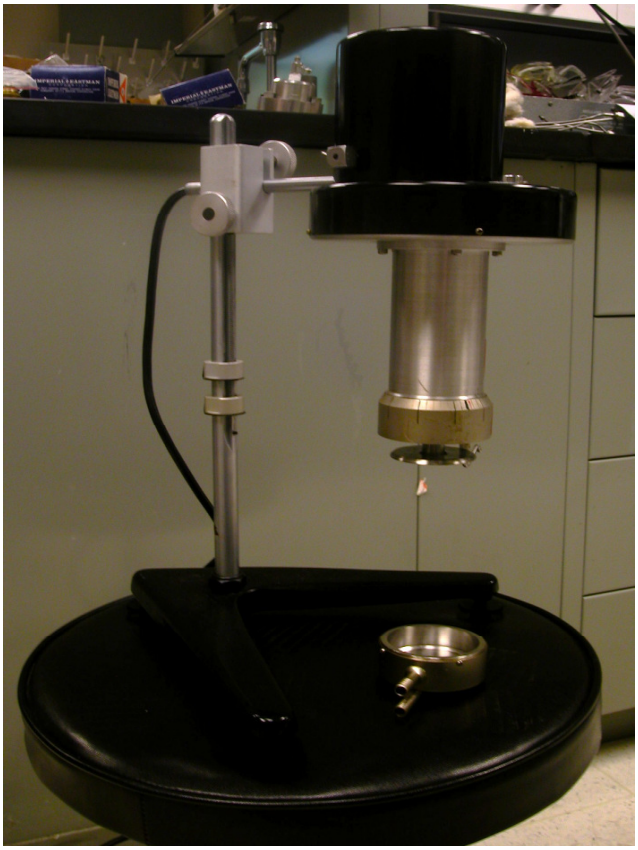

Figure 25: Viscometer

3.3.5. Digital Camera

A Nikon Coolpix 5000 model digital camera is used for this work to take the images through the microscope for the pore scale to make sure that the pores was filled completely saturated with the injected fluid and to observe whether there is any emulsion or pore blocking by polymers. The micromodel was also photographed directly at meso scale to observe the front movement of the displacement processes, inlet and the outlet fractures. The entry of the fluid into the micromodel was also captured by the camera.

3.4. THE INJECTION PROCESS

The injection process is basically carried out by using a syringe pump, metal tubes, a micromodel and a microscope. The figure below shows an empty silicon wafer at pore scale. This image is taken before any fluid entered into the micromodel. This is typically how the micromodel looks

like after anodic-bonding of the pyrex glass to the silicon wafer which is the last step of the construction process.

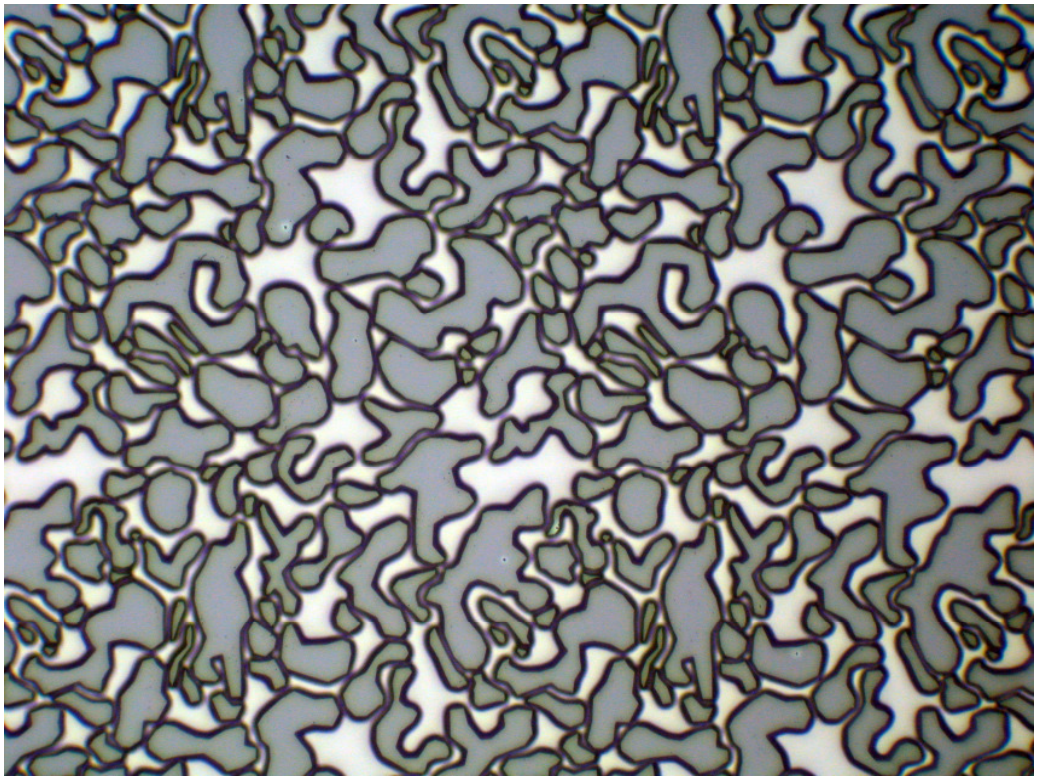

Figure 26: An empty silicon-wafer at pore scale

3.4.1. CO_2 Injection

After the construction process is completed, the CO_2 injection is initiated. CO_2 injection is carried out for every experiment to remove any dirt or junk from the micromodel. So this way, the pore spaces are clean and ready for the experiment. CO_2 is injected into the micromodel by using a CO_2 tank and transparent plastic tubing. The plastic tubing provides the connection between the micromodel and the CO_2 tank. A pressure gauge is mounted to the CO_2 tank to adjust the pressure. To protect the pyrex glass which was bounded to the wafer, a pressure limit is applied. The maximum pressure was 60 psi which could be applied during CO_2 injection.

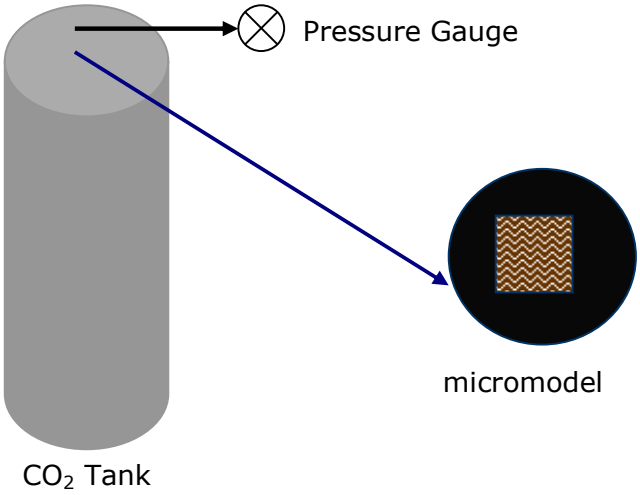

Figure 27: Schematic apparatus for CO_2 Injection

The figure above shows the apparatus schematically. The black arrow indicates the mounted pressure gauge, and the blue arrow indicates the plastic tubing which connects the micromodel to the CO_2 tank. After connection, pressure was increased up to 60 psi and micromodel outlets are checked to make sure that CO_2 was being injected through the micromodel. The injection is run about 15 minutes. Afterwards, the micromodel is being observed through the microscope to make sure that it is completely clean.

3.4.2. Oil Injection

The figure below is a schematic illustration of oil injection into the micromodel. Basically, water pushes oil and oil enters the micromodel. The observation of the pore spaces during the saturation is followed through the microscope. The blue arrows indicate the plastic tubings which were connected to provide the fluid connection. The apparatus for polymer injection is the same as oil injection process. Instead of oil cylinder, the polymer-filled cylinder is placed between the syringe pump and the micromodel. The procedure is followed the same way.

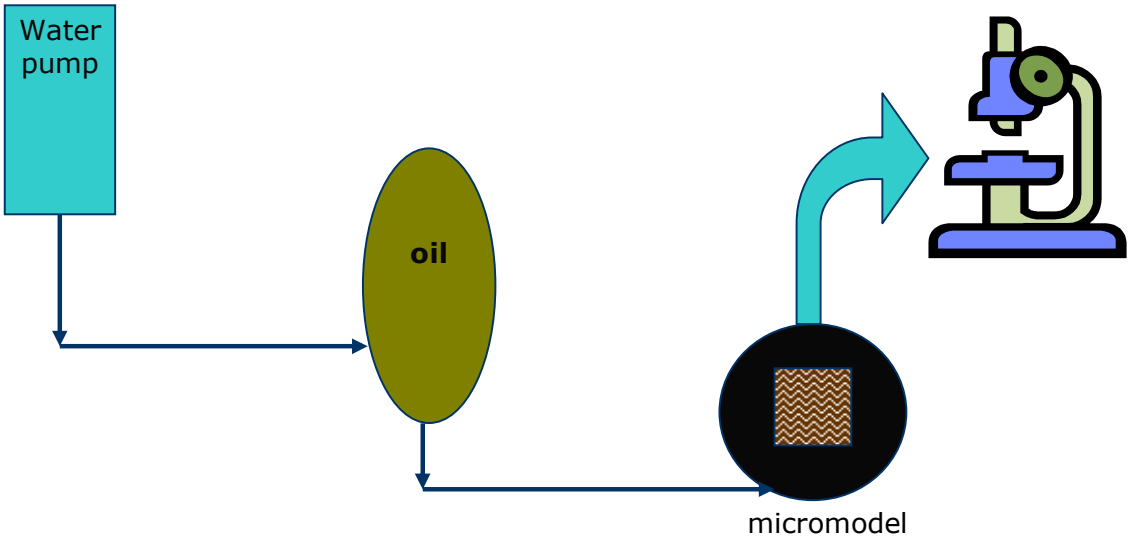

Figure 28: Schematic apparatus for oil injection

During injection process, first visual observation is made by looking at the micromodel directly at meso scale, and observing the oil saturation, but to make sure that all the pores are filled with oil, it is necessary to look through the microscope and check the pores whether there is still brine or gas bubbles between the pore spaces. Sometimes it takes days to get the micromodel completely oil saturated, and sometimes it can take just hours to make sure it is oil-saturated. This is likely due to the success at the end of the cleaning process or CO_2 injection at the very beginning of the experiment to get the dirt or the junk out of the micromodel. In order to get accurate and reliable results, in all the experiments, it was made sure that the micromodel was 100% oil saturated to observe the front movement and the displacement pattern of the polymer flood in a better way.

The image below was taken after one hour oil injection. It is clearly seen that some pores are not oil filled yet. In order to avoid this, the injection is still being run, until all the pores are completely oil filled.

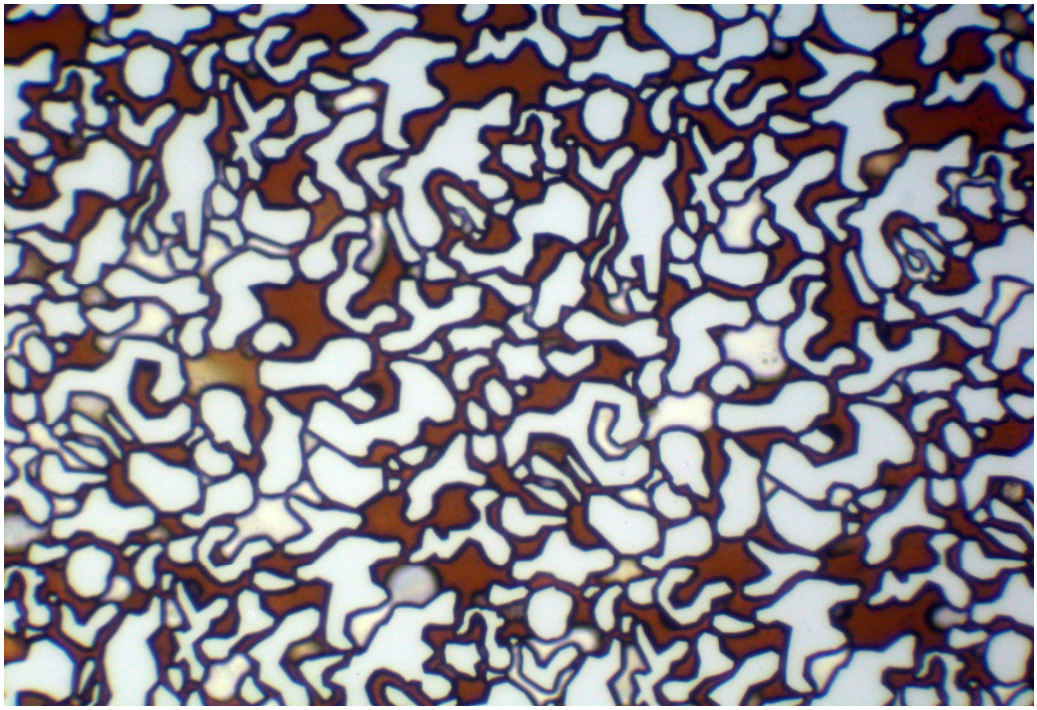

Figure 29: Partially oil-saturated silicon wafer (pore scale)

The image below depicts a hundred percent oil saturated silicon wafer. Images are taken after stopping the injection of oil into the micromodel. It is clear to see that there are not any gas bubbles or any junk in the micromodel.

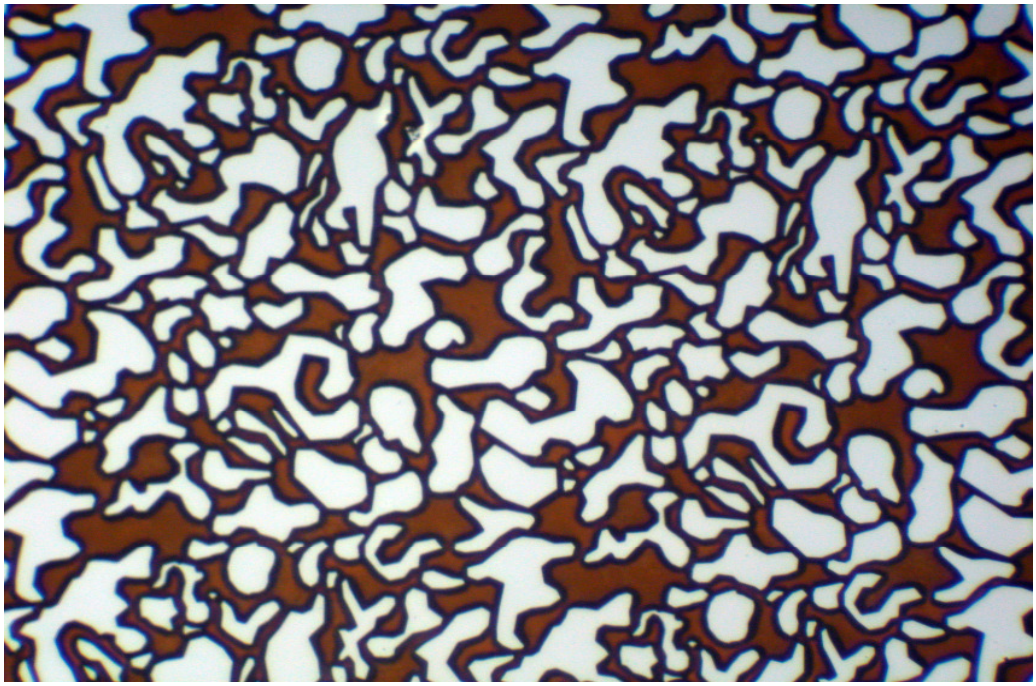

Figure 30: Fully oil – saturated wafer (pore scale)

3.4.3. Brine Injection

The figure below is a schematic illustration of brine injection into the micromodel. In this step, a tube which was filled up with decane is placed between the syringe pump and the brine tube in order to avoid corrosion problems in the syringe pump because of the Sodium Chloride content in the brine solution. Syringe pump is connected to the decane tube, and the decane tube is connected to the brine tube and brine tube is connected to the micromodel inlet in order to provide the injection. All the connections were made by using plastic tubing which are shown as blue arrows in the image below. Transparent plastic tubings were chosen in order to observe the fluid movement between the tubes. Basically, in the brine injection process, water pushes decane and decane pushes brine and brine enters the micromodel. The observation of the pore spaces during the saturation is followed through the microscope.

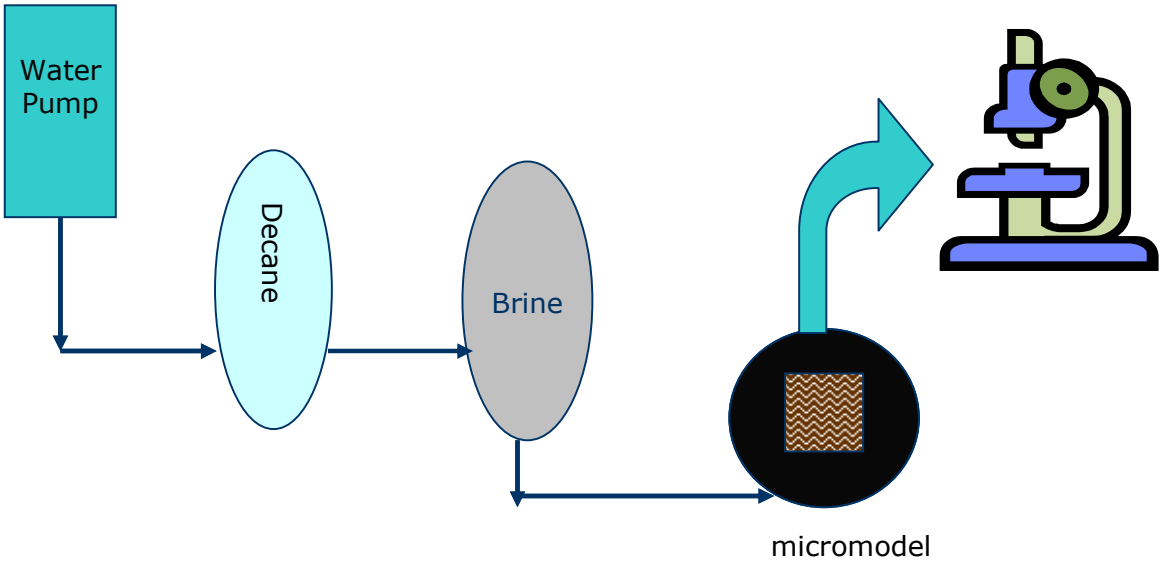

Figure 31: Schematic apparatus for brine injection

The image below depicts a hundred percent brine saturated silicon wafer. Images are taken after stopping the injection of brine into the micromodel.

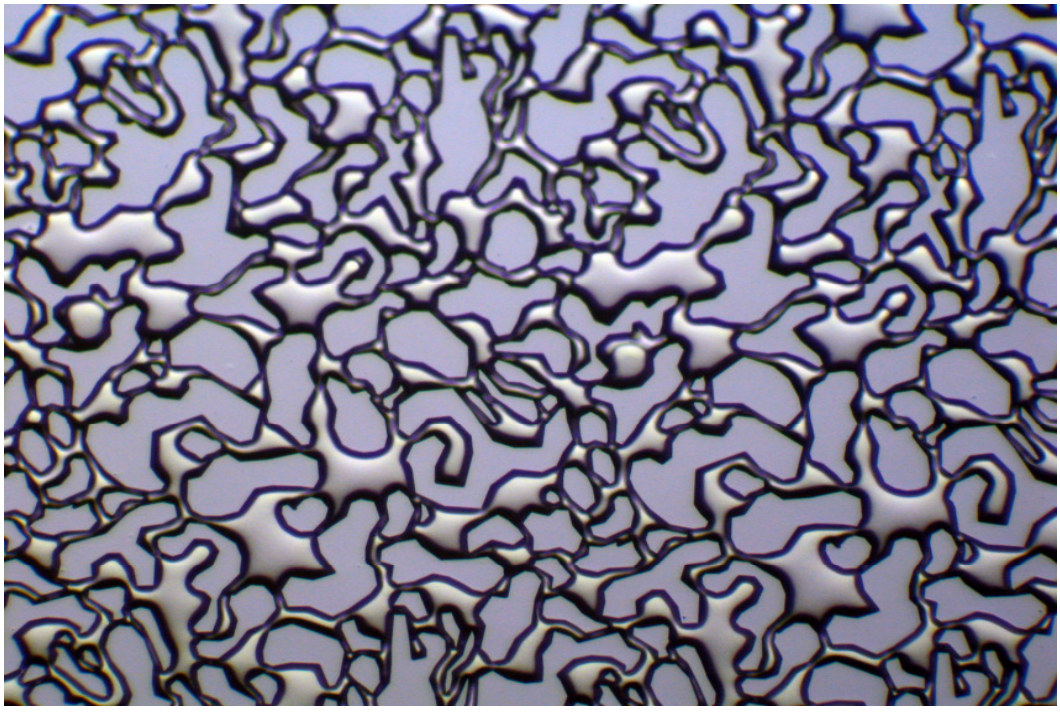

Figure 32: Brine – saturated wafer (pore scale)

3.5. THE CLEANING PROCESS

After each experiment, the aluminum holders and the silicon wafer should be cleaned carefully in order to prepare micro model for the next experiment.

3.5.1. Cleaning of the Aluminum Holders

Cleaning process of the aluminum holders is done with the Toluene via a solvent pump. After taking off the screws out of the holders, the O-rings and the spaces which were filled with the O-rings should be cleaned with the Toluene. A little amount of toluene can be poured into those spaces and vacuum it from the outlets in order to clean the entries. It should be repeated until toluene comes out of the vacuum tube. The screws should be assembled into the micromodel star-wise in order to apply the same pressure between the holders. This way, problems related to the leaking can be avoided. The same method should be used when taking the screws out of the micromodel. Applying the same pressure on the holders can avoid the problems related to the silicon wafer. Silicon wafer can be shifted during assembling; in this case, vacuum should be applied to observe if there is any flow through the holes.

3.5.2. Cleaning of the Silicon Wafer

After each experiment, all the fluid which was injected into the micromodel should be removed from the silicon wafer.

❖ Decane Flooding

Decane is used to remove the residual oil saturation (Sor) after each trial. It flushes the oil which was stuck between pore spaces during trials. In order to inject the decane, the decane cylinder should be connected to the water pump from one side and the other side of the cylinder should be connected to one of the inlets of the micromodel. This way, water pushes decane, and decane comes into the micromodel by applying the constant pressure. After decane goes through the inlet fracture, it comes out from the outlet. The outlet should be capped in order to get the decane to go towards opposite outlets. One T-cable should be connected to the opposite outlets of the micromodel in order to see if decane comes out of the tubing. If decane comes out, the micromodel can be considered clean but in order to ensure the cleanness, the pore spaces should be observed through a microscope. The figure below shows apparatus schematic for decane flooding.

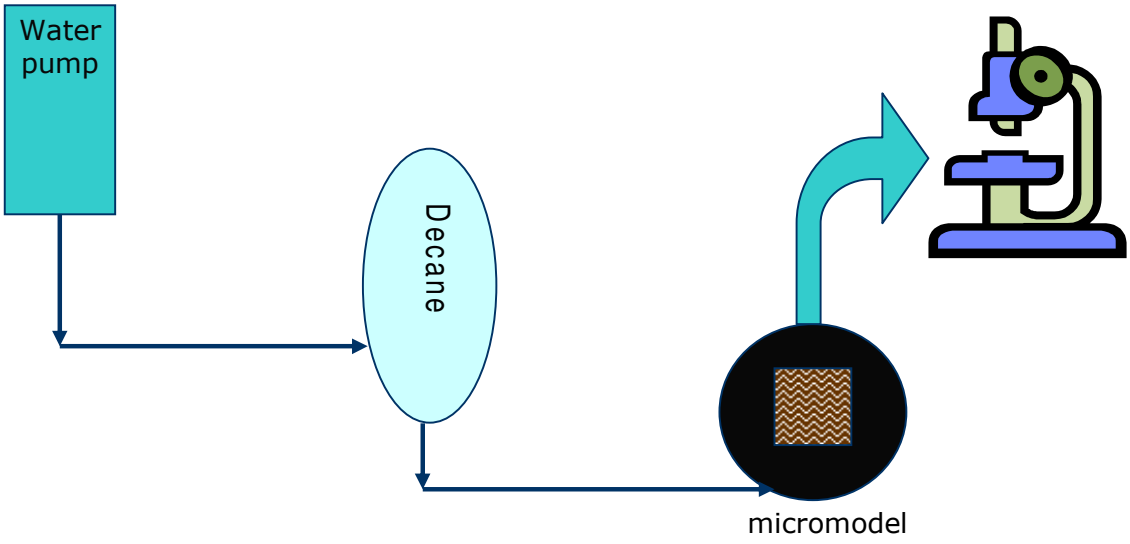

Figure 33: Schematic apparatus for decane injection

3.6. PROBLEMS AND CHALLENGES

There are some challenges and problems in cleaning processes because of the stuck oil between the pore spaces. One of the biggest problems was the cleaning process of the silicon wafers. It was avoided to continue with the same wafer for the next experiment, because it was not possible to flush all the injected fluids out of the micromodel.

3.6.1. Problems with the Cleaning Process

The figure below shows decane flood for several hours followed by three alternating cycles of toluene and CO_2. Pressure should not be over 60 psi when using CO_2 to avoid any accidents.

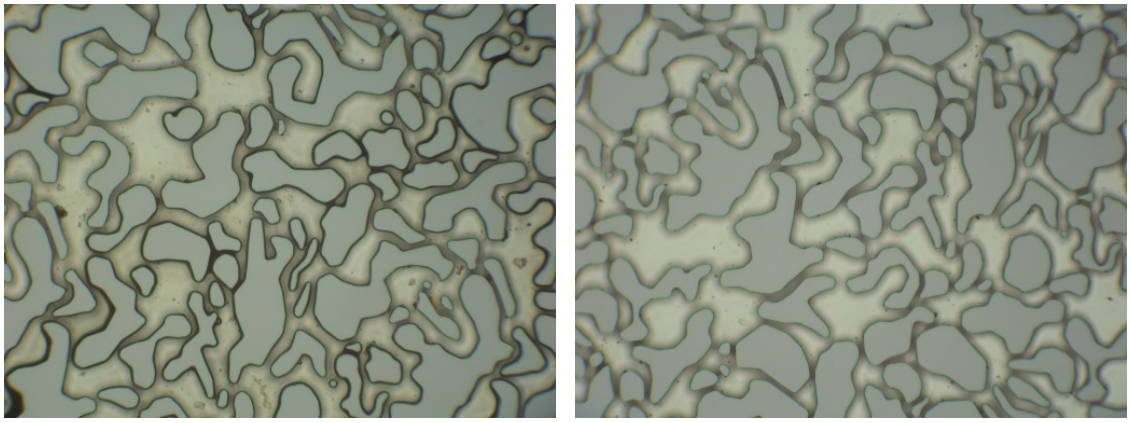

Figure 34: Decane flooded micromodel (pore scale) [10]

In the case of the early decane trials, the micromodel was cleaned with water, CO_2 and a heat lamp but this method is inadequate for flushing the heavier crude components. Even with the use of toluene, it has not been possible to flush the crude oil fully out of the micromodel. To ensure repeatability, it may be necessary to use a new micromodel for each individual trial. The figure below shows crude oil remaining in the intermediate and small-sized portions of the pore space.

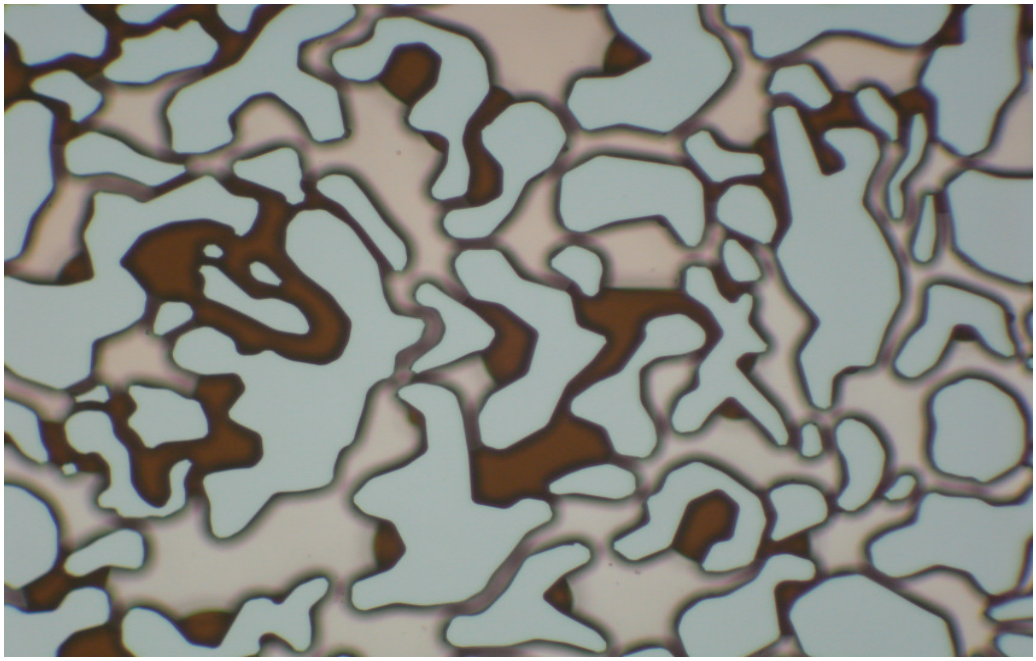

Figure 35: Residual Oil saturation at pore scale [10]

3.6.2. Uneven Pressure Distribution

The silicon wafer is covered by two aluminum holders which were assembled with screws. The screws should be tightened up very carefully to avoid any damage to the silicon wafer. A star-wise method is used when tighten the screws in order to apply the same pressure on each screw point.

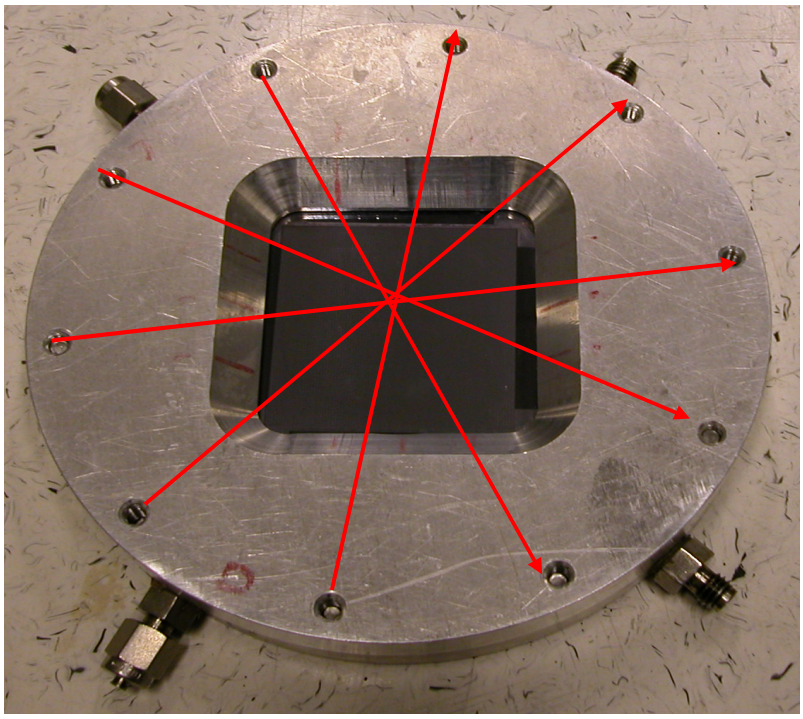

Figure 36: Star-wise method

Uneven pressure distribution can cause damage on the wafer and wafer can get broken in the middle of the experiment. Consequently, the experiment should be stopped and start all over again with a new wafer.

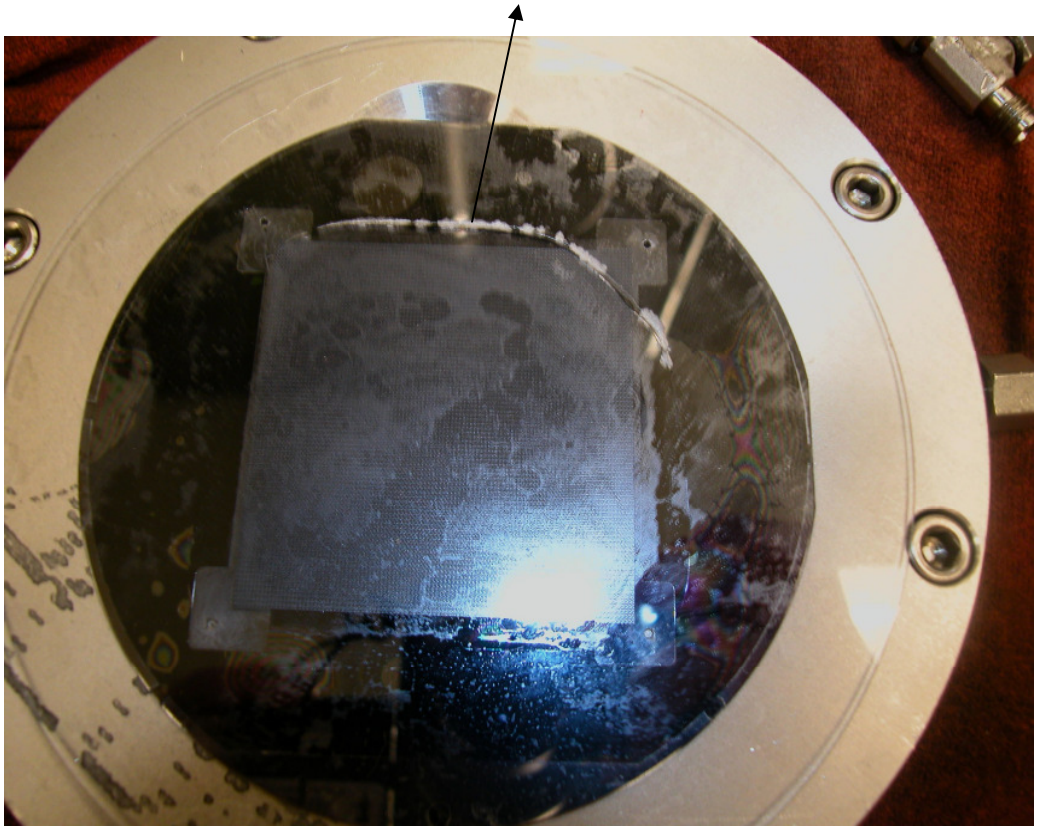

Figure 37: A broken wafer – 1

The figure below shows a broken silicon wafer during a brine injection. As the brine was being injected into the micromodel, because of applied uneven pressure on the holders, the wafer got broken and the injected fluid came out of the crack, shown in the image above.

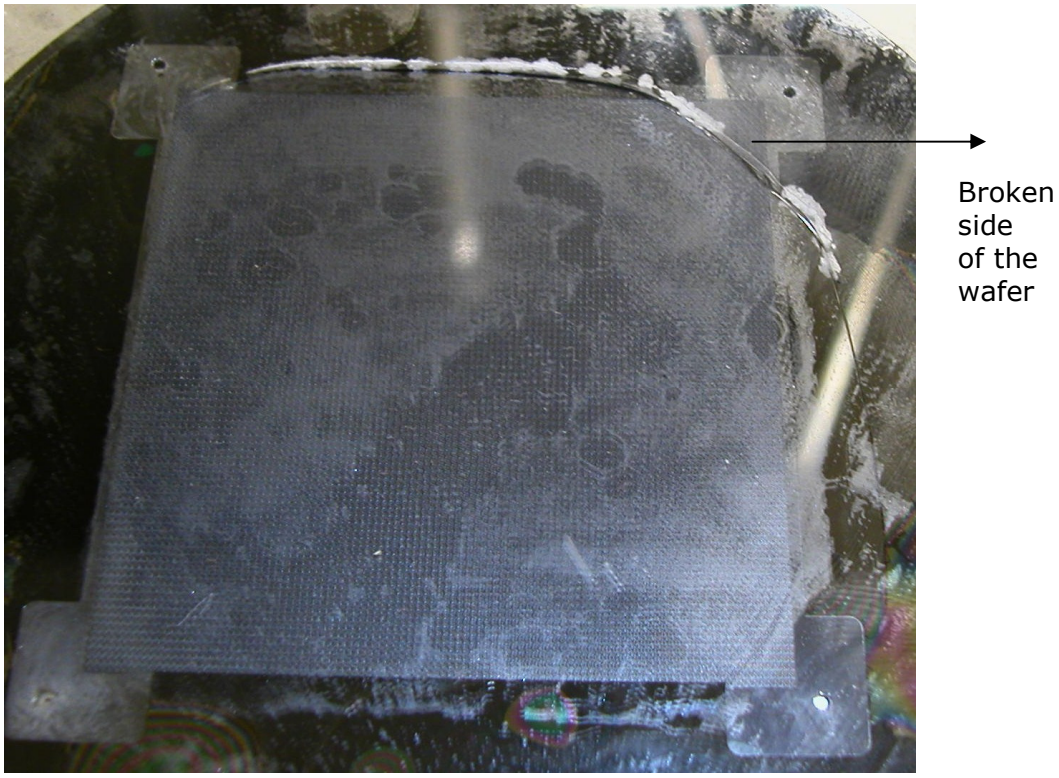

Figure 38: A broken wafer - 2

Consequently, if the wafer is broken, the experiment must be stopped and a new wafer should be placed into the micromodel. In between the aluminum holders, the entries and the outlets should be cleaned carefully in order to avoid any residual fluid from the previous experiment to enter into the micromodel for the next experiment.

A broken wafer causes time problem. The experiment for which 3 weeks was invested is being wasted if the wafer gets broken. Since it is an expensive tool, it also has an economical effect.

CHAPTER 4

4. EXPERIMENTAL WORK

4.1. IMAGE ANALYSIS

Image analysis is carried out by using Adobe Photoshop CS3 Extended software. The aim of the analysis was to find out the residual oil saturation, oil recovery and the porosity values. All the images were first gray scaled, and then the software leads us to the threshold option where the histogram percentage is obtained. This percentage gives us the ratio of the dark spaces on the image. So, basically what the software gives us is the percentage of dark spaces on an image.

In order to calculate porosity of the model, a completely brine saturated and a completely oil saturated wafer image is used. Since the software gives us the percentage of the dark spaces, an edge effect should be taken into consideration at this step. Because, even in a completely brine saturated image, because of the pores edges, software still gives us approximately 20 percent of dark spaces. In order to get more reliable values, the edge effect should be subtracted from the original percentage of the image.

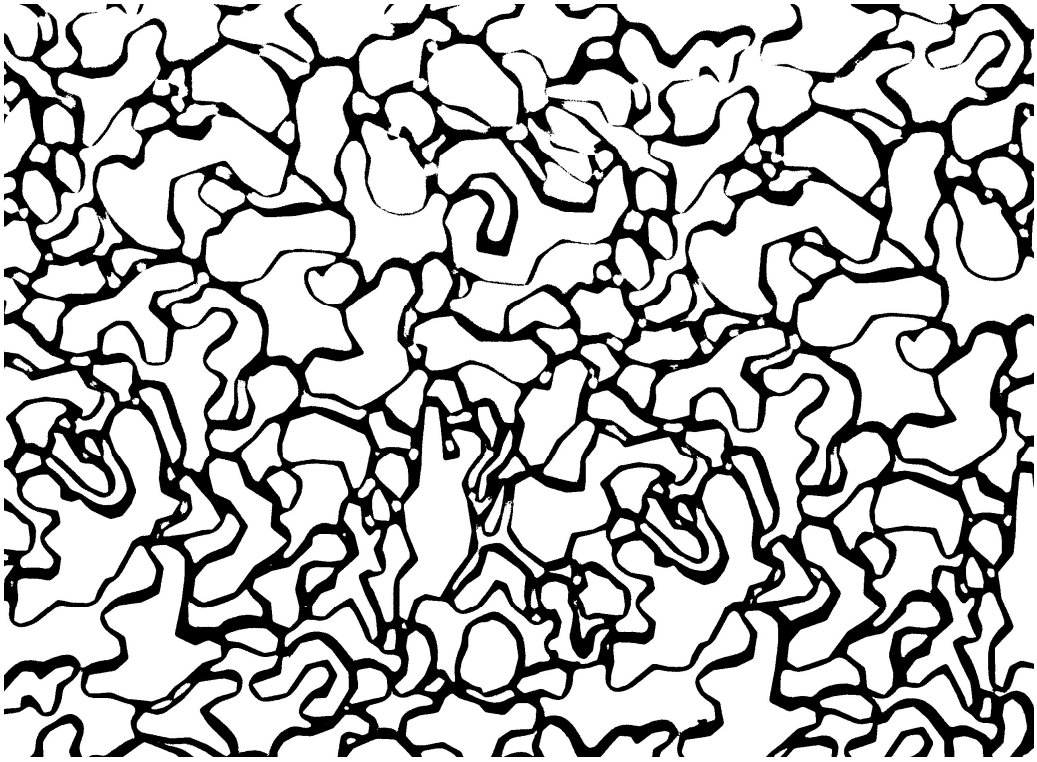

Figure 39: The edges of the grains (pore scale)

As it can be seen on the image above, the edges of the grains are black and they cause then a difficulty in obtaining the oil saturation value in an image where oil and brine / polymer are present. Even though the image above is brine saturated (no oil present), still the software gives us a percentage of black spaces. The histogram percentage that is obtained by the software gives us then the oil saturation value including the edges of the grain. In order to get a more accurate oil saturation and recovery value, the edge effect should be subtracted from the histogram percentage.

The calculated edge effect is 27.8 %. This value is calculated by using a completely brine saturated image and subtracted from every original percentage of the images.

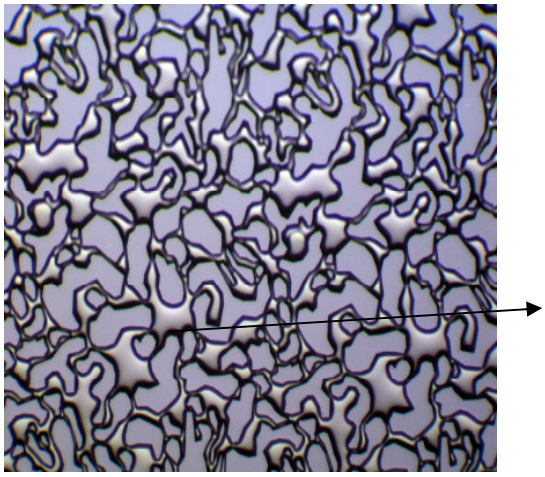

(a)

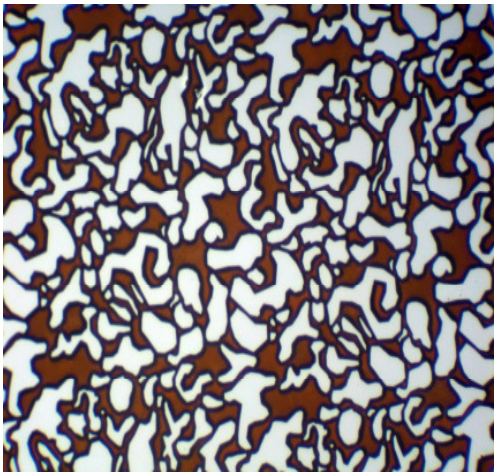

(b)

Figure 40: (a): brine saturated micromodel, (b): oil saturated micromodel (Pore scale)

The calculated porosity value of the model from the image analysis was 22.1. After calculating the edge effect and the porosity value, the residual oil saturations are calculated. In order to get the overall percentage, the micromodel, after each experiment, was gridded 4 * 4 to take 16 images of the pores. The images are taken from the middle point of each grid at pore scale (through the microscope).

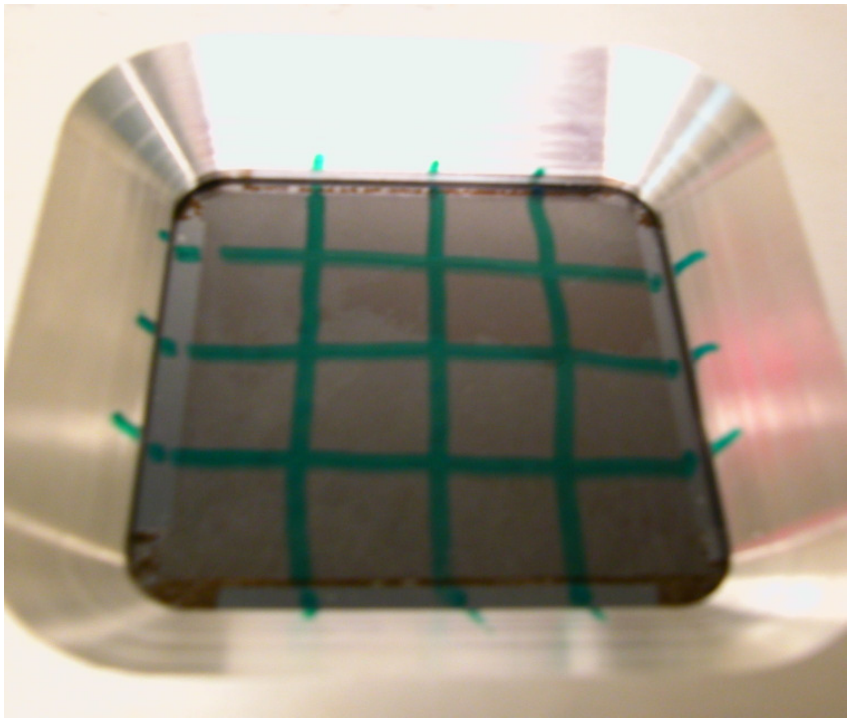

Figure 41: The gridded micromodel for the image analysis

The equation for calculating the residual oil saturation is following:

So = (Original Percentage – Edge Effect) / Porosity

At the end of the analysis, 16 values were calculated. They are summed up and divided by the overall percentage which was considered 1600 % since there was 16 images. The end value gave us the approximate residual oil saturation; consequently, the oil recovery value was calculated by subtracting the residual oil saturation from 100 %.

4.2. PERMEABILITY AND IN-SITU VISCOSITY MEASUREMENT

In every experiment, the Darcy's Law is used for the calculation of permeability and viscosity.

Darcy's Law:

$$q = \frac{k \times A \times \Delta P}{\mu \times L} \quad \text{.....(2)}$$

In the equation 2 above, q (cc/min) is the flow rate that is applied in syringe pump. A (m^2) is the cross-sectional area of the micromodel. L (m) is the length of the micromodel and μ (Pa.s) is the viscosity of the brine solution and ΔP (psi) is the stabilized pressure.

For the calculation of the permeability of the model, brine is injected into the micromodel at constant flow rate until the pressure is stabilized. The syringe pump gives the flow rate and the pressure values. Since the length and the cross sectional area of the micromodel are known, the permeability is calculated by using brine viscosity. (0.001 Pa.s)

Viscometer is used for determining the viscosity of the polymers at room temperature. For the in-situ viscosity measurements, again the Darcy's Law is used. Polymer injection is carried out at constant flow rate until the pressure is stabilized. Since the permeability of the model was obtained from the previous calculation, the viscosity of the polymer in the porous medium is calculated by using the flow rate and pressure values from the syringe pump.

The results of the calculations are shown in further sections.

4.3. FIRST EXPERIMENT

4.3.1. Oil Displacement by Associative Polymer

The aim of this experiment was to observe the displacement process of crude oil by the associative polymer which is called SuperPusher 255. It is an anionic water soluble white powder polymer. The solutions of brine and polymer are prepared according to the instructions. First, viscosity of the polymer solution is measured at room temperature (22ºC) in the viscometer which was 12 cP. And the measured viscosity of brine solution was 1.00 cP. It was measured at the same room temperature and in the same viscometer. After viscosity measurement, the injection process started.

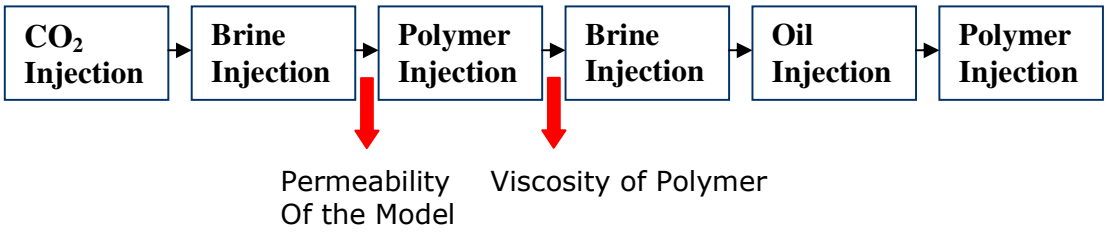

Figure 42: The Injection steps during 1. Experiment

The figure above depicts a schematic illustration of the injection steps. Black arrows indicate the end of an injection and the start point of the

next injection. The red arrows indicate the calculations that were made after the pressure was stabilized and the injection was stopped. First, CO_2 is injected into the micromodel for 15 minutes in order to clean the wafer completely to prepare it for the experiment. The second injection step was the injection of brine solution. Brine is injected into the micromodel in order to calculate the permeability of the model by using Darcy's Law.

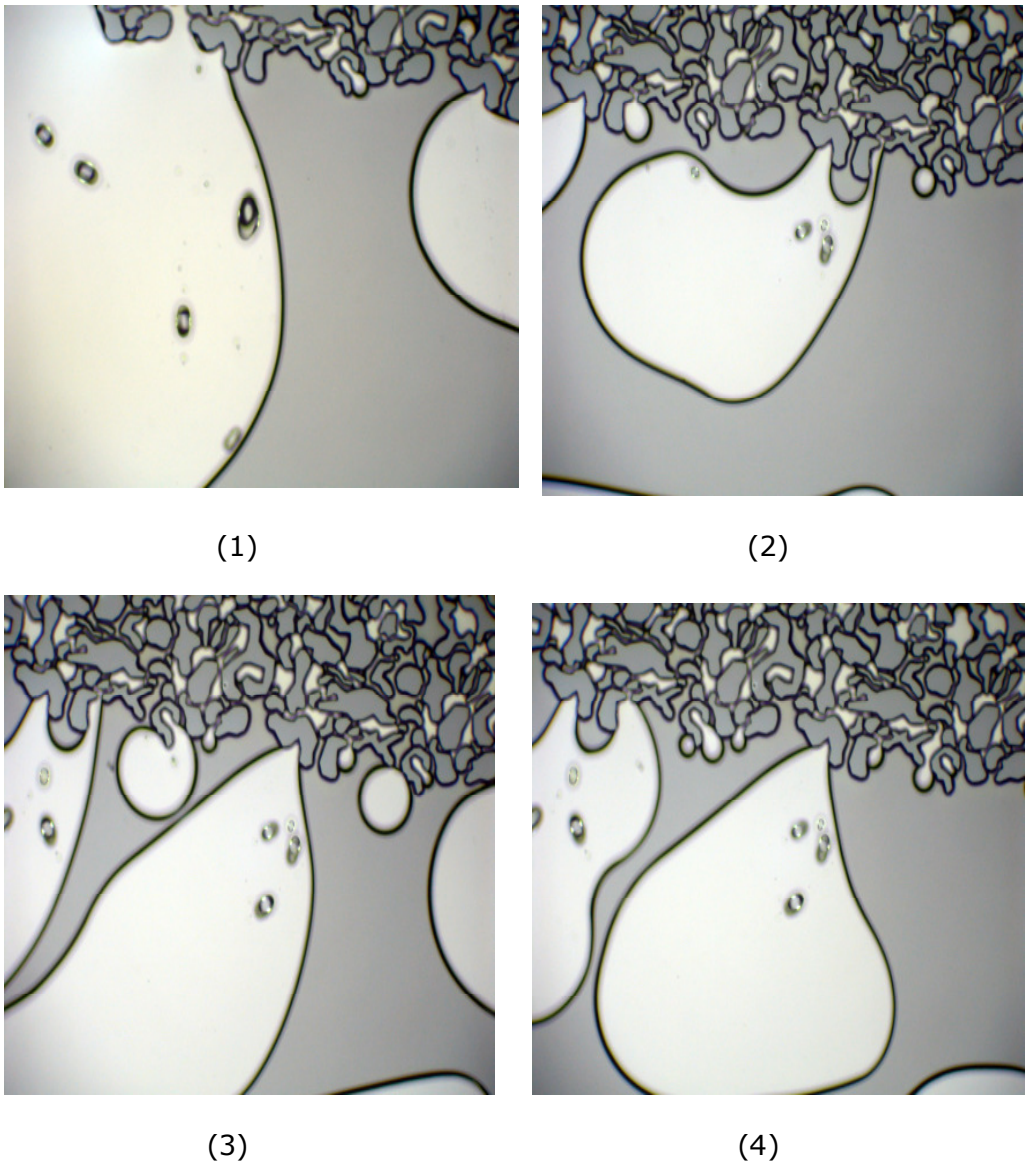

(1) (2)

(3) (4)

Figure 43: Gas displacement by brine injection (pore scale)

The figure above shows the displacement of the gas bubbles by brine on the outlet fracture. The pore spaces are observed through the microscope

in order to flush out all the gas bubbles and get the wafer completely brine saturated.

The micromodel is saturated with brine at constant pressure (45 psi), and then constant flow rate (0.006cc/min) is used to reach the stabilization of pressure. After the pressure was stabilized at 8 psi, the permeability of the model is calculated.

L (Length)	0.05	m		
μ (Viscosity)	0.001	Pa.s		
A (Area)	1.25E-06	m2		
ΔP (Pressure)	8	psi	5.52E+04	Pa
Conversion factor from psi to Pa	6.89E+03			
Q (Flow rate)	0.006	cc/min	1.00E-10	m3/s
Conversion factor from cc/min to m3/s	6.00E+07			
k (Permeability)	**7.25E-14**	**m2**		
Conversion factor from m2 to Darcy	1.00E-12	7.25E-02	D	
Conversion factor from Darcy to milidarcy	0.001	7.25E+01	mD	

Table 2: Permeability Calculation for the first experiment

After calculating the permeability of the model, the third step of injection started which was Polymer injection to find out its viscosity in the porous medium.

L (Length)	0.05	m		
A (Area)	1.25E-06	m2		
ΔP (Pressure)	25	psi	1.72E+05	Pa
Conversion factor from psi to Pa	6.89E+03			
Q (Flow rate)	0.00015	cc/min	2.50E-12	m3/s
Conversion factor from cc/min to m3/s	6.00E+07			
k (Permeability)	**7.25E-14**	m2		
μ (Viscosity)	1.25E-01	**Pa.s**		
conversion factor from cP to Pa.s	0.001	1.25E+02	cP	

Table 3: Viscosity Calculation for the first experiment

Note that the viscosity of the same polymer solution in porous medium is increased up to 125 cP, which could mean that the shear rate in the porous medium is much more less and increases the viscosity.

After calculations, brine is injected into the micromodel again to provide a clean wafer for the oil injection so wafer could get completely oil saturated.

The API gravity of the oil is measured at the same room temperature (22ºC), which was 30 APIº. And its measured viscosity from the viscometer was 35 cP. After getting the wafer completely brine saturated, the images through the microscope are taken with a digital camera.

Figure 44: The inlet and the outlet fractures of the micromodel, meso scale. (Inlet fracture is being filled with the oil)

The figure above shows the inlet and the outlet fractures of the micromodel. The oil injection started from the right-down side of the micromodel. When the inlet fracture was filled with oil and a little amount of oil came out of the left side of the inlet fracture, in order to push the movement towards the outlets, the left side of the inlet fracture was capped with a fitting.

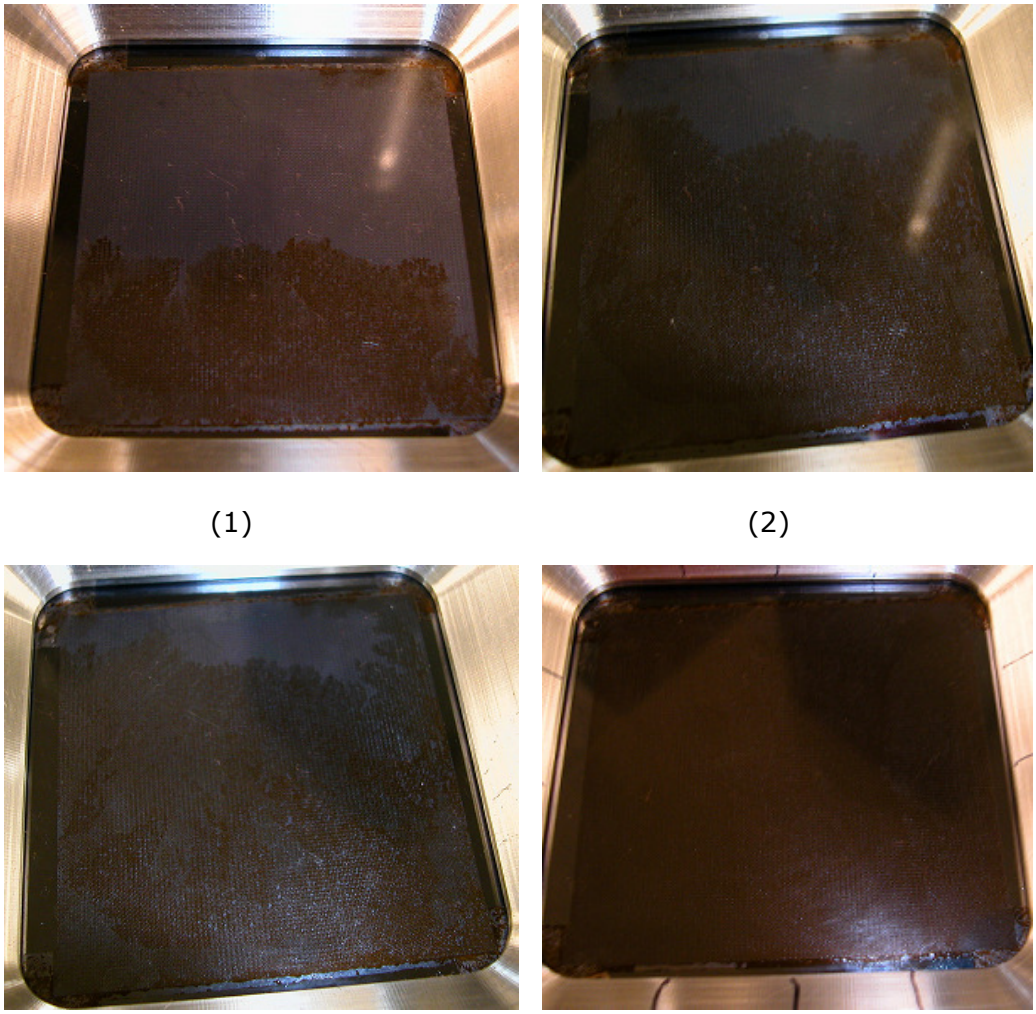

(1) (2)

(3) (4)

Figure 45: The images of the Oil Injection into the Micromodel at meso scale

After getting the micromodel completely oil saturated, the pore spaces are observed through the microscope to make sure that there was not any gas bubbles or brine in the micromodel.

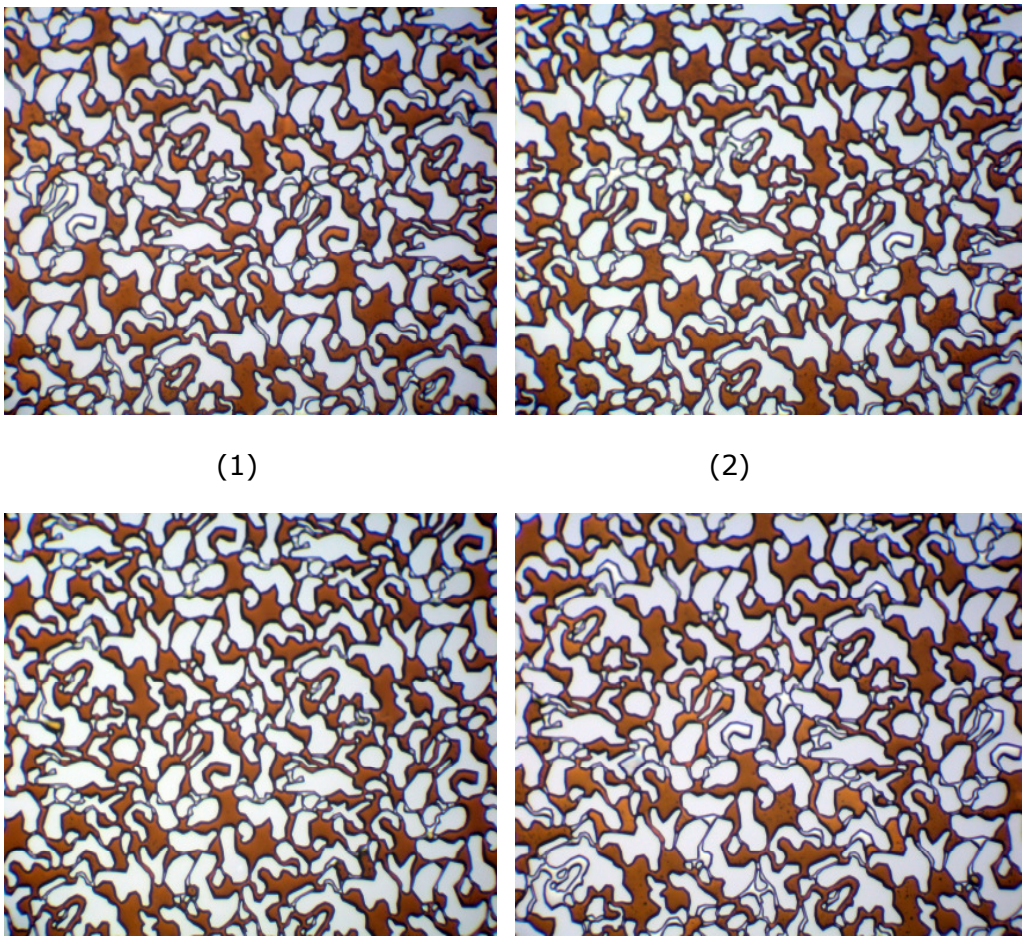

(1) (2)

(3) (4)

Figure 46: Images of the oil-filled pore spaces taken through the microscope at pore scale

It was very difficult to make the heavy oil flow into the micromodel. In order to make the process faster, two heat lamps are used. One of them was mounted to the injection tube clamp and pointed to the oil tube and the other one was directed to the micromodel. The heat decreased the viscosity of oil and made the flow faster into the micromodel. After reaching 100% oil saturation, the associative polymer (Superpusher 255) injection was started at constant flow rate (0.0001cc/mL).

(1)

(2)

(3)

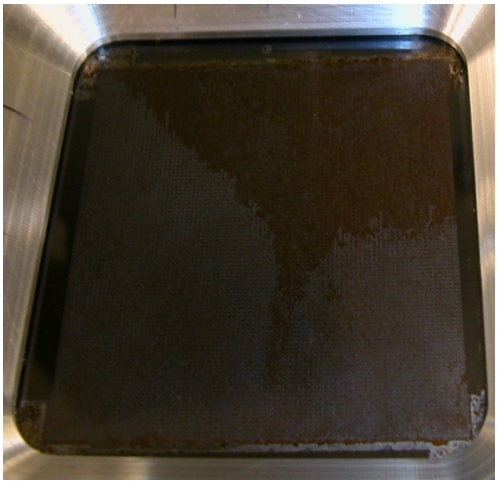

(4)

(5) (6)

Figure 47: Oil Displacement by associative polymer (meso scale)

The images above are taken with a digital camera at meso scale. The polymer is injected from the right entry of the inlet fracture but it started to sweep the oil from the left side of the inlet fracture as soon as the left entry was closed. This is likely due to the bonding of the micromodel. Sometimes there is a bit of an edge effect and the permeability along the side of the micromodel is a bit larger than in the middle of the micromodel. After reaching breakthrough, polymer started entering into the micromodel and sweeping the oil from the injection entry. A stable displacement is observed. Viscous fingering did not occur during the displacement process. The swept area is observed through the microscope and 16 images are taken for the image analysis to find out the residual oil saturation and the recovery values.

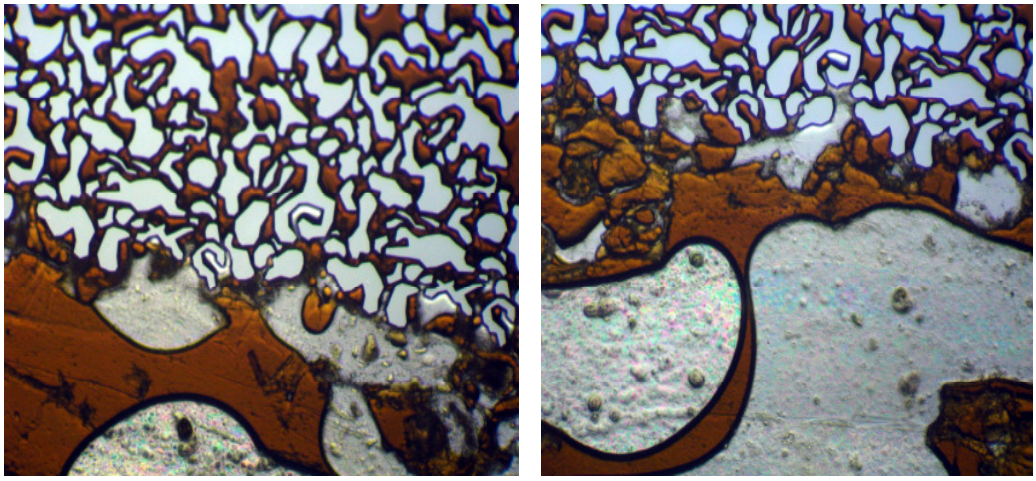

(1) (2)

Figure 48: Displacement of crude oil by associative polymer at the outlet fracture (pore scale)

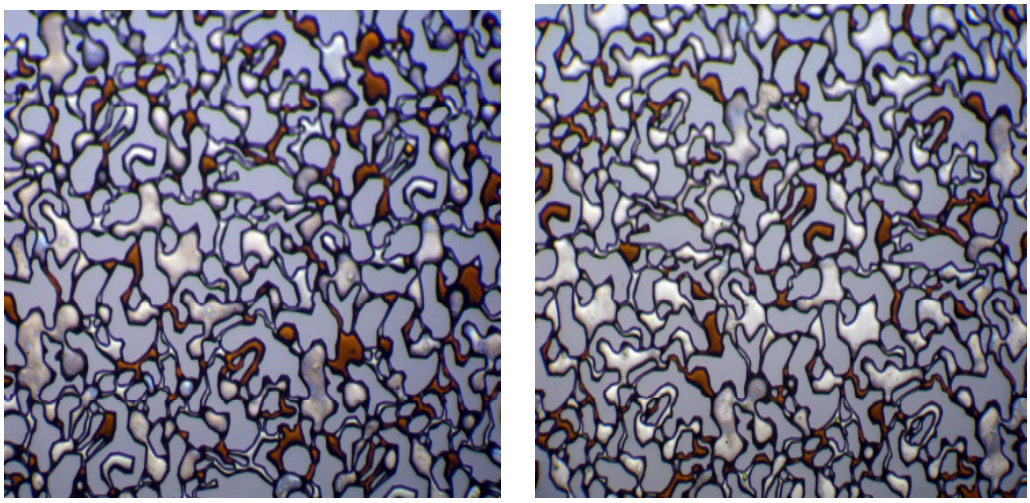

(1) (2)

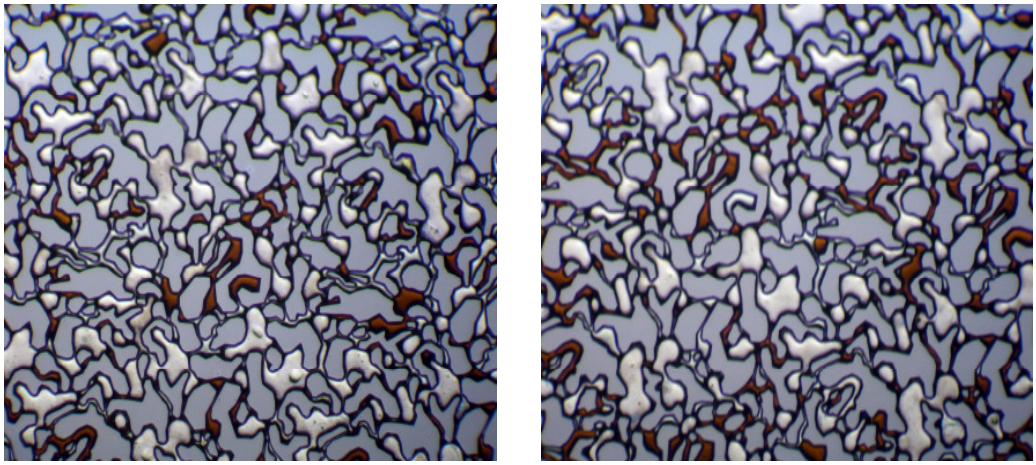

(3) (4)

Figure 49: Residual Oil in the pore spaces after polymer flood (pore scale)

The pore scale images show that polymer swept the oil out of the pore spaces very clearly. There is little amount of oil left in the micromodel. The images are analyzed by using the image software to find out the residual oil saturation value. The results of analyze are given in the last part of this chapter.

The amount of the polymer volume injected is 10.17 mL until breakthrough including four entry volumes. The dead volume should be taken into consideration and subtracted from the total amount of the injected volume. Since there are 4 entries, it makes 4 times dead volume which is 0.9 mL (for each) * 4 = 3.6mL. The total amount of volume injected into the micromodel is (10.17-3.6=) 6.57mL. Stable displacement is observed.

4.3.2. Results of the Image Analysis

As it was described in the image analysis, 16 images are taken from the grids on the micromodel at the end of the experiment. Basically, the injection had already been stopped before the images were taken.

Image Nr.	Edge effect	Porosity	Original Percentage	Oil saturation (So)
1	27.80%	22.10%	33.99%	**28%**
2	27.80%	22.10%	35.54%	**35%**
3	27.80%	22.10%	31.74%	**18%**
4	27.80%	22.10%	34.77%	**32%**
5	27.80%	22.10%	32.54%	**21%**
6	27.80%	22.10%	34.65%	**31%**

7	27.80%	22.10%	35.05%	**33%**
8	27.80%	22.10%	34.90%	**32%**
9	27.80%	22.10%	35.14%	**33%**
10	27.80%	22.10%	36.65%	**40%**
11	27.80%	22.10%	34.31%	**29%**
12	27.80%	22.10%	33.72%	**27%**
13	27.80%	22.10%	37.21%	**43%**
14	27.80%	22.10%	33.97%	**28%**
15	27.80%	22.10%	39.58%	**53%**
16	27.80%	22.10%	31.71%	**18%**
				501%

Overall percentage	**1600%**
So	**31%**
Oil Recovery	**69%**

Table 4: Image Analysis results of the first experiment

Since the overall percentage is 1600%, it gives us the oil saturation value which is 31%. From there, the calculated oil recovery is 69%.

4.4. SECOND EXPERIMENT

4.4.1. Oil Displacement by Brine

The aim of this experiment was to observe the displacement process of crude oil by brine in order to compare its displacement efficiency with the associative polymer. The same solution of brine is prepared according to the instructions. And the measured viscosity of brine solution was 1.00 cP. It was measured at the same room temperature and in the same viscometer. After viscosity measurement, the injection process started.

The steps followed were:

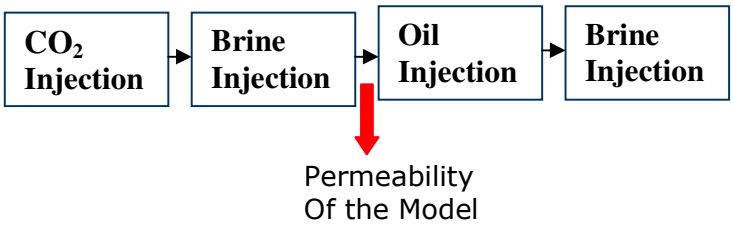

Figure 50: The Injection steps during 2. Experiment

The figure above depicts a schematic illustration of the injection steps. Black arrows indicate the end of an injection and the start point of the next injection. The red arrows indicate the calculations that were made after the pressure was stabilized and the injection was stopped. First, CO_2 is injected into the micromodel for 15 minutes in order to clean the wafer completely to prepare it for the experiment. The second injection step was the injection of brine solution. Brine is injected into the micromodel in order to calculate the permeability of the model by using Darcy's Law.

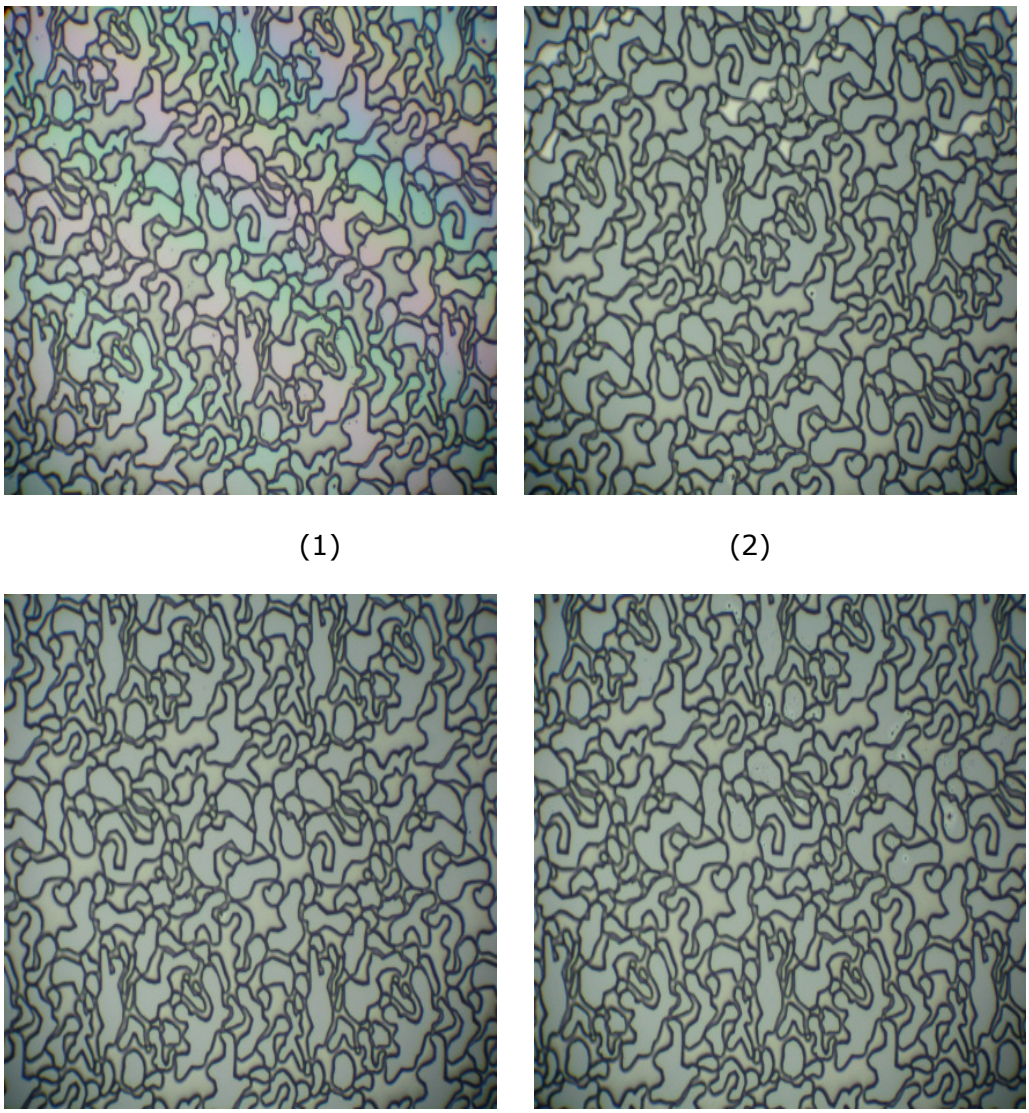

(1) (2)

(3) (4)

Figure 51: Completely brine saturated micromodel (pore scale)

The images in the figure 51 above show the brine-filled pore spaces which are taken through the microscope. The pore spaces are observed carefully in order to flush out all the gas bubbles and get the wafer completely brine saturated. The micromodel is saturated with brine at constant pressure (45 psi), and then constant flow rate (0.003 cc/min) is used to reach the stabilization of pressure. After the pressure was stabilized at 30 psi, the permeability of the model is calculated.

L (Length)	0.05	m		
μ (Viscosity)	0.001	Pa.s		
A (Area)	1.25E-06	m2		
ΔP (Pressure)	30	psi	2.07E+05	Pa
Conversion factor from psi to Pa	6.89E+03			
Q (Flow rate)	0.03	cc/min	5.00E-10	m3/s
Conversion factor from cc/min to m3/s	6.00E+07			
k (Permeability)	**9.67E-14**	**m2**		
Conversion factor from m2 to Darcy	1.00E-12	9.67E-02	D	
Conversion factor from Darcy to milidarcy	0.001	9.67E+01	mD	

Table 5: Permeability Calculation for the second experiment

After calculations, oil is injected into the micromodel again. The API gravity of the oil is measured at the same room temperature (22ºC), which was 30 APIº. And its measured viscosity from the viscometer was 35 cP.

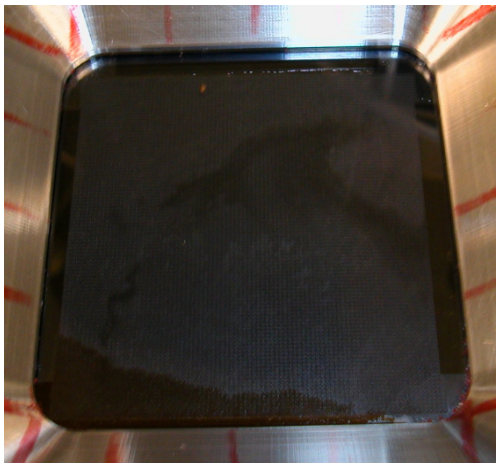

(1)

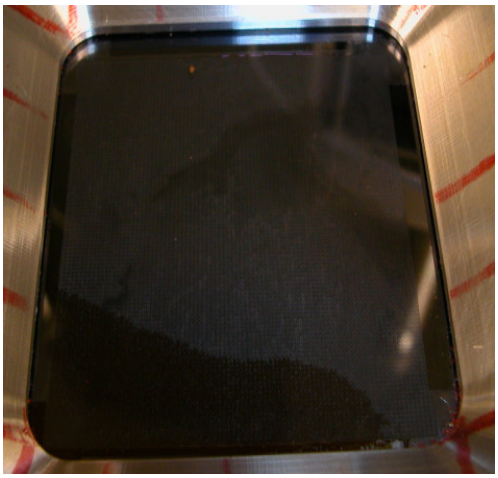

(2)

(3)

(4)

Figure 52: The oil injection into the micromodel, observation at meso scale

The images above show the oil injection into the micromodel in order to provide an oil-saturated wafer for the brine flood. After getting the micromodel completely oil saturated, the pore spaces are observed through the microscope to make sure that there was not any gas bubbles or brine in the micromodel.

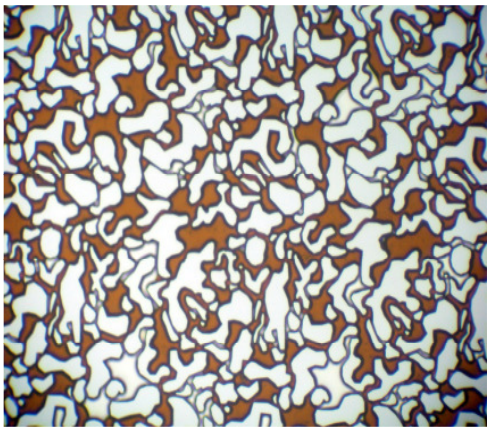

(1)

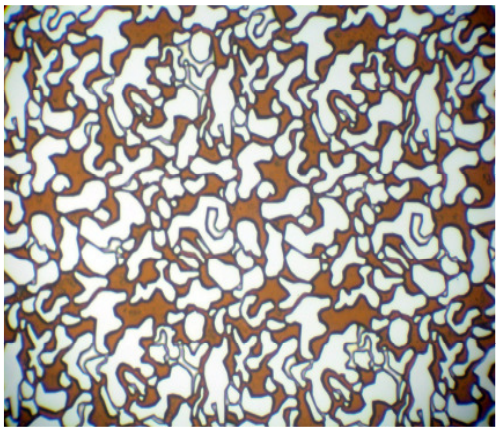

(2)

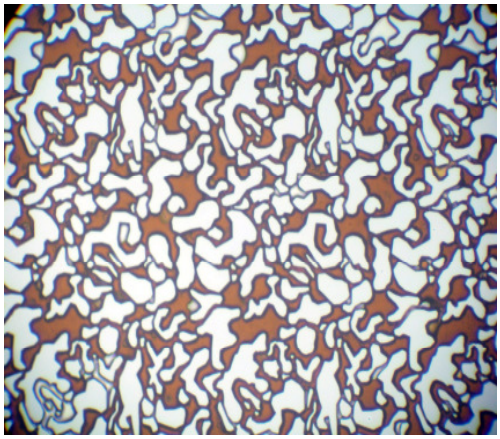

(3)

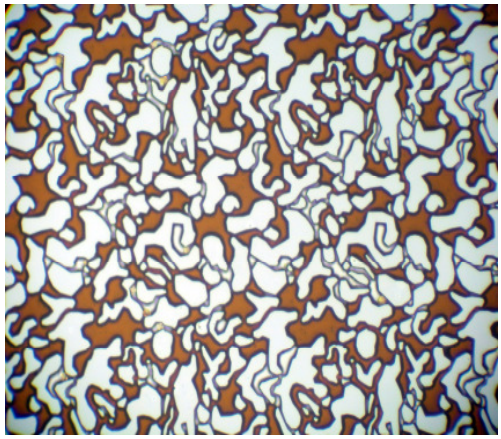

(4)

Figure 53: Images of the oil-filled pore spaces taken through the microscope (observation at pore scale)

Since it was the same oil, there were again some difficulties in getting the oil flow into the micromodel. The same heat lamp method is used to decrease its viscosity; consequently its movement was accelerated. After reaching 100% oil saturation, the brine injection was started at constant flow rate (0.00015cc/mL).

(1)

(2)

(3)

(4)

(5)

Figure 54: Oil displacement by brine (meso scale)

The images above are taken with a digital camera at meso scale. The brine is injected from the right entry of the inlet fracture but it started to sweep the oil from the left side of the inlet fracture as soon as the left entry was closed. When brine entered into the micromodel, it started to create fingering. At the beginning, fingers were thin but with the increasing time, they became thicker and consequently reached breakthrough. After reaching breakthrough, fingers started to disappear and at the end it was completely brine flood. An unstable displacement is observed. The swept area is observed through the microscope and 16 images are taken for the image analysis to find out the residual oil saturation and the recovery values.

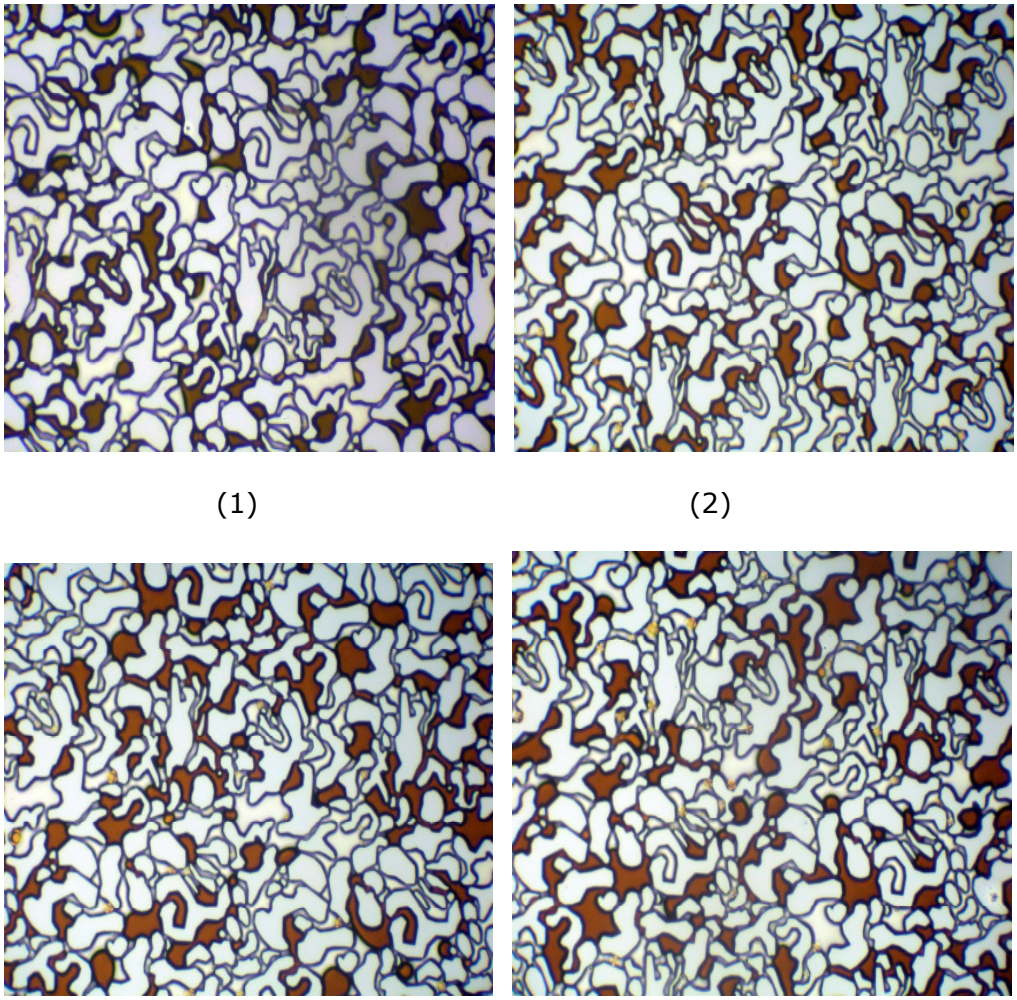

(1) (2)

(3) (4)

Figure 55: Residual oil in the pore spaces after brine flood (pore scale)

The pore scale images show that there is still a great amount of oil left in the micromodel. The images are analyzed by using the image software to find out the residual oil saturation value. The results of analyze are given in the last part of this chapter.

The injected volume from the injection until breakthrough is 8.9mL (without dead volumes). The cumulative water cut at the end of the experiment was 1.0 mL. The amount of the produced oil was 0.5 mL.

The water cut is 1.0 / 1.5 = 0.66 = % 66.

4.4.2. Results of the Image Analysis

In this experiment, first the recovery value and the residual oil saturation value are calculated at the brine breakthrough. Basically, the images were taken after brine reached the breakthrough and the injection had been stopped before the images were taken.

Image Nr.	Edge effect	Porosity	Original Percentage	Oil saturation (So)
1	27.80%	22.10%	45.69%	**81%**
2	27.80%	22.10%	44.58%	**76%**
3	27.80%	22.10%	45.44%	**80%**
4	27.80%	22.10%	46.00%	**82%**
5	27.80%	22.10%	44.81%	**77%**
6	27.80%	22.10%	46.02%	**82%**
7	27.80%	22.10%	45.18%	**79%**
8	27.80%	22.10%	46.01%	**82%**
9	27.80%	22.10%	44.48%	**75%**
10	27.80%	22.10%	44.91%	**77%**
11	27.80%	22.10%	43.74%	**72%**
12	27.80%	22.10%	44.06%	**74%**
13	27.80%	22.10%	45.37%	**80%**
14	27.80%	22.10%	44.17%	**74%**
15	27.80%	22.10%	45.21%	**79%**
16	27.80%	22.10%	43.93%	**73%**
				1243%

Overall percentage	**1600%**
So	**78%**
Oil Recovery	**22%**

Table 6: Image analysis results of the second experiment at brine breakthrough

The results show that the residual oil saturation at the brine breakthrough is 78%. And the oil recovery is 22%. This indicates that brine injection results in poor sweep efficiency and there is still a great amount of oil left in the micromodel. The second step in this experiment was to analyze the images which are taken at the end of the experiment. The end of the experiment means that the injection of brine was stopped because the water cut was reached 100 percent. 16 more images are taken in order to

determine the values again. The values shown in table 7 below are calculated from the images that are taken at the end of the experiment.

Image Nr.	Edge effect	Porosity	Original Percentage	Oil saturation (So)
1	27.80%	22.10%	37.55%	**44%**
2	27.80%	22.10%	36.39%	**39%**
3	27.80%	22.10%	39.18%	**51%**
4	27.80%	22.10%	36.46%	**39%**
5	27.80%	22.10%	38.52%	**49%**
6	27.80%	22.10%	40.41%	**57%**
7	27.80%	22.10%	38.53%	**49%**
8	27.80%	22.10%	39.13%	**51%**
9	27.80%	22.10%	39.59%	**53%**
10	27.80%	22.10%	38.09%	**47%**
11	27.80%	22.10%	37.68%	**45%**
12	27.80%	22.10%	38.06%	**46%**
13	27.80%	22.10%	39.55%	**53%**
14	27.80%	22.10%	39.96%	**55%**
15	27.80%	22.10%	38.78%	**50%**
16	27.80%	22.10%	38.38%	**48%**
				776%

Overall percentage	**1600%**
So	**48%**
Oil Recovery	**52%**

Table 7: Image analysis results at the end of the second experiment

The results show that at the end of the experiment, oil recovery was improved from 22% up to 52%.

4.5. THIRD EXPERIMENT

4.5.1. Oil Displacement by Conventional Polymer

The aim of this experiment was to observe the displacement process of crude oil by the conventional polymer which is called FLOPAAM 3630 S. Flopaam 3630 S is a copolymer of two monomers. First one is acrylamide and the second one is acrylic acid. Acrylic acid monomer gives the anionic properties to the polymer therefore this is an anionic water-soluble

polymer. Its PH is between 4 and 9 at 5 g/l. The solutions of brine and polymer are prepared according to the instructions. First, viscosity of the polymer solution is measured at room temperature (22ºC) in the viscometer which was 11 cP. And the measured viscosity of brine solution was 1.00 cP. It was measured at the same room temperature and in the same viscometer. After viscosity measurements, the injection process started. The steps followed were:

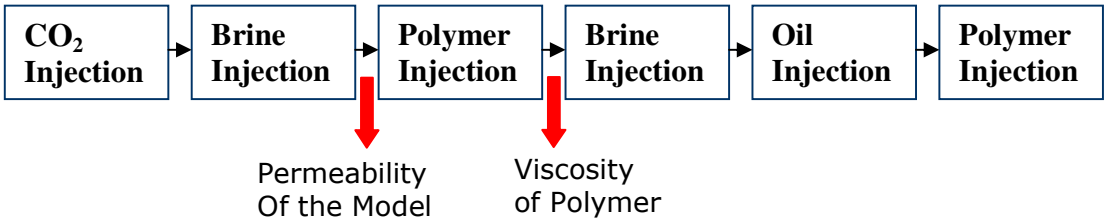

Figure 56: The injection steps during 3. Experiment

The figure above depicts a schematic illustration of the injection steps. Black arrows indicate the end of an injection and the start point of the next injection. The red arrows indicate the calculations that were made after the pressure was stabilized and the injection was stopped. First, CO_2 is injected into the micromodel for 15 minutes in order to clean the wafer completely to prepare it for the experiment. The second injection step was the injection of brine solution. Brine is injected into the micromodel in order to calculate the permeability of the model by using Darcy's Law. The pore spaces are observed through the microscope in order to flush out all the gas bubbles and get the wafer completely brine saturated.

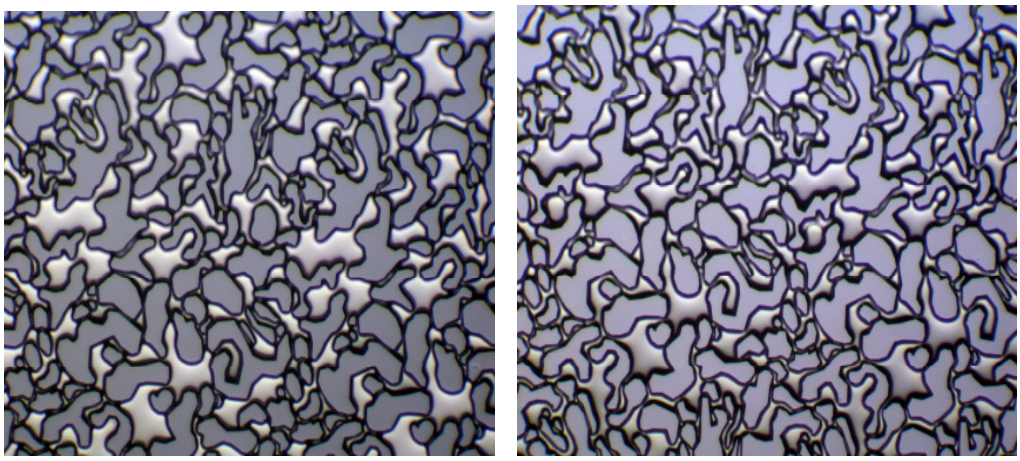

(1) (2)

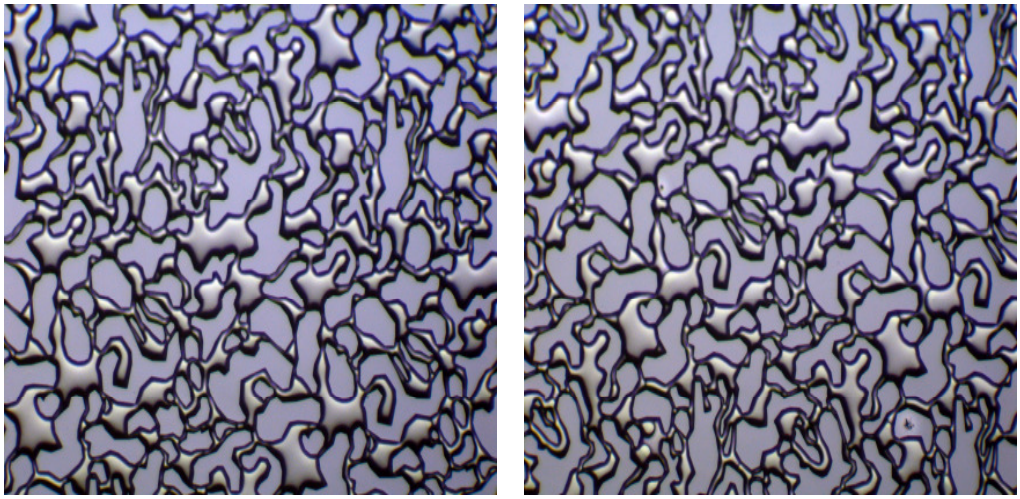

(3) (4)

Figure 57: Fully brine saturated micromodel, pore scale

The micromodel is saturated with brine at constant pressure (45 psi), and then constant flow rate (0.003cc/min) is used to reach the stabilization of pressure. After the pressure was stabilized at 30 psi, the permeability of the model is calculated.

L (Length)	0.05	m		
μ (Viscosity)	0.001	Pa.s		
A (Area)	1.25E-06	m2		
ΔP (Pressure)	30	psi	2.07E+05	Pa
Conversion factor from psi to Pa	6.89E+03			
Q (Flow rate)	0.03	cc/min	5.00E-10	m3/s
Conversion factor from cc/min to m3/s	6.00E+07			
k (Permeability)	**9.67E-14**	**m2**		
Conversion factor from m2 to Darcy	1.00E-12	9.67E-02	D	
Conversion factor from Darcy to milidarcy	0.001	9.67E+01	mD	

Table 8: Permeability Calculation for the third experiment

After calculating the permeability of the model, the third step of injection started which was polymer injection to find out its viscosity in the porous medium.

L (Length)	0.05	m		
A (Area)	1.25E-06	m2		
ΔP (Pressure)	9	psi	6.21E+04	Pa
Conversion factor from psi to Pa	6.89E+03			
Q (Flow rate)	0.01	cc/min	1.67E-10	m3/s
Conversion factor from cc/min to m3/s	6.00E+07			
k (Permeability)	**9.67E-14**	m2		
μ (Viscosity)	9.00E-04	**Pa.s**		
conversion factor from cP to Pa.s	0.001	9.00E-01	cP	

Table 9: Viscosity Calculation for the third experiment

There was a difficulty in measuring the viscosity of the conventional polymer in porous medium. Again, constant flow rate (0.01) is used. After pressure was stabilized at 9 psi, the viscosity is measured by Darcy's law. But it did not give a meaningful result since it is less than brine viscosity according to the conclusion. In order to get more accurate results, the first two steps are repeated. Since the wafer was already used, it was difficult to clean it completely, so consequently the permeability decreased down to 35.8 mD.

L (Length)	0.05	m		
μ (Viscosity)	0.001	Pa.s		
A (Area)	1.25E-06	m2		
ΔP (Pressure)	27	psi	1.86E+05	Pa
Conversion factor from psi to Pa	6.89E+03			
Q (Flow rate)	0.01	cc/min	1.67E-10	m3/s
Conversion factor from cc/min to m3/s	6.00E+07			
k (Permeability)	**3.58E-14**	**m2**		
Conversion factor from m2 to Darcy	1.00E-12	3.58E-02	D	
Conversion factor from Darcy to milidarcy	0.001	3.58E+01	mD	

Table 10: Permeability Calculation for the third experiment (repeat)

Again, its viscosity in porous medium is calculated after the pressure was stabilized.

L (Length)	0.05	m		
A (Area)	1.25E-06	m2		
ΔP (Pressure)	46	psi	3.17E+05	Pa
Conversion factor from psi to Pa	6.89E+03			
Q (Flow rate)	0.0005	cc/min	8.33E-12	m3/s
Conversion factor from cc/min to m3/s	6.00E+07			
k (Permeability)	**3.58E-14**	m2		
μ (Viscosity)	3.41E-02	**Pa.s**		
conversion factor from cP to Pa.s	0.001	3.41E+01	cP	

Table 11: Viscosity Calculation for the third experiment (repeat)

Note that the viscosity of the same polymer solution in porous medium is increased up to 34.1 cP.

After calculations, brine is injected into the micromodel again to provide a clean wafer for the oil injection so wafer could get completely oil saturated. The API gravity of the oil is measured at the same room temperature (22ºC), which was 30 APIº. And its measured viscosity from the viscometer was 35 cP. The oil injection started from the right-down side of the micromodel. When the inlet fracture was filled with oil and a little amount of oil came out of the left side of the inlet fracture, in order to push the movement towards the outlets, the left side of the inlet fracture was capped with a fitting. Oil is injected at constant pressure (52 psi). After getting the micromodel completely oil saturated, the pore spaces are observed through the microscope to make sure that there was not any gas bubbles or brine in the micromodel.

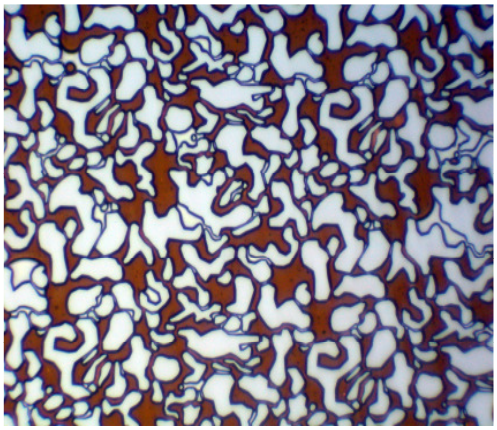

(1)

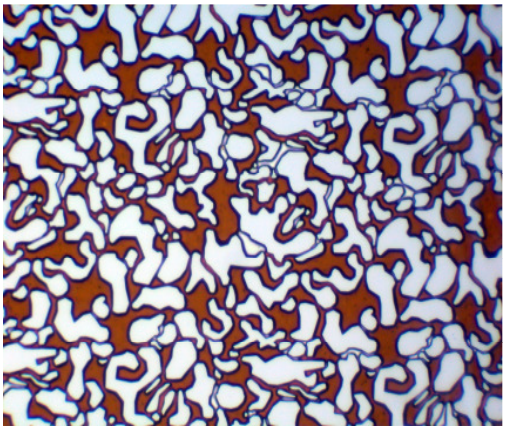

(2)

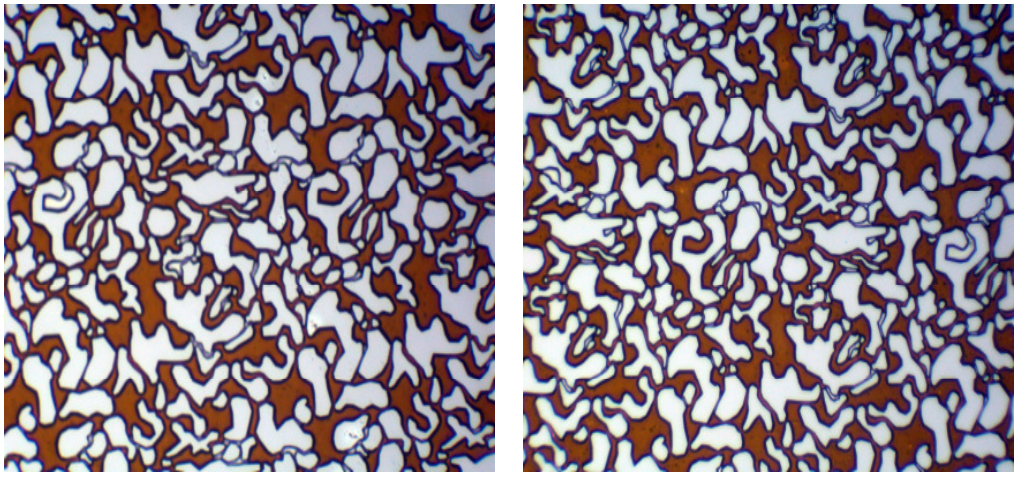

(3) (4)

Figure 58: Images of the oil-filled pore spaces taken through the microscope at pore scale

After reaching 100% oil saturation, the associative polymer (FP-3630-S) injection was started at constant flow rate (0.0001cc/mL).

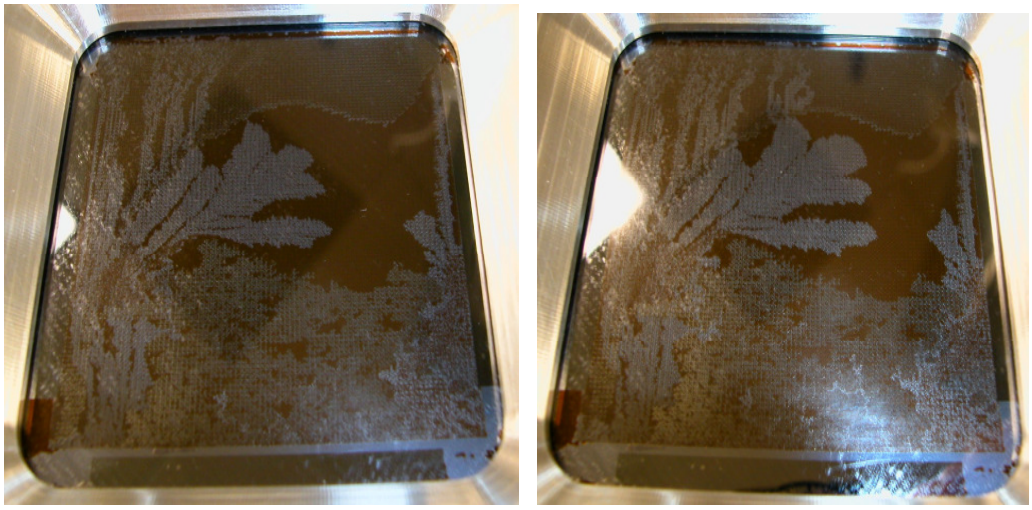

(1) (2)

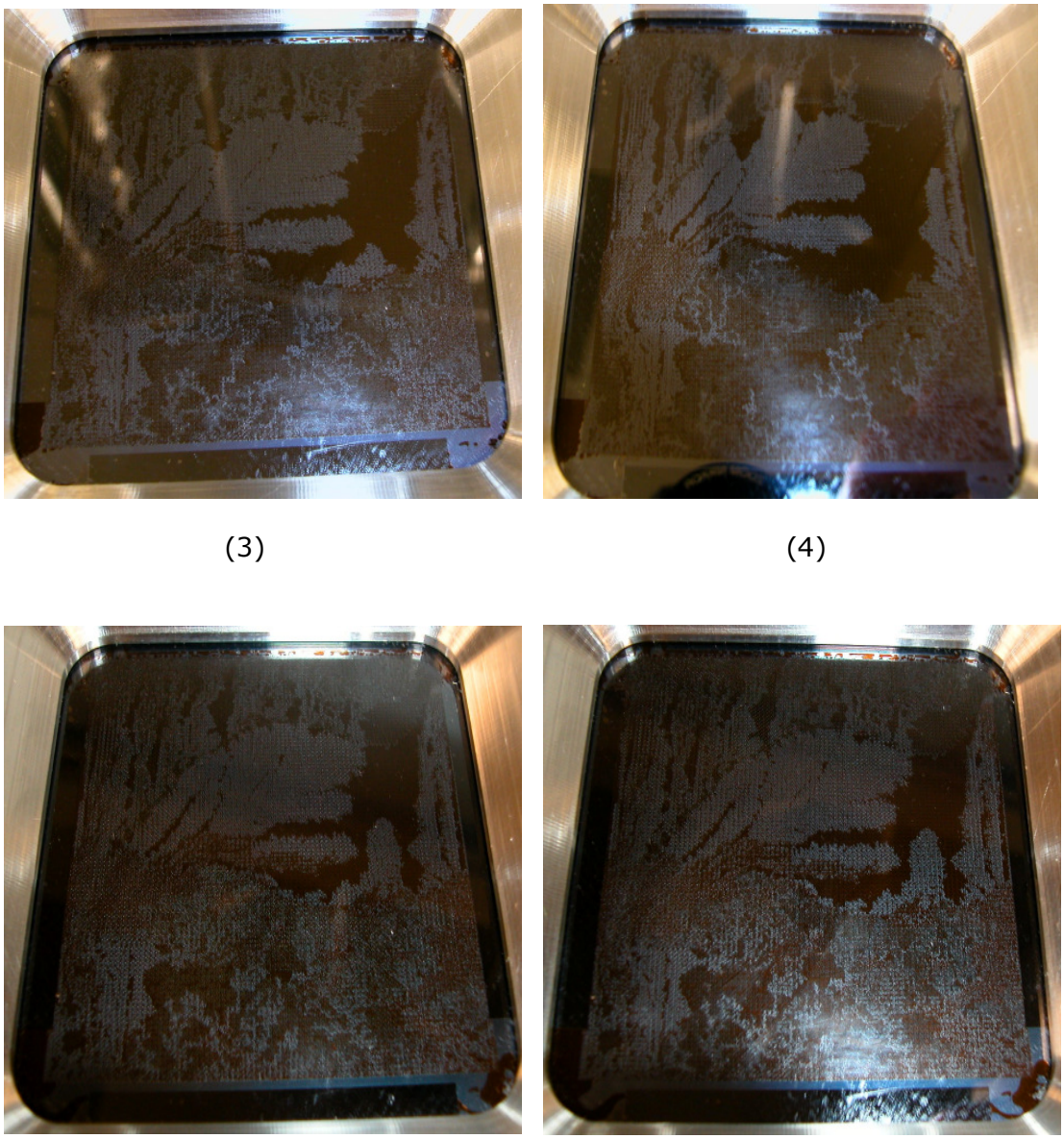

(3) (4)

(5) (6)

Figure 59: Oil Displacement by conventional polymer (FP-3638-S) at meso scale

The images above are taken with a digital camera at meso scale. The polymer is injected from the right entry of the inlet fracture but it started to sweep the oil from the left side of the inlet fracture as soon as the left entry was closed as it did in the first experiment. An unstable displacement is observed. Viscous fingers occurred during the displacement process. Except the biggest finger, there were some little

fingers right in front of the inlet fracture and they became thicker with increasing time. The swept area is observed through the microscope and 16 images are taken for the image analysis to find out the residual oil saturation and the recovery values.

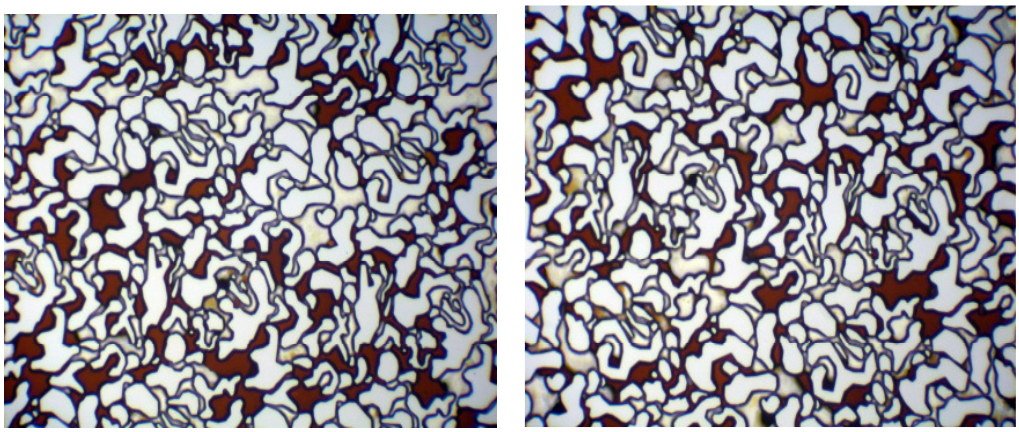

(1) (2)

Figure 60: Residual Oil in the pore spaces after polymer flood (pore scale)

The pore scale images show that there is still a great amount of oil left in the micromodel. The images are analyzed by using the image software to find out the residual oil saturation value. The results of analyze are given in the last part of this chapter. The injected volume until BT is 8.7 mL (without entry volumes). Total amount of injected volume is 13.00mL.

4.5.2. Results of the Image Analysis

16 images are taken from the grids on the micromodel at the end of the experiment by following the same procedure as in the previous experiments.

Image Nr.	Edge effect	Porosity	Original Percentage	Oil saturation (So)
1	27.80%	22.10%	33.65%	**26%**
2	27.80%	22.10%	36.92%	**41%**
3	27.80%	22.10%	34.76%	**31%**
4	27.80%	22.10%	40.48%	**57%**
5	27.80%	22.10%	35.42%	**34%**
6	27.80%	22.10%	34.35%	**30%**
7	27.80%	22.10%	33.02%	**24%**
8	27.80%	22.10%	35.91%	**37%**

9	27.80%	22.10%	41.00%	**60%**
10	27.80%	22.10%	40.32%	**57%**
11	27.80%	22.10%	45.86%	**82%**
12	27.80%	22.10%	47.07%	**87%**
13	27.80%	22.10%	35.64%	**35%**
14	27.80%	22.10%	37.52%	**44%**
15	27.80%	22.10%	38.22%	**47%**
16	27.80%	22.10%	29.91%	**10%**
				702%

Overall percentage	**1600%**
So	**44%**
Oil Recovery	**56%**

Table 12: Image analysis results of 3. Experiment

Image analysis results show that at the end of polymer flood, there is a 56% oil recovery.

4.6. FOURTH EXPERIMENT

4.6.1. Oil Displacement by Associative Polymer after Brine breakthrough

The aim of this experiment was to observe the displacement process of crude oil by the same brine solution and inject the associative polymer right after brine breakthrough in order to observe whether the associative polymer mitigates the viscous fingering which was created by brine previously. The same associative polymer is used (SuperPusher 255). The solutions of brine and polymer are prepared according to the instructions. First, viscosity of the polymer solution is measured at room temperature (22ºC) in the viscometer which was 12 cP. And the measured viscosity of brine solution was 1.00 cP. It was measured at the same room temperature and in the same viscometer. After viscosity measurement, the injection process started.

The steps followed were:

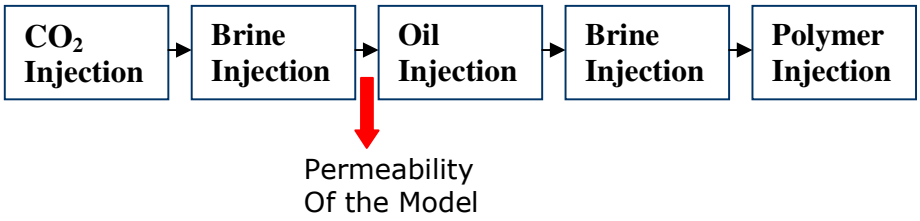

Figure 61: The injection steps during 4. Experiment

The figure above depicts a schematic illustration of the injection steps. Black arrows indicate the end of an injection and the start point of the next injection. The red arrows indicate the calculations that were made after the pressure was stabilized and the injection was stopped. First, CO_2 is injected into the micromodel for 15 minutes in order to clean the wafer completely to prepare it for the experiment. The second injection step was the injection of brine solution. Brine is injected into the micromodel in order to calculate the permeability of the model by using Darcy's Law. The pore spaces are observed through the microscope in order to flush out all the gas bubbles and get the wafer completely brine saturated.

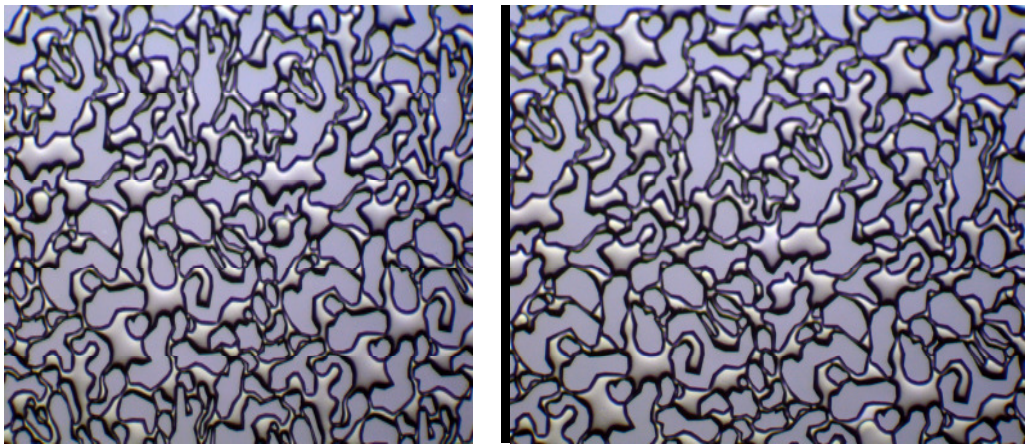

(1) (2)

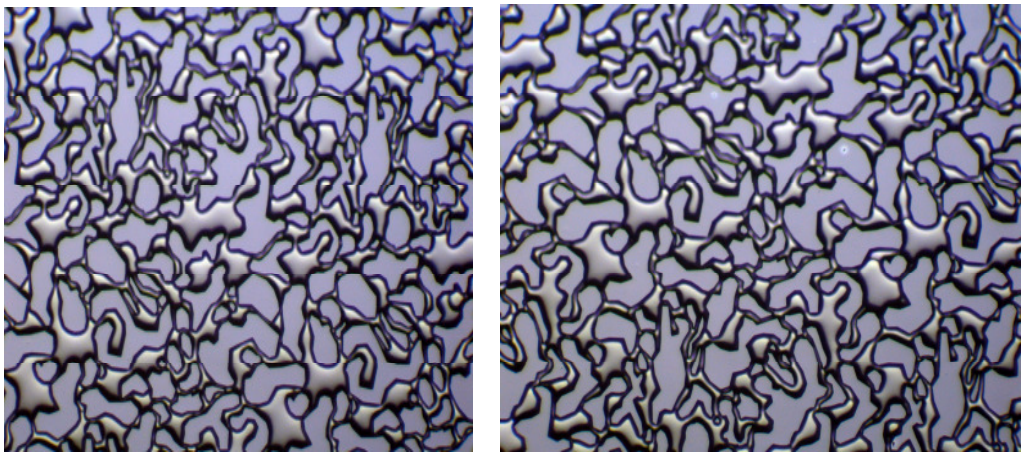

(3) (4)

Figure 62: Brine saturated wafer (pore scale)

The micromodel is saturated with brine at constant pressure (45 psi), and then constant flow rate (0.02cc/min) is used to reach the stabilization of pressure. After the pressure was stabilized at 12 psi, the permeability of the model is calculated.

L (Length)	0.05	m		
μ (Viscosity)	0.001	Pa.s		
A (Area)	1.25E-06	m2		
ΔP (Pressure)	12	psi	8.27E+04	Pa
Conversion factor from psi to Pa	6.89E+03			
Q (Flow rate)	0.02	cc/min	3.33E-10	m3/s
Conversion factor from cc/min to m3/s	6.00E+07			
k (Permeability)	**1.61E-13**	**m2**		
Conversion factor from m2 to Darcy	1.00E-12	1.61E-01	D	
Conversion factor from Darcy to milidarcy	0.001	1.61E+02	mD	

Table 13: Permeability calculation for the third experiment

After getting the wafer brine saturated, heavy oil is injected. The total amount of injected volume of heavy oil is 21.97 mL. The API gravity of the oil is measured at the same room temperature (22ºC), which was 30 APIº. And its measured viscosity from the viscometer was 35 cP. After getting the wafer completely oil saturated, the images through the microscope are taken with a digital camera. After getting the micromodel completely oil saturated, the pore spaces are observed through the microscope to make sure that there was not any gas bubbles or brine in the micromodel.

The injection process is then continued with the brine injection at constant flowrate (0.00015cc/mL).

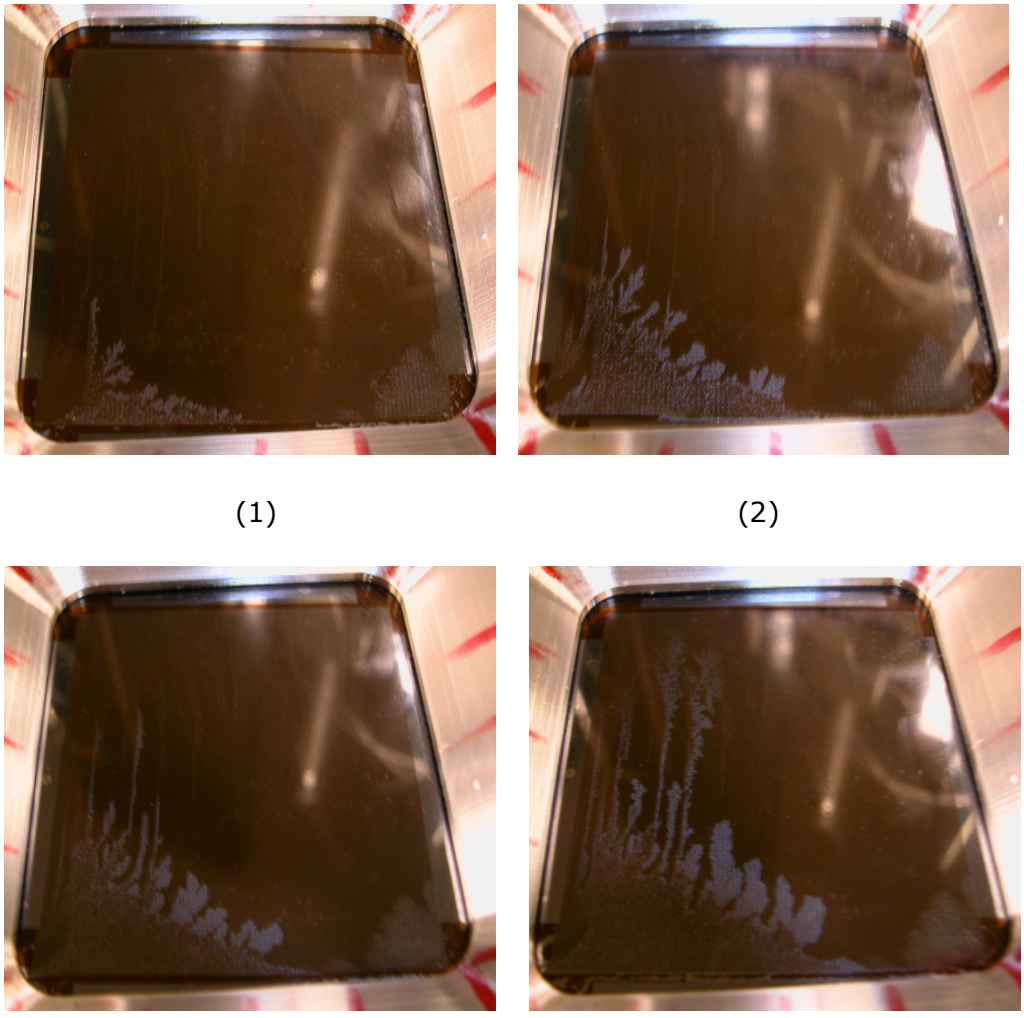

(1) (2)

(3) (4)

Figure 63: Brine Injection into a oil-saturated micromodel until Breakthrough (meso scale)

The images above are taken with a digital camera at meso scale. The brine is injected from the right entry of the inlet fracture but it started to sweep the oil from the left side of the inlet fracture as in the first experiment as soon as the left entry was closed. An unstable displacement is observed. Viscous fingering occurred during the displacement process. The swept area is observed through the microscope and 16 images are taken for the image analysis to find out the residual oil saturation and the recovery values.

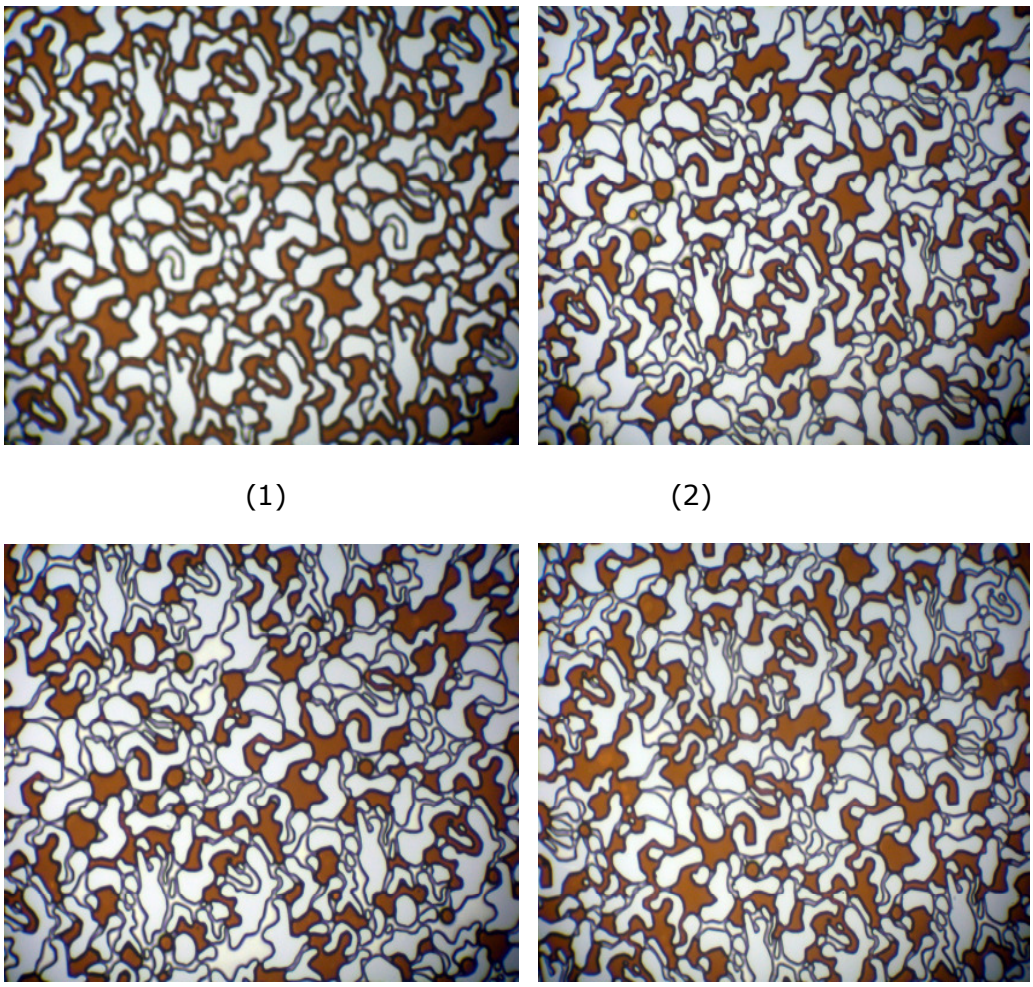

(1) (2)

(3) (4)

Figure 64: Residual Oil after brine flood until breakthrough (pore scale)

After brine reached the breakthrough, brine injection is stopped and the associative polymer injection started. Images that are taken of the displacement process were neither understandable nor clear. Because of this problem, a schematic illustration of the oil displacement is prepared. The illustration is shown below is depicting the inlets and the outlets of the micromodel. The grey part is the brine injection at meso scale, which was shown in the figure 63. The polymer front movement and its displacements pattern are shown in yellow.

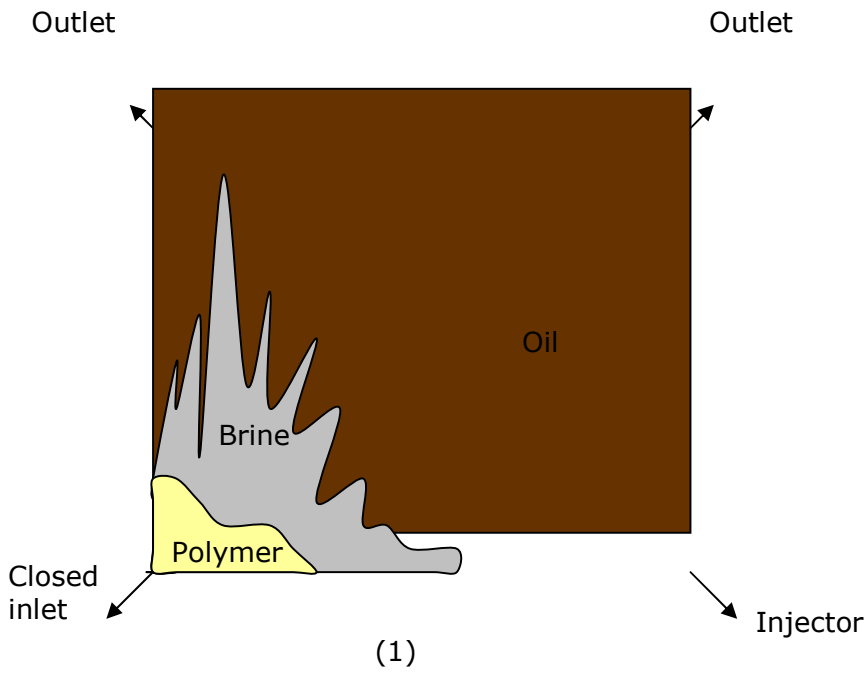
Outlet
Outlet
Oil
Brine
Polymer
Closed
inlet
Injector

(1)

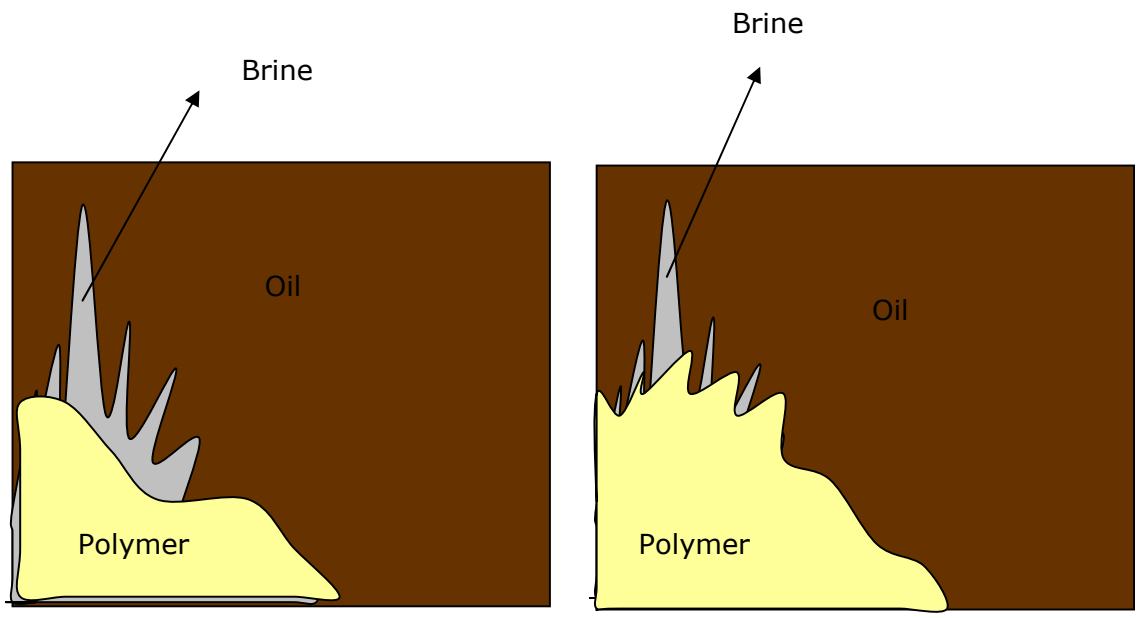
Brine
Oil
Polymer
Brine
Oil
Polymer

(2) (3)

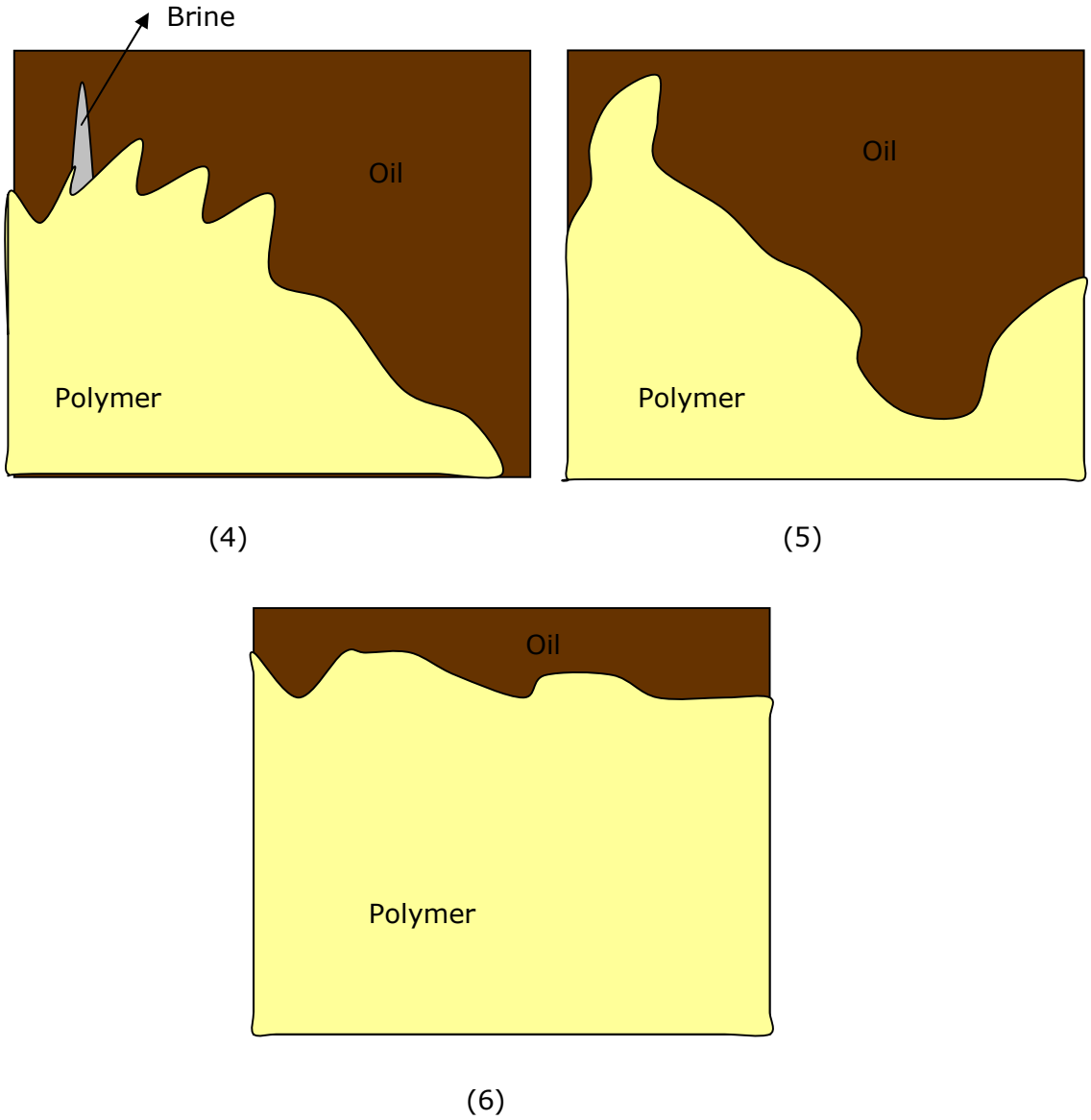

Figure 65: Schematic illustration of the oil displacement by associative polymer after brine breakthrough

Polymer is injected into the micromodel at the constant flow rate (0.00015cc/mL). Polymer is injected from the right injection side and the left side is closed to observe the front movement. Polymer first entered into the micromodel from the left side of the inlet fracture as it did in the first experiment (1). This is likely due to the anodic bonding. During the bonding of pyrex glass to the silicon wafer, because of placing the weights on the glass unsymmetrical, the permeability could be different, so

accordingly polymer starts sweeping the oil from the left side even though the injection entry is the right side of the micromodel. It was not clear to observe the polymer flood at meso scale before it reached the fingers (2). Then, as it reached the fingers, it started expanding the fingers sideways and made them thicker (3, 4). As in the first experiment, it led to a stable displacement and mitigated the viscous fingers which were caused by the brine injection in the previous step (5, 6). Afterwards, 16 images are taken for the image analysis and residual oil saturation is observed.

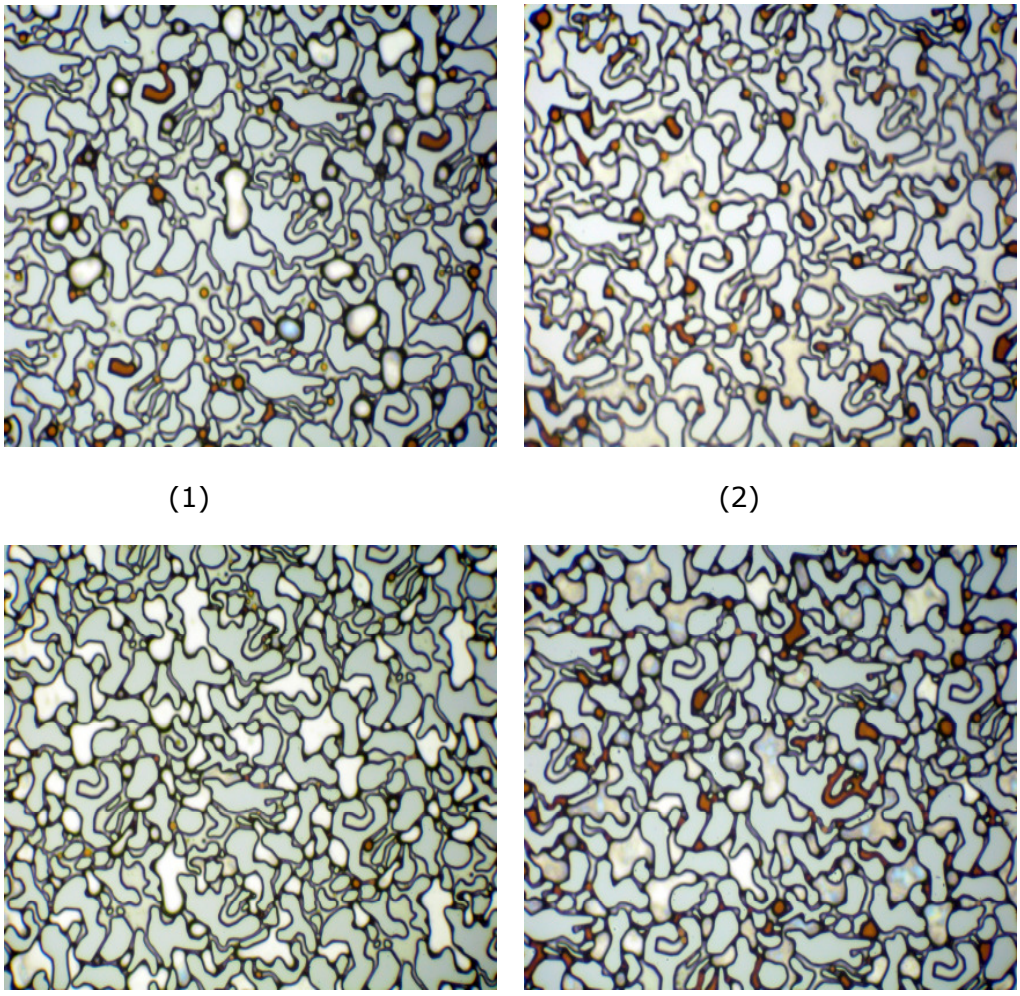

(1) (2)

(3) (4)

Figure 66: Residual Oil saturation after polymer flood, pore scale

The pore scale images show that polymer swept the oil out of the pore spaces very clearly. There is very little amount of oil left in the micromodel. The images are analyzed by using the image software to find

out the residual oil saturation value. The results of analyze are given in the last part of this chapter.

4.6.2. Results of the Image Analysis

In this experiment, similar to the second experiment, first the residual oil saturation and the recovery values are calculated at the brine breakthrough. Table 14 below shows the oil saturation and the recovery values which were calculated after brine reached the breakthrough which means, brine injection was stopped and the images were taken before the polymer injection started.

Image Nr.	Edge effect	Porosity	Original Percentage	Oil saturation (So)
1	27.80%	22.10%	43.98%	**73%**
2	27.80%	22.10%	40.27%	**56%**
3	27.80%	22.10%	46.16%	**83%**
4	27.80%	22.10%	48.70%	**95%**
5	27.80%	22.10%	43.18%	**70%**
6	27.80%	22.10%	41.58%	**62%**
7	27.80%	22.10%	43.16%	**70%**
8	27.80%	22.10%	40.69%	**58%**
9	27.80%	22.10%	43.12%	**69%**
10	27.80%	22.10%	44.27%	**75%**
11	27.80%	22.10%	40.82%	**59%**
12	27.80%	22.10%	43.50%	**71%**
13	27.80%	22.10%	46.05%	**83%**
14	27.80%	22.10%	49.00%	**96%**
15	27.80%	22.10%	39.78%	**54%**
16	27.80%	22.10%	32.92%	**23%**
				1097%

Overall percentage	**1600%**
So	**69%**
Oil Recovery	**31%**

Table 14: Image analysis results of 4. Experiment at brine breakthrough

The results show that it is very similar to the second experiment in which brine flood was carried out. Again poor sweep efficiency occurred until brine breakthrough. The second part of the analysis is made after polymer flood which was injected right after brine breakthrough. (shown in table 15 below)

Image Nr.	Edge effect	Porosity	Original Percentage	Oil saturation (So)
1	27.80%	22.10%	32.24%	**20%**
2	27.80%	22.10%	42.52%	**67%**
3	27.80%	22.10%	30.54%	**12%**
4	27.80%	22.10%	37.11%	**42%**
5	27.80%	22.10%	36.87%	**41%**
6	27.80%	22.10%	33.49%	**26%**
7	27.80%	22.10%	30.36%	**12%**
8	27.80%	22.10%	35.80%	**36%**
9	27.80%	22.10%	33.76%	**27%**
10	27.80%	22.10%	28.20%	**2%**
11	27.80%	22.10%	29.68%	**9%**
12	27.80%	22.10%	36.38%	**39%**
13	27.80%	22.10%	32.50%	**21%**
14	27.80%	22.10%	30.39%	**12%**
15	27.80%	22.10%	30.23%	**11%**
16	27.80%	22.10%	31.06%	**15%**
				391%

Overall percentage	**1600%**
So	**24%**
Oil Recovery	**76%**

Table 15: Image analysis results at the end of 4. Experiment

Results show clearly that associative polymer flood results in good sweep efficiency and increases the oil recovery from 31% up to 76%.

4.7. FIFTH EXPERIMENT

Finally, a viscosity measurement is carried out. The aim was to compare the concentrations of polymers for the same acquired viscosity. The same associative polymer (S255) and the same conventional polymer (FP-3630-S) are used.

Temperature	22ºC			
	FP3630S		**S255**	
Brine amount in solution	199.9	g	199.9	g

Polymer amount in solution	0.05	g	0.05	g
Viscosity in Viscometer (μ)	**3**	**cP**	**7**	**cP**

Table 16: Viscosity measurements of polymer in viscometer at room temperature (22ºC)

Viscosity measurements show that associative polymer results in higher viscosities at the same concentrations as conventional polymers. The conventional polymer gives the viscosity of 3 cP where the associative polymer gives 7 cP viscosities at the same concentrations. All the measurements are carried out in the same viscometer and at the same room temperature.

4.8. COMPARISON OF THE IMAGE ANALYSIS RESULTS

The table below shows the recovery values and gives a comparison of the experiment results. Note that the second and third experiments, between a normal brine flood and a conventional polymer flood, there is not much difference in recovery values. Associative polymer gives a clear result in first and fourth experiments. It indicates that stable displacement results in better sweep efficiency and better recovery values compared to the experiment in which conventional polymer flood was carried out or the experiment in which brine flood was carried out.

Experiment No	Experiment Title	Oil Recovery at BT	Oil Recovery at the end
1st	**Oil Disp. by Asso. Polymer (S255)**		**69 %**
2nd	**Oil Disp. by Brine**	**22 %**	**52 %**
3rd	**Oil Disp. by Conv. Polymer (FP3630S)**		**56%**
4th	**Oil Disp. by Asso. Poly (S255) after Brine BT**	**31 %**	**76 %**

Table 17: Comparison of Oil Recoveries

CHAPTER 5

5. CONCLUSIONS AND RECOMMENDATIONS

5.1. SUMMARY AND CONCLUSIONS

This experimental and theoretical study was concerned with the behavior of polymer in porous media at the pore level. The oil recovery and sweep efficiency were also obtained in two-dimensional silicon micromodels which replicate the flow in Berea sandstone. All the micromodels used for this study were exact duplicates of each other. Two phase displacements are conducted with brine, oil and new type so-called associative polymers. The trials were respectively:

a) Oil Displacement by Associative polymer
b) Oil Displacement by conventional Polymer
c) Oil displacement by Brine
d) Oil Displacement by Associative Polymer right after brine Breakthrough

Prior to polymer flood, the models were saturated with brine first, and then oil was injected into the micromodel to observe the sweep pattern at meso scale and the pore spaces through the micromodel.

Consequently, the conclusions below are made.

1. The silicon micromodels that are used for this project, were constructed to observe pore level interactions of oil, water and polymer and fabricated at Stanford NanoFabrication Facility in California, USA. They were exact duplicates of eachother. Fluid flow within model replicates a two dimensional flow through a thin section of Berea sandstone.

2. New types of polymers –so-called Associative Polymers- are used for this project. They are developed to decrease the cost of polymer flooding.

3. This study investigates the displacement process of medium viscosity oil (10-100 cP) by aqueous solutions of associative polymers and compared its results to the oil displacement processes by brine and the conventional Polymers.

4. Laboratory measurements show that associative polymers result in greater fluid viscosities at the same concentration as conventional polymers.

5. Generally, we find that conventional polymers and brine result in viscous fingering during the displacement fluid. However, associative polymers lead to more stable displacement characteristics at these concentrations. The displacement pattern while injecting brine displays fingers clearly.

6. Injection of associative polymers after breakthrough mitigates fingering, leads a stable displacement and improves viscous oil displacement accordingly.

7. Experimental results show that associative polymers are a promising method to improve the displacement efficiency of viscous oils.

8. For consistency, further research is required to understand the full range of the fluid interactions. Data comparison of the micromodel investigations with the core floods could be done to confirm these experimental results.

9. The fifth experiment showed that associative polymer results in higher viscosities at the same concentrations as conventional polymers which mean that in order to get the same viscosity as associative polymer, more amount of conventional polymer is required.

5.2. RECOMMENDATIONS

Since it was an experimental work, difficulties regarding the laboratory equipment and accidents with the micromodel were expected. In order to be able to make comparisons as many as possible and get more accurate results, investing more time would be the first recommendation for the further experiments with these associative polymers. Comparison with different concentrations of polymers (different viscosities) would also help to understand the rheological effects.

The images taken through the microscope at pore scale and directly over the micromodel at meso scale were the most important parts of this study. Capturing good images would allow the researcher explain and prove the conducted experiment very clearly.

For consistency, further research is required to understand the full range of the fluid interactions. Data comparison of the micromodel investigations with the core floods could be done to confirm these experimental results.

The injected pore volumes could not be determined due to the experimental set-up. Because of this problem, the injected volumes were not same, so the image analysis method which is used in this study may have not given trustable values. A new method for evaluating the residual oil saturation and the recovery values could be developed to obtain more reliable and accurate values.

REFERENCES

1. Schlumberger Oil Field Glossary, http://www.glossary.oilfield.slb.com/

2. Paulo R. Filoco, SPE, Petrobas and Mukul M. Sharma, SPE, University of Texas at Austin,: "Effect of Brine Salinity and Crude Oil Properties on Relative Permeabilities and Residual Saturations", paper prepared for presentation at the 1998 SPE Annual Meeting in New Orleans, LA, September 1998, SPE 49320.

3. R.R.Jennings, SPE-AIME, The Dow Chemical Co., J.H.Rogers, The Dow Chemical Co., T.J. West, The Dow Chemical Co.,: "Factors Influencing Mobility Control by Polymer Solutions", SPE 2867.

4. Frank W. Smith, SPE – AIME, Atlantic Richfield Co.: "The Behavior of Partially Hydrolyzed Polyacrylamide Solutions in Porous Media", February, 1970, *Journal of Petroleum Technology*, 2422.

5. http://www.snf-oil.com/, SNF Group - Manufacturer of Polymers for EOR.

6. Fredrick Woody, *Stanford University*, Diploma Thesis,: "Pore Level Visualization of Foam in a Silicon Micromodel", June 1995.

7. R. Lenormand, C. Zarcone, and A. Sarr.: "Mechanism of the Displacement of one fluid by another in a network of capillary ducts", *Journal of Fluid Mechanics*, 1983.

8. R. Shankar Subramanian, R. Balasubramaniam,: "Non-Newtonian Flows". *Cambridge University Press, Cambridge, UK* (2001).

9. Don W. Green, G. Paul Willhite,: "Enhanced Oil Recovery, SPE Textbook Series Vol 6", 1998, *Society of Petroleum Engineers.*

10. Sarah B. Inwood and Anthony R Kovscek, Stanford University, SUPRI-A Research Group Affiliates Meeting 2007 Presentation,: "High-Resolution, Microvisual Study of High Mobility Ratio, Immiscible Displacements", April, 2007.

11. http://www.fys.uio.no/~eaker/thesis/node17.html

12. Larry W. Lake,: "Enhanced Oil Recovery", 1989 by *Prentice-Hall, Englewood Cliffs,* New Jersey 07632.

13. Michael A. Janeczko, Member SPE-AIME, Texaco Inc.: "Skull Creek Newcastle Sand Unit – A Successful Polymer Flood" paper presented at the 54th Annual Fall Technical Conference and Exhibition of the Society of Petroleum Engineers of AIME held in Las Vegas, Nevada, U.S.A, SPE 8380.

14. Ian Martin, Central Del Rio Oils Ltd., and Wally Lozanski, Consulting Engineer, Members AIME,: "Taber South - Canada's First Polymer Flood", paper presented at the 21st Annual Technical Meeting of the Petroleum Society of CIM, SPE 3180.

15. Ivonete P.Gonzalez de Silva, Maria Aparecida de Melo, and Jose Marcelo Luvizotto, Petrobas SA, and Elizabete F. Lucas, Federal University of Rio de Janerio,: "Polymer Flooding: A Sustainable Enhanced Oil Recovery in the Current Scenario" paper prepared for presentation at the 2007 SPE Latin American and Caribbean Petroleum Engineering Conference held in Buenos Aires, Argentina, SPE 107727.

16. Balram K. Maitin and Hartwig Volz, Deutsche Texaco, SPE/DOE 9794.: „Performance of Deutsche Texaco AG'S OERREL and Hankensbuettel Polymer Floods", paper presented at the 13th Annual OTC in Houston, TX, U.S.A.

17. W.B. Gogarty, Member AIME, Marathon Oil CO., Littleton, COLO.: "Mobility Control with Polymer Solutions". *Society Petroleum Engineers Journal*, June, 1967, SPE 1566.

18. R.L.Jewett, SPE-AIME, The Dow Chemical Co., G.F.Schurz, SPE-AIME, The Dow Chemical Co.,: "Polymer Flooding – A Current Appraisal", *Journal of Petroleum Technology*, 2545, June, 1970.

19. N. Mungan, F. W. Smith, J.L. Thompson, Sinclair Oil & Gas Co. Tulsa, OK,: "Some Aspects of Polymer Floods", SPE 1628.

20. Sarah B. Inwood and Anthony R Kovscek, *Stanford University*, SUPRI-A Research Group,: "High-Resolution, Microvisual Study of High Mobility Ratio, Immiscible Displacements", April, 2007